2-1-2015

Use of alginate/montmorillonite nanocomposites as drug delivery system for curcumin

Marwa Fathy Ahmed

THE AMERICAN UNIVERSITY IN CAIRO
School of Sciences and Engineering

Department of Chemistry

Use of alginate/montmorillonite nanocomposites as a drug delivery system for curcumin

Marwa Fathy Abdelfattah Ahmed

A thesis submitted in partial fulfillment of the requirements for the degree of

Master of Science in Chemistry

September 2015

Advisor

Prof. Adham Ramadan

The American University in Cairo

Use of alginate/montmorillonite nanocomposites as a drug delivery system for curcumin

A Thesis submitted by

Marwa Fathy Abdelfattah Ahmed

To the Chemistry Graduate Program

September 2015

In partial fulfillment of the requirements for the degree of Master of Science in Chemistry with concentration in Food Chemistry

Has been approved by

Thesis Committee Supervisor /Chair: Dr. Adham R. Ramadan

Affiliation: Professor of Chemistry and Dean of Graduate Studies, the American University in Cairo.

Thesis Internal Examiner: Dr. Mayyada El Sayed

Affiliation: Visiting Assistant Professor of Chemistry, Chemistry Department, School of Sciences and Engineering, the American University in Cairo.

Thesis External Examiner: Dr. Omaima N. El Gazayerly

Affiliation: Professor and Chair of the Pharmaceutics and Industrial Pharmacy Department, Faculty of Pharmacy, Cairo University.

Thesis Committee Moderator: Dr. Tamer Shoeib

Affiliation: Associate Professor and Chair of the Chemistry Department, School of Sciences and Engineering, the American University in Cairo.

Program Director	Date	Dean	Date

Acknowledgement

Actually, many people have contributed to this work and made my graduate experience one of the most enriching and interesting steps in my life. First of all, I have to dedicate this work to my great family, with especial gratitude to my great parents who were always behind me. None of this would have been possible without their love and prayers. I have been fortune to have them in my life, I wish I could thank them.

I would like to give my deepest gratitude and appreciation to my dear husband Ahmed Abdelwadoud, who gave me all his support and love. He was the source of encouragement and confidence during my graduate journey. Really, I would like to express my immense appreciation for all he has done for me.

My deepest gratitude is to my brother, Mohammed, my sisters Mona and Yassmeen and their families, who always gave me all their love and support.

My deepest gratitude is to my advisor, Dr. Adham Ramadan. I actually enjoyed working with him throughout my graduate study. I have been incredibly fortunate to have an advisor who gave me all his support, encouragement and continuous guidance. He was always generous with his knowledge, time and effort.

I owe a debt of gratitude of my husband's family who gave me their love and support. I also would like to thank my lab colleges for listening, offering me advice, and supporting me through the whole thesis work. They really made the lab time a very interesting and encouraging time.

I would like to give special thanks to all the members of the Chemistry Department at AUC for their dedication to their work and the family-like environment that is felt everywhere and with everyone in the department.

List of Abbreviations

Abbreviation	Meaning
Alg.	Alginate
C-EC	curcumin-ethylcellulose
C-ECMC	curcumin-ethylcellulose/meyhylcellulose
COX-II	Cyclooxygenase-II
CS	Chitosan
Cur.	Curcumin
EE	Entrapment efficiency
e-MMT	Exfoliated montmorillonite
FaSSGF	Fast state simulated gastric fluid
FaSSIF-V2	Fast state simulated intestinal fluid version 2
FeSSIF	Fed state simulated intestinal fluid
FL	Flexible liposomes
FTIR	Fourier transform infrared
G unit	L-guluronic acid
Hyb.	Hybrid
MMT	Montmorillonite
M unit	D-mannuroinic acid
NC	Nanocomposites
PCNC	Polymer-clay nanocomposites
PEG	Polyethylene glycol
PVA	Polyvinyl alcohol

PVP K-30	Polyvinypyrrolidone K-30
SDS	Sodium dodecyl sulfate
SEM	Scanning electron microscopy
SGF	Simulated gastric fluid
SIF	Simulated intestinal fluid
SPC	Soybean hosphatidylcholine
TEM	Transmission electron microscopy
TMC	N-trimethyl chitosan
TPGS	D-α-tocopheryl polyethylene glycol 1000
TPP	Tripolyphosphate
XRD	X-ray diffraction

Abstract

Curcumin (Cur.) is a well known traditional medicine due to its anti-inflammatory and antioxidant properties. Its pharmacological mechanism of action and safety have been extensively studied to investigate its use in clinical and therapeutic applications. However, its low water solubility and rapid metabolism are main obstacles. Different techniques were used to overcome the drawbacks of curcumin, with recent attention focusing on approaches based on nanotechnology. Clay-polymer nanocomposites are getting to play a role in nanoformulations for drug delivery. This is due to their improved rheological and mechanical properties, and controlled drug release characteristics compared to their individual components, clays and polymers. Alginate/ montmorillonite (MMT) nanocomposites are used as drug delivery system for a wide variety of drugs due to numerous advantages of both components such as the high loading capacity of MMT and the ability of alginate release encapsulated drugs in a controlled manner. Accordingly, this study aimed at the preparation of curcumin loaded alginate/MMT nanocomposites and the investigation of their release properties.

Exfoliated MMT clay was first prepared by stirring the clay in an aqueous suspension for 4 hours, followed by filtration and drying at 70 °C. Exfoliation was confirmed by X-ray diffraction (XRD) and Fourier Transform infrared (FTIR) spectroscopy. Curcumin loaded MMT was then prepared by dispersing the exfoliated clay into an ethanoic curcumin solution. Different parameters were tested, namely stirring time, curcumin solution concentration and ratio of MMT to curcumin, in order to find out the maximum loading conditions. Stirring exfoliated MMT into curcumin solution of 1 mg/ml for 1 hour and in 5% W/V ratio was found to be the best condition for maximum loading (6.56 mg/g, corresponding to entrapment efficiency of 25.62 %). The hybrid sample (curcumin loaded MMT) was thus prepared. Visible spectrophotometric measurements of the curcumin solution were used to determine the amount of curcumin loaded by measuring the absorbance of curcumin solution before and after the dispersion of the clay. The hybrid sample was then encapsulated into alginate beads with different hybrid to alginate ratios (W/W) using the ionotropic technique.

XRD and FTIR analysis were used for the characterization of the prepared hybrid and nanocomposites. They revealed the increase in the degree of clay exfoliation upon drug loading and encapsulation into the alginate beads and the loss of the crystalline nature of curcumin upon

adsorption onto the clay surface without any chemical interaction between the clay and curcumin.

The release of curcumin from different alginate/MMT nanocomposites was studied in different biorelevent media: fast gastric (FaSSGF), fast intestinal (FaSSIF) and fed intestinal media (FeSSIF). The curcumin release in gastric media was negligible and this was attributed to its low solubility in these media and to the shrinkage of alginate beads in the acidic pH environment. Curcumin release in intestinal media was significantly higher and was found to be affected by both the feeding state and the ratio of hybrid to alginate. Increasing the hybrid to alginate ratio decreased the percentage of curcumin release because of the decrease of the swelling ratio of alginate due to the crosslinking effect of the clay. Consequently, the 1:20 (W/W) hybrid to alginate ratio nanocomposite sample (NC 1) showed the highest release percentage in both fast and fed intestinal media (71% in the FaSSIF and 15.5 % in the FeSSIF). On the other hand, the 1:2 (W/W) hybrid to alginate ratio nanocomposite sample (NC 4) demonstrated the lowest release percentage in both media (17.4% in FaSSIF and 6.6 % in FeSSIF). The feeding state played additional role in the percentage of curcumin released as it was found to affect both the pH and the concentration of the natural solubilizing components such as phospholipids and bile salts of the intestine. Accordingly, the percentage of curcumin released was higher in the fasting state than in the fed state due to the higher pH of the former media (88.4% in the FaSSIF and 16.6% in the FeSSIF for NC 1. Curcumin release in both intestinal media demonstrated different behaviors: in FaSSIF sustained release behavior was found to occur for 24 hours, while curcumin release reached a plateau by 8 hours in the FeSSIF.

This study reveals the promising use of alginate/MMT nanocomposites as sustained release drug delivery system for curcumin through surface adsorption of curcumin onto the surface of exfoliated clay and encapsulation of the loaded clay into alginate beads. The release of curcumin would be hindered into the gastric environment and start into the intestine. For maximum and sustained release behavior a fasting state is preferred.

Table of Contents

List of Figures

List of Tables

1 Introduction

1.1 Curcumin

Curcumin is a hydrophobic polyphenolic phytochemical extracted from the rhizome of turmeric (*Curcuma longa*) that is mainly cultivated in South Asian countries. Curcumin extract is a mixture of polyphenolic compounds called curcuminoids in addition to proteins, fats, and carbohydrates [1]. Curcuminoids consist of three main compounds which are curcumin I, demethoxycucumin (curcumin II) and bisdemethoxycucumin (curcumin III)[2] and they differ chemically in the number of the methoxy substituents on the two phenolic rings. Curcumin-I is found to be the most predominant polyphenol (represents 77% of the curcuminoids) and most of the therapeutic benefits of curcumin extract is attributed to it. Chemical formula of curcumin (Figure 1-1) is $C_{21}H_{20}O_6$, with molecular weight of 368.37 g/mol. It is oil soluble and has high solubility in alkaline solutions, however it is practically water insoluble in acidic and neutral pH [3][4][5][6][7]. Figure 1-1 represents the change in chemical structure of curcumin under different pH ranges. Under acidic to neutral pH curcumin acts as H-donor because of its keto form. However, alkaline pH (≥8) the enolate form convert curcumin into a strong electron donor [1].

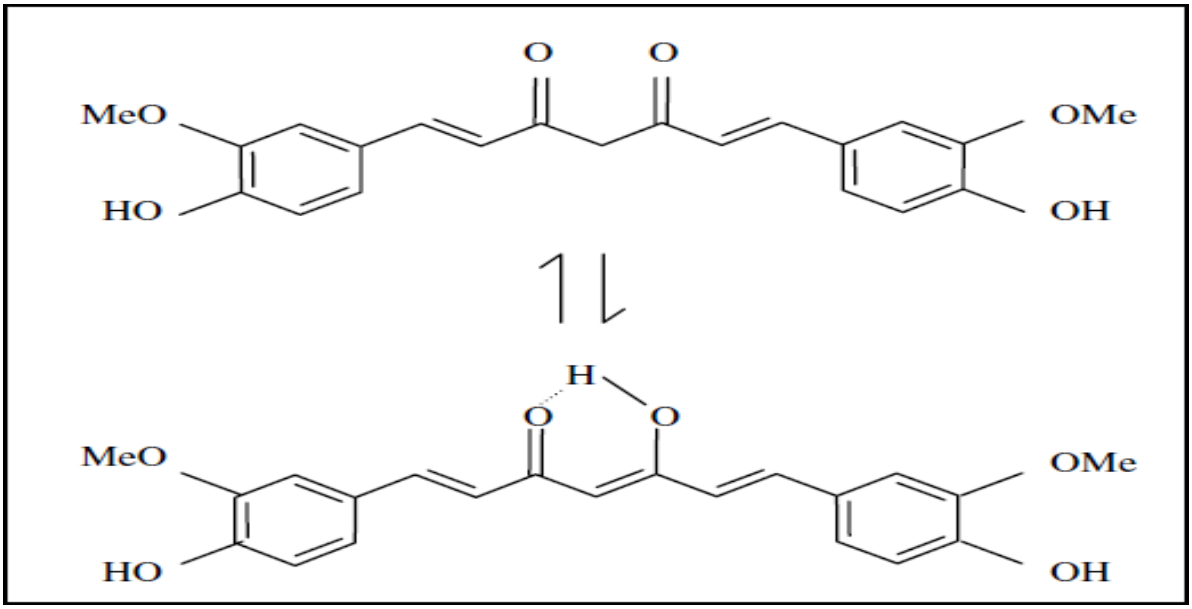

Figure 1-1: Curcumin Tautomers in neutral and acidic medium (bis-keto form) and in alkaline medium (enol form). [1]

Curcumin has been used for centuries in India and the surrounding region as a spice and coloring agent. Traditionally, curcumin has been used in the treatment and prevention of variety of chronic and acute diseases based on its anti-inflammatory and anti-oxidant activities. Figure 1-2 represents a summary of the target diseases that are known to be either treated or prevented by curcumin [6]. Although curcumin is used for centuries for the treatment and prevention of such diseases, the scientific bases for these applications were recently studied to find out the pharmacological and molecular targets of curcumin. Recent studies revealed that curcumin has the ability to affect different cell signaling pathways through targeting different biochemical molecules such as enzymes, proteins, growth factors, growth factor receptor, and transcription factors. Different preclinical and clinical studies in mice, rats and humans have been conducted to investigate the safety of curcumin [1], [4], [5]. One study involving oral administration of 5g/day for one month to Sprague–Dawley rats revealed that there is no apparent toxicity (1, 4). In humans, phase-I clinical studies showed that curcumin is safe in a dose up to 12 g/day[1], [4], [5].

Among different types of cancer that are affected by curcumin is colon cancer. In this regard, curcumin can act alone as anti-carcinogenic agent or as a potentiating agent for other pharmaceutical compounds such as 5-fluorouracil, doxorubicin, and celecoxib. Curcumin has antioxidant activity as it can sequester mutagenic reactive oxygen species such as superoxide anions, hydroxide radicals, and peroxides. Consequently, phase I clinical studies have been developed for curcumin, in addition to its enrollment in phase II clinical studies. Cyclooxygenase II (COX-II) is one of the common biomolecules that are associated to the incidence of colon cancer, so targeting this biomolecule has been the aim for the treatment of colon cancer. Curcumin has showed inhibitory effect on COX-II but with higher safety and minimal side effect compared to other COX-II inhibitors such as celecoxibe as the post market analysis of the latter showed an increase in the risk of acute myocardial infarction upon chronic administration. This safety of curcumin as a COX-II inhibitor is attributed to the difference in its mechanism of actions. For curcumin, the inhibitory effect is based on the regulation of the transcription factors rather than competitive inhibition of COX enzyme such as in case of celecoxib [8].

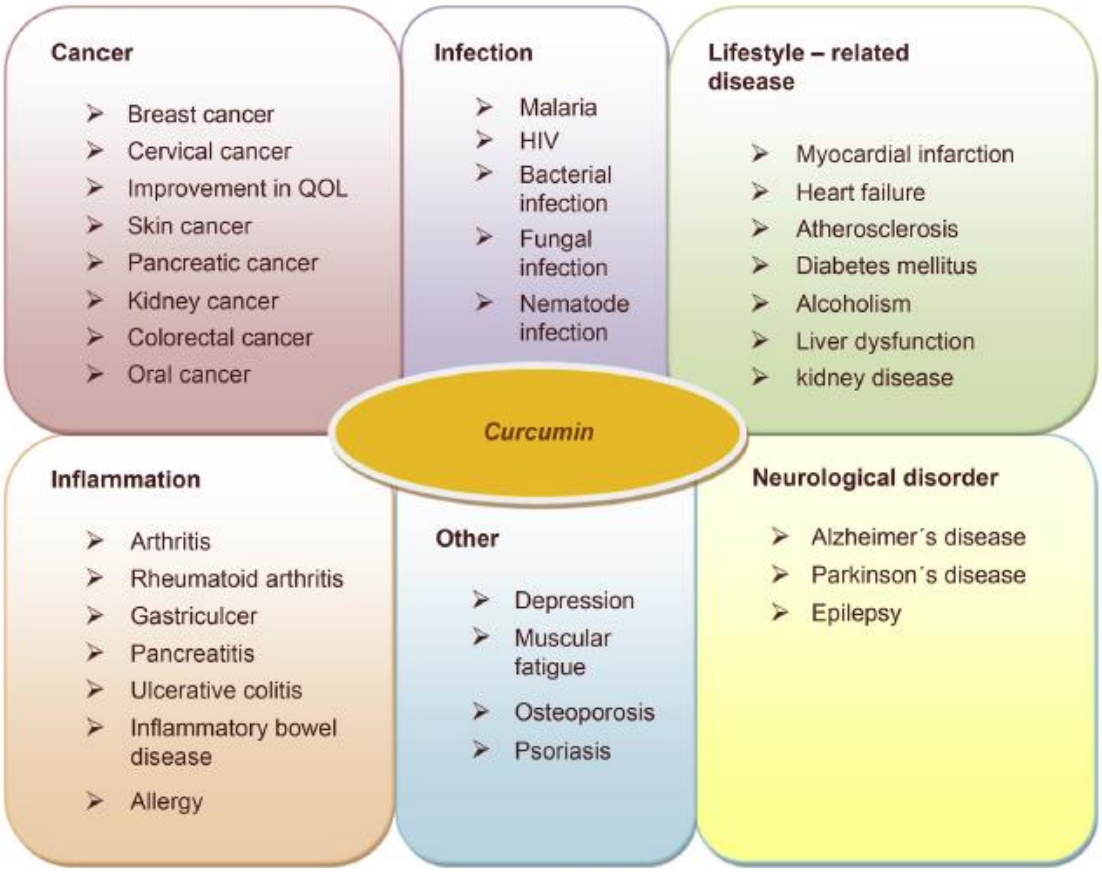

Figure 1-2: Curcumin target diseases. [6]

1.1.1 Physiological Limitations

Although of all its health benefits, curcumin could not have the expected clinical and therapeutic application. The limited application of curcumin is mainly attributed to its water insolubility that limits its absorption, in addition to its rapid metabolism and elimination from physiological systems. Curcumin low water solubility, less than 0.0004 mg/ml at pH 7.3, is the main limiting factor for its therapeutic application [7]. Clinical studies showed very low or even negligible amounts of curcumin in human serum after oral administration of high doses. According to Sharma et al., oral administration of 3.6 gm of curcumin resulted in plasma concentration of curcumin of 11.1 nM after one hour of dosing. Increasing the dose up to 8 g showed a jump in plasma concentration up to1.75 µM after one hour of administration while at doses less than 4 g curcumin levels in serum were below the detectable value [1]. These studies and others indicate that serum bioavailability of curcumin after oral administration depends on the administrated dose and is considered very low compared to the dosing amount. However, this low bioavailability is not only attributed to insolubility of curcumin in water but also to its rapid

metabolism. It is metabolized into different active and inactive products in the intestine and liver and these compounds are excreted in the form of glucuronids and sulfate conjugates [2], [3], [7].

In consequence to the above, curcumin has been the scope of investigations with the aim of developing new strategies for its administration and formulation in order to enhance its therapeutic uses and improve its bioavailability. Different formulations have been developed to achieve these goals with more emphasis on the application of nanotechnology for the preparation of new delivery systems for curcumin [3], [6], [7]. Among the investigated curcumin nanoformulations are polymer nanoparticles, polymeric micelles, solid/lipid nanoparticles, nanoemulsions, liposomes, nanogel and self-assemble. Figure 1-3 represents some of the developed curcumin nanoformulations [7].

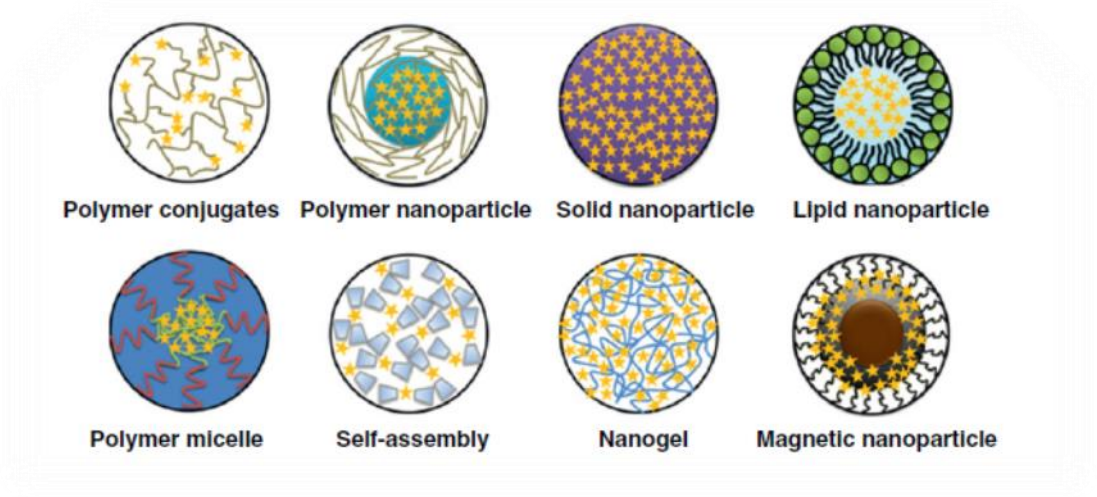

Figure 1-3: Different types of recently developed curcumin nanoformulations. [7]

1.2 Biopolymer-Clay Nanocomposites as Drug Delivery System

One of the recently developed nanoformulations with wide applications in drug delivery systems entails biopolymer-clay nanocomposites. Nanocomposites are hybrid materials in which the filler material has at least one of its dimensions in the nanoscale. The combination of a polymer material and a clay nanofiller form what is known as polymer-clay nanocomposites (PCNC). These have been widely studied to investigate the improvement of the properties of both of the polymer and clay, especially as drug delivery systems. Each component of PCNC can be used separately to provide controlled site specific drug delivery pattern. However, each of them has some limitations and could not fulfill all the needs as a drug delivery system. Nevertheless, the

combination a polymer material with nanoclays could improve the mechanical and barrier properties of the polymer on one hand and dispersion stability, ion exchange capacity and drug release rate of the clay on the other hand [9]. For example, Kevadiya et al reported the decrease in the release rate of procainamide in the gastric media from MMT gallery by compounding it with alginate and further coating it with chitosan. Additionally, the two polymers provided more slow and controlled release behavior to procainamide in the intestinal media compared to the drug/clay hybrid alone [10]. On the other hand, direct loading of drugs into polymers matrix only suffers from low entrapment efficiency and burst release effects. These disadvantages were improved by the incorporation of inorganic clays into the polymer matrix as proved by the study done by Kaygusuz and Erim for the entrapment of bovine serum albumin into alginate/montmorillonite nanocomposites [11]. The entrapment efficiency was increased from 40% to 78% by the addition of 2%W/V MMT and the release rate was slower from the naanocomposites (45-55% within 9 hours) compared the alginate beads (85% within 2 hours).

1.2.1 Biopolymers

Biopolymers are polymers that are capable of undergoing decomposition either enzymatically or by the microbial effect to produce environment friendly materials such as carbon dioxide, water, biomasses and inorganic materials [12]. Polysaccharides are considered the most abundant biopolymers on earth as they represent the basic elements in the skeleton of both plants and animals. Polysaccharides are composed of sugar monomers that are connected by glycosidic linkage and their properties depend mainly on the type and arrangement of sugar units, and molecular weight. The diversity in chemical groups and molecular weights of natural polysaccharides are the reason for the wide range of their chemical reactivity and properties [13]. Alginate is a polysaccharide, extensively studied in drug delivery for controlled and targeted release and enhancement of drug bioavailability [14]–[16]. It is used either alone or as a composite with clay minerals or even in combination with other polymers such as chitosan [12],[14],[18].

Alginic acid is a linear polysaccharide that is consisting of alternating blocks of D-mannuronic acid and L-glucuronic acids, these homogenous blocks are separated by blocks of either alternating or random sugar units of D-mannuroinic(M unit) and L-guluronic (G unit) acids (Figure 1-4). The main source of alginic acid is brown seaweeds of different species [14], [15],

[17], [19]. The extraction process, source, and the degree of purification give rise to more than 200 grades of alginate that vary in sequence and composition of the building block in addition to its molecular weight [14], [19]. The properties of different alginate grades such as transmittance, swelling, and gel strength depend on the mannuronate/guluronate ratio [19].

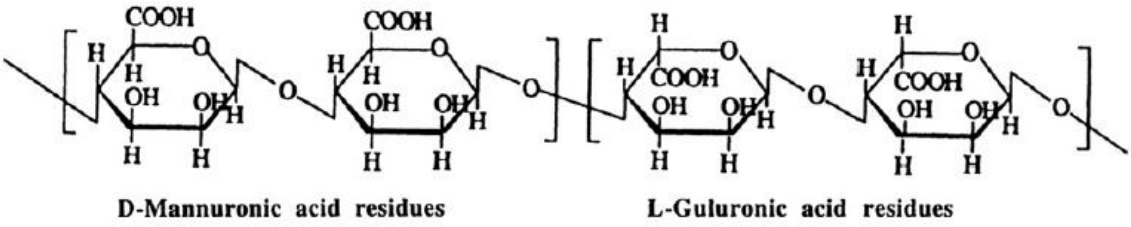

Figure 1-4: Main building blocks of alginate. [19]

Sodium alginate is the most used form of alginate products as it is slowly soluble in cold water and forms a viscous solution. However, it is practically insoluble in alcohol, hydroalcoholic solutions that contain more than 30% alcohol, and other organic solvents such as chloroform and ether [17]. On the other hand, calcium alginate salt is insoluble in both water and organic solvent but soluble in sodium citrate solution which acts as chelating agent for calcium leading to degradation of the calcium cross linking structure between different alginate molecules. Both alginic acid and its salts with di and multivalent cations can form high viscosity gels. In case of alginic acid, the gel is formed upon hydration due to the formation of intermolecular bonds. On the other hand, di and multivalent alginate salts (except for Mg^{+2} salt) form ionotropic hydrogels due to the selective ion binding properties of the polymer. The strength of the ionotropic gel depends on the mannuronic : guluronic ratio (M/G ratio) because guluronate residues demonstrate higher affinity to divalent cations [17], [19]. Consequently, alginate grades with low guluronate content demonstrate faster drug release profile compared to those of high guluronate residues. Additionally, the M/G ratio affect the composition of the storing media of calcium alginate beads, so for high guluronate alginate the storing media should contain high concentration of calcium ions and the Na^{+1}:Ca^{+2} should be less than 25:1. On the other hand, for low guluronate alginate the Na^{+1}:Ca^{+2} should be less than 3:1 [17]. These two types of hydrogels, acid and ionotropic gels, greatly affect the drug release properties from the dosage form by affecting both the physicochemical properties and the swelling process of the gel. Moreover, alginates have the ability to form strong complexes with poly cations such as chitosan

and polypeptides and these complexes are very effective in both stabilizing the gel and reducing its porosity. Accordingly, its drug release properties can be adjusted with compounding with such materials and can form more stable drug delivery system. On the biological side, alginate was found to have strong mucoadhesive properties compared to other polymers such as chitosan, polystyrene and poly (lactic acid) due to its polyanionic properties, consequently it is more effective in mucosal drug delivery such as in the gastrointestinal tract [20]. The mucoadhesive properties of alginate are found to be important in increasing the drug residence time at the site of action, and consequently its bioavailability and effectiveness [15], [16].

1.2.2 Clay

Years ago clay was used in drug formulation both as excipients (disintegrating or emulsifying agents) and as active ingredient (anti-diarrhea and antacid), however, later on co administration of some drugs such as promazine (antidepressant) with clay containing formulations showed reduced absorption of these drugs [22]–[24]. By studying this phenomenon, scientists discovered that clays minerals can be used in modified drug delivery systems for delayed, sustained and/or targeted drug delivery [23], [24].

Clays are characterized by layered structures that consist mainly of octahedral and tetrahedral sheets. The tetrahedral sheet consists of silicon atom surrounded by four oxygen atoms while the octahedral one consists either of aluminium or magnesium atoms that is surrounded by eight oxygen atoms. These sheets are connected together by sharing the oxygen atoms while free unshared oxygen atoms are present as hydroxyl group (OH). According to the arrangement of these sheets two main groups of clays or layers are formed: the kaolin group in which one tetrahedral sheet is fused to only one octahedral sheet (1:1) with total layer thickness 0.7nm and the phyllosilicate group in which one octahedral sheet is sandwiched between two tetrahedral sheets (2:1) with total layer thickness 0.94nm [25]. Phyllosilicate group may be present in two different electrostatic states: neutral such as in case of pyrophyllite which has no inter layer ions and cannot swell in water, or negative such as in case of mica and smectite. For mica one of the silicon atoms in the tetrahedral sheet is substituted with aluminium atom which creates negative charge that is compensated by potassium ions in the interlayer space [25]. These potassium ions are equal in size to the hole created by the Si/Al tetrahedral sheets so there is no interlayer spacing created and consequently mica layers are fused strongly and cannot undergo swelling or

exfoliation. On the other hand smectite clays are characterized by the presence of the negative charges on the octahedral sheets due to the replacement of aluminium atoms with magnesium ions and this replacement is compensated by inserting either sodium or calcium cations in the interlayer spaces (Figure 1-5) [25]. However, the size of compensating cations is not equal in size to the hole created on the octahedral sheet, so an interlayer space is created and smectite clays have the ability to swell in solutions and the layers undergo exfoliation by different techniques. Due to the variation between layers in the negative charge created by atoms replacement, the average charge value is measured by cation exchange capacity [25]–[27]. Being dispersible in solution allows smectite clays to have high aspect ratio which enhance its surface interaction with polymers during the preparation of polymer-clay nanocomposites, and consequently they are considered very effective as reinforcement filler for polymers [25]. Nevertheless, the high intrinsic hydrophilicity and stacking force of clay layers make their dispersion in many polymer solutions, especially hydrophobic polymers, difficult and cannot by easily achieved by physical mixing of the polymer and clay. To improve this compatibility with hydrophobic polymers, clays are subjected to surface modification with hydrophobic agents that decreases their surface energy and enhance the polymer-clay interaction that produce nanocomposites of improved properties [24], [25].

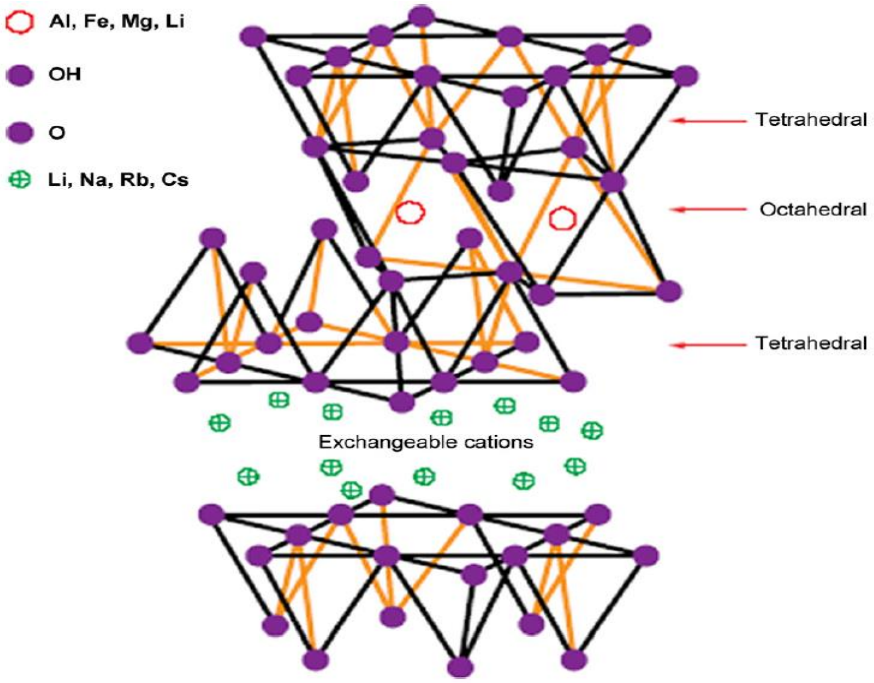

Figure 1-5: Clay schematic structure. [24]

Different approaches have been proposed for the clay-drug interactions and were found to depend on the type of clay used, and drug's physicochemical properties and functional groups. The most known and used technique is cation exchange in which cationic drug molecules exchange with the small cations such as Na^+ and Li^+ that occur naturally intercalated between the clay layers to compensate for the negative charge of the clay layers. This mechanism is also important for drug release kinetics within the body as it allows drug release in biological systems that have compensating counter ions of the clay as demonstrated in Figure 1-6 [22], [24]. However, other types of clay-drug interactions were found to take place, such as van der Waal interactions, hydrogen bonding, and ion-dipole interaction [22]. Two methods describe clay-drug hybrid preparations: the wet and the dry methods. The first one is more common and involves the dispersion of clay particles in drug aqueous solution for certain time under mild agitation followed by drying process to obtain clay-drug hybrid [24]. The dry method is used for poorly soluble drugs in which clay particles and drug molecules are mechanically mixed to interact under harsh conditions such as strong milling or at the melting temperature of the drug [24]. Variability in clay-drug interactions and consequent variation in drug release kinetics promoted the use of clay in modified drug delivery systems as extended-release system, site-specific release system and/or solubility enhancing carrier for poorly soluble drugs [22], [24]. Improving solubility of poorly soluble drugs is a great challenge facing pharmaceutical scientists as many of the newly discovered drug candidates are water insoluble, presenting a critical barrier for drug absorption. Mineral clays could promote the solubility of both anionic and nonionic drugs that are weakly bonded to their surfaces, through increasing the drug surface area exposed to dissolution media and drug wettability due to the hydrophilic properties of clays [22].

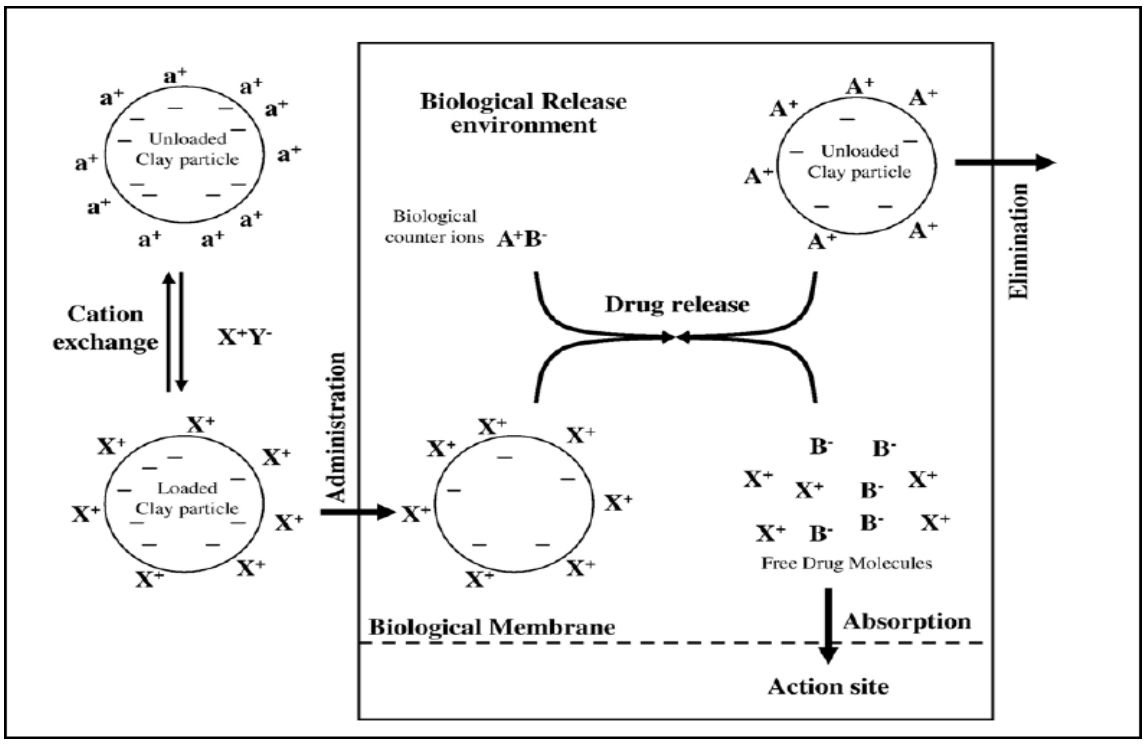

Figure 1-6: Clay-Drug Interaction By Cation Exchange Mechanism and In Vivo Drug Release Mechanism. Clay surface charge (-), compensating cations (a+), cationic drug (X+), drug associated anions (Y-), in vivo counter ions (A+), anions associated with the counter ion. [22]

Among both natural and synthetic clays Montmorillonite (Figure 1-7)has been widely used in drug delivery applications either alone or in combination with different polymers to form polymer-clay nanocomposites [22]. This is mainly attributed to its very high ion exchange capacity compared to other pharmaceutical silicates clays, such as kaolin and talc, as well as low cost and hydrophilicity [28]–[31]. Nevertheless, it could also be modified to be more compatible with hydrophobic drugs and polymers by exchanging the small inorganic cations such as sodium with larger hydrophobic ones such alkyl ammonium cations which increase both the interlayer space between the clay layers and also alter its surface properties to be more hydrophobic [12].

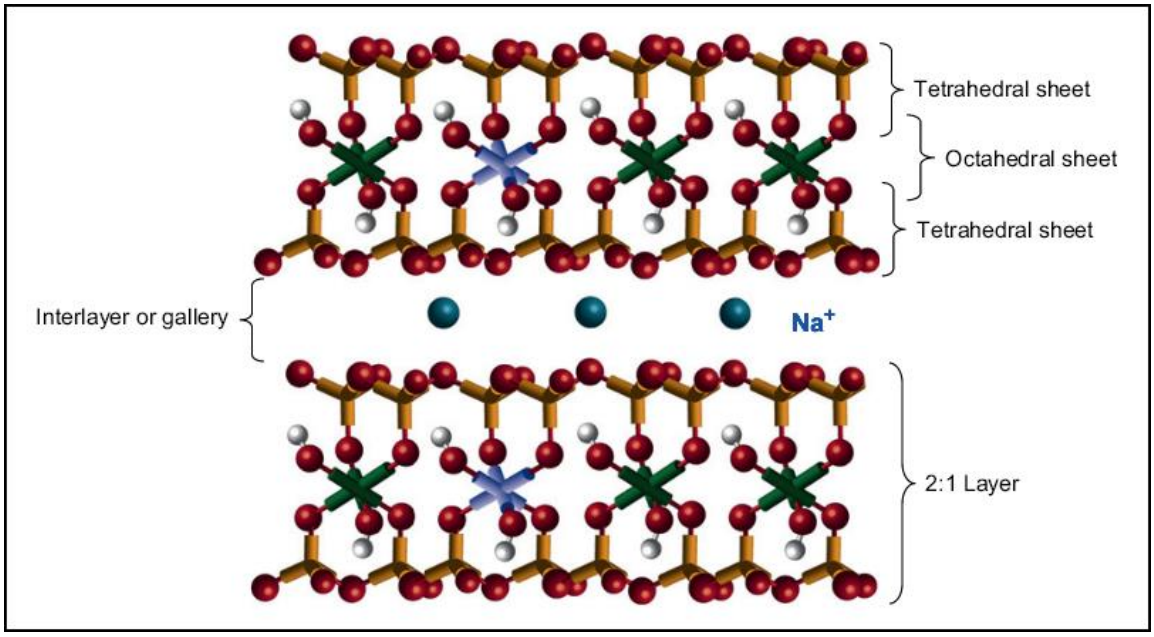

Figure 1-7: Montmorillonite basic structure. [26]

1.2.3 Preparation Techniques and Types of Polymer-Clay Nanocomposites

There are three main methods for the preparation of biopolymer- clay nanocomposites which are in-situ polymerization, solvent intercalation and melt intercalation. These methods would form different biopolymer-clay nanocomposites morphologies according to preparation conditions, and polymer/clay affinities. These morphologies are described based on the degree of the clay layers separation from each other and their dispersion into the polymer matrix. Figure 1-8 demonstrates different types of polymer-clay nanocomposites morphologies which are phase separated, intercalated and exfoliated structures [12], [25][32]. *Phase separated structures* show some interaction between the polymer and clay (mostly the clay surface) without any intercalation between the polymer molecules and the clay interlayer spaces. This structure almost has the same properties of traditional micro composites as the clay particles occur as aggregates of stacked layers in the polymer matrix. *Intercalated structures* are characterized by the increase of the clay interlayer space while keeping its periodic array arrangement, the increase in clay d-spacing is due to the insertion of one or more of the polymer chains between the clay layers. This structure can be described as a well ordered multilayered hybrid with high interaction between its components. Exfoliated structures, also known as delaminated structures, have individual clay layers totally dispersed in the polymer matrix losing the clay periodic array arrangement. This is achieved when the increase in the interlayer d-spacing is more than 8-10nm. Accordingly, there

is a great increase in clay aspect ratio which explains the high interaction between the polymer and clay leading to great improvement of the polymer properties and the use of fewer amounts of clay [12]. As mentioned before, these different structures of polymer-clay nanocomposites depend on the nature and properties of the clay and polymer as well as the preparation technique.

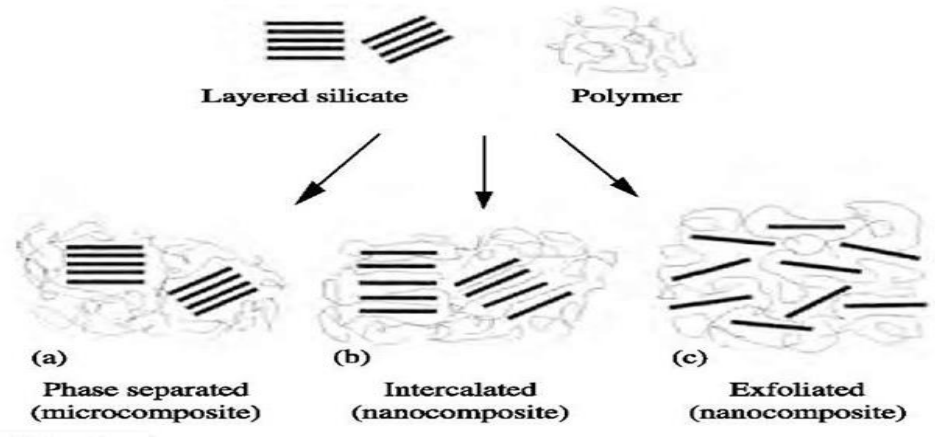

Figure 1-8: Polymer-clay nanocomposites structures. [27]

A. *In-situ polymerization*

This technique involves the polymer synthesis from its monomer building blocks solution. The clay is suspended and swollen in the monomer solution before the initiation and propagation of the polymerization process. During the polymerization process, the polymer matrix penetrates the layers of the clay forming intercalated structure and in some cases leading to complete exfoliation of the clay layers. For synthetic polymers, this technique seems suitable but for natural biopolymers, it is not possible to use as the polymers are naturally synthesized and there is no way to incorporate the clay into the polymer matrix during its synthesis [9], [12], [33].

B. *Solvent intercalation*

This technique is used for polymer/clay systems in which the clay can be swollen in a solvent which can either dissolve the polymer, or which is miscible with another solvent for the polymer of interest. After mixing the polymer solution and clay suspension, the solvent is evaporated. This typically results in an intercalated nanocomposite structure [9], [12], [33].

C. *Melt Intercalation*

This technique entails mixing the polymer and clay at a temperature corresponding to the melting temperature of the polymer. Extruders are typically used to induce sheer force that leads to clay exfoliation or delamination giving the polymer matrix the chance to penetrate the clay layered

structure. Consequently, the technique depends on the preparation conditions which are the sheering force and the residence time in addition to polymer/clay affinity. This means that monitoring the process parameters is necessary to avoid polymer degradation due to mechanical, thermo-mechanical and/or high residence time. Some biopolymers such as chitosan and pectin have high thermal or thermo-mechanical degradation properties so cannot be melt-processed [9], [12], [33].

1.2.4 Structural Characterization of Polymer-Clay Nanocomposites

The main goal in polymer-clay nanocomposite characterization is to define the degree of clay dispersion into the polymer matrix because this is responsible for the improvement in different properties of the hybrid material. Structural characterization can be done using two techniques, X-ray diffraction analysis (XRD) and transmission electron microscopy (TEM) [25], [33]. Due to the regular layered structure of clays, they give characteristic peak in XRD analysis. Consequently, applying peak parameters such as peak width at half maximum height and peak position (2θ) in Bragg's law (eq.1-1) will help us to quantitatively find out the change in interlayer spacing of clay (d-spacing) upon interaction with the polymer molecules [25].

$$\text{Sin } \theta = n\,\lambda/2d \qquad \text{Equation 1-1}$$

where θ is the measured diffraction angle, λ is the wavelength of the used x-ray radiation, and d is the interlayer spacing. Accordingly, any change in the peak intensity, broadness, and position can be indicative for the degree of intercalation or exfoliation [25], [27]. Figure 1-9 is another demonstration for the use of XRD to estimate the structure of the formed nanocomposites. It depicts the XRD results of three polymer/organoclays mixtures, and demonstrates the three possible interactions and structures of polymer/clay composites. For immiscible polyethylene/organoclay mixture, the XRD pattern of the clay did not change and the basal spacing was conserved, at a value of d = 2.2 nm, while the basal spacing of the organoclay is increased to d= 3.0 nm in case of its interaction with polystyrene due to the intercalation of the polymer chains into the clay layers. The third type of change involves the complete exfoliation of the clay layers by its interaction with the polymer chains as in case of siloxane/silicate nanocomposite and this is confirmed by the disappearance of the diffraction beak in the XRD spectrum [25]. Additionally, Transmission Electron Microscopy (TEM) can also be used to qualitatively elucidate the composite structure [25], [27], [33].

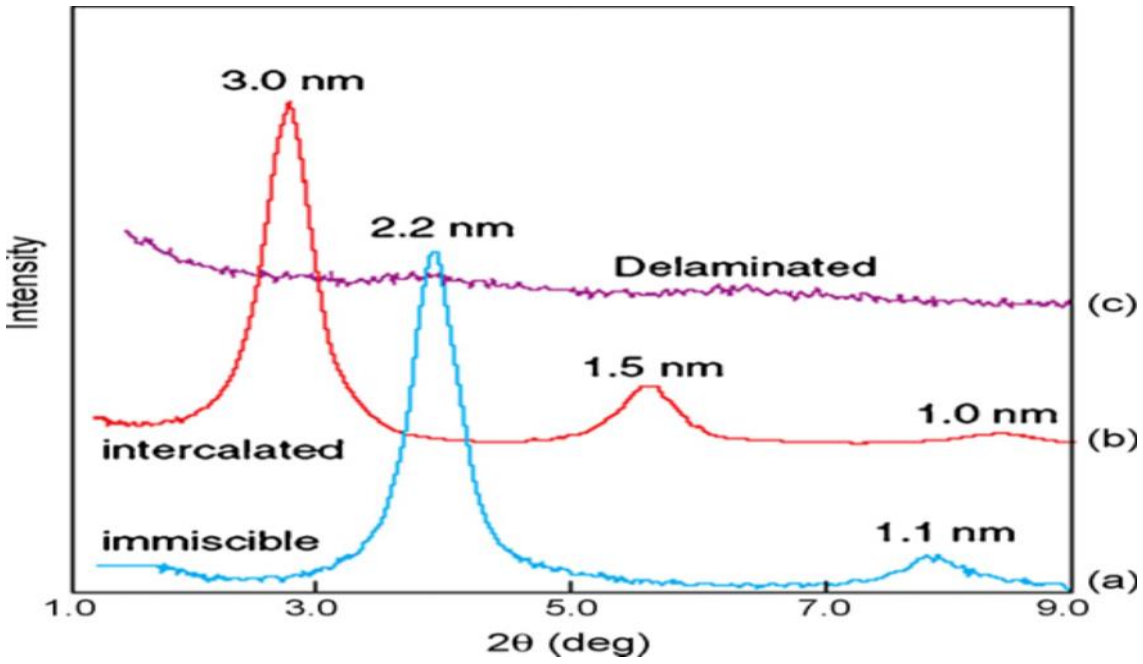

Figure 1-9: Typical XRD patterns from polymer/layered silicates: (a) is Polyethylene/layered silicate (nanocomposites are not formed) immiscible mixture, (b) Polystyrene/organoclay nanocomposite (the polymer is intercalated into the silicate layers), and (c) silo

1.2.5 Alginate-Montmorillonite Nanocomposite Drug Delivery Systems

For patients, orally administered dosage forms are the most convenient and consequently special attention is paid to them. Successful oral formulation should deliver the required therapeutic dose to the specific site of action throughout the treatment period. Decreasing the dosing frequency increases the patient compliance, so sustained release formulations are extensively studied. Additionally, drug delivery systems that effectively increase the drug stability throughout the gastrointestinal tract during the time of treatment are investigated. Alginate is a biopolymer that is widely applied in controlled oral drug delivery systems mainly due to its ability to form cross-linked gel structure in the presence of divalent ions, the most used ion is Ca^{+2}. This gel structure allows the entrapment of small drug molecules, proteins, cells and enzymes. Moreover, alginate is a pH sensitive hydrogel, i.e. it shrinks at acidic pH (in the stomach) and its pore size decreases. Consequently, it prevents the release of drug molecules in gastric fluids. However, at neutral and slightly alkaline pH, alginate gel swells and the pore size increase to allow the leakage of the entrapped molecules therefore alginate is suitable carrier for drugs that are sensitive to the harsh conditions of the stomach. The preparation of alginate gel is achieved at mild agitation conditions and does not require any heating or harsh conditions. Accordingly, it is a suitable entrapment for sensitive molecules such as proteins [14]–[17], [19], [20]. On the other hand,

alginate suffers from the low entrapment efficiency and burst release of drugs in the intestinal media. Therefore, the combination of alginate with other biodegradable materials has been investigated in order to overcome these drawbacks. Clay minerals are one of the fillers that are used in combination with many biopolymers to improve their drug delivery characteristics. Montmorillonite is one of the widely used clay in pharmaceutical applications due to its biocompatibility, low cost and mucoadhesive properties. In addition, its high surface area and layered structure allow the intercalation of drug molecules into its layered gallery. The incorporation of MMT into alginate gel has been studied with the aim of adjusting the drug delivery properties for both of these components. The addition of MMT to alginate increases the entrapment efficiency of alginate due to the large surface area of the clay. The clay also improves the surface strength of alginate, thus reducing the loss of drug molecules during the preparation process [31]. The addition of MMT to alginate also slows down the drug release and provides diffusion release instead of erosion mechanisms. The combination of alginate montmorillonite has been studied for the delivery of drugs such as diclofenac sodium, lidocain HCl, vitamin B1, B2 and B6, and bovine serum albumin [31].

1.3 Biorelevant Dissolution media

The bioavailability challenges of new formulations and delivery systems evoked the need for accurate dissolution experiments. Consequently, conventional dissolution tests that are used for quality control, were applied for the prediction of in vivo behavior of dosage forms through establishing in vitro in vivo correlations. For oral dosage forms, dissolution media described in international pharmacopeia focused on simulating the pH of the gastrointestinal tract and the use of some enzymes such as pepsin and pancreatine to estimate the in vivo behavior of drug formulation. For water insoluble drugs, artificial surfactants were added to these media to estimate their dissolution upon the presence of the natural ones such as bile salts and phospholipids. However, these media did not take into account many other factors that can significantly affect the intraluminal dissolution and solubility of active ingredients such as the ionic strength, surface tension, viscosity and osmolality. In addition to effect of food on both the composition and pH of the gastrointestinal tract contents which in consequence affect the bioavailability of ingested dosage forms[34].

Establishing in vitro dissolution experiments that simulate the in vivo conditions is needed to predict bioavailability of new active ingredients and formulation. This would provide a useful tool to save time and cost needed for pharmacokinetic and clinical studies done to estimate the fate of dosage form after administration. For orally administered formulations, solubility and dissolution of the active ingredients are vital processes to predict their bioavailability since only soluble molecules can permeate the mucosal membrane of the gastrointestinal tract at the specific site of absorption[35], [36]. The dramatic increase in the knowledge of intraluminal environment and the strong need to develop optimum formulations evolved the biorelevant dosage form performance testing. This testing refers to the simulation of gastrointestinal conditions, both the content and hydrodynamic, during the in vitro testing of different dosage forms [35].

For drugs with solubility and bioavailability problems to achieve their therapeutic effect, dissolution testing should be carefully designed to predict their in vivo behavior. According to the biopharmaceutical classification system (BCS), dissolution rate of class II drugs (poorly soluble but highly permeable) is considered the rate limiting step for drug absorption and prediction of its in vivo performance [34]–[38]. For example, Phenytoin is a weak acid lipophilic antiepileptic drug and is classified as BCS class II drug. Comparing the dissolution profile of phenytoin in both traditional and biorelevant media with studies performed in human volunteers, confirms the predictive power of biorelevant media to estimate the in vivo behavior of such drugs. Phenytoin showed enhanced drug release in fed state simulated intestinal fluids (50%) compared to fasting state (36%). Studies in human volunteers also confirmed the enhancement of drug release when ingested with food. This result is attributed to the increase of bile components in the fed state which provide solubilizing effect to phenytoin [37]. Accordingly, the use of biorelevant media in dissolution testing of pharmaceutical dosage forms would provide us with information that can be correlated to their in vivo performance.

2 Literature Review

2.1 Introduction

Curcumin is the primary phenolic compound extracted from the turmeric spice of curcuma longa. It has been used for many centuries in Asia as a spice, food coloring agent, and dietary supplement as well as a component in Asian traditional medicine. Recent studies revealed that curcumin can exert many important pharmacological actions that target many chronic diseases such as type II diabetes, rheumatoid arthritis, Alzheimer's disease, and multiple sclerosis [1]–[7]. In addition there is strong evidence of curcumin having the ability to both prevent and treat different types of cancers through various pathways including inhibition of cell proliferation, metastasis and induction of apoptosis by modulating many pro-inflammatory factors. Furthermore curcumin demonstrated high safety in oral doses up to 12 g/day and free pass through cellular membranes due to its lipophilicity [5], [7]. However, pharmacokinetic studies proved very low bioavailability of curcumin due to is low water solubility (0.0004 mg/ml at pH 7.3), rapid degradation and elimination by the intestine and the liver [5]. Consequently, many approaches have been adopted to improve curcumin bioavailability especially by applying nanotechnology [1]–[7].

Nanotechnology has wide application in drug delivery and could be used to improve drug solubility, stability, and to provide targeted and sustained drug delivery. Different materials have been used to formulate nanosized drug delivery systems such as synthetic and natural polymers, lipids, proteins and metals. Nano-sized curcumin loaded drug delivery systems have been designed and studied to enhance curcumin bioavailability through improving its water solubility, reducing its metabolism and elimination from the body and enhancing its stability in biological system [1][5], [7]. One of the extensively studied nanosized drug delivery systems is polymer-clay nanocomposites in which clay nanoparticles dispersed in a polymer matrix provide large interfacial interactions with the polymer molecules, consequently improving of both the polymer and clay physicochemical properties. The drug delivery properties of nanocomposites can be adjusted by changing the type and ratio of the used polymer or the clay mineral and/or by adjusting the preparation conditions [7]. Additionally, this system was found to improve the drug delivery properties of both the polymer and clay. They were found to have improved rheological

and mechanical properties relative to individual components, in addition to the enhanced drug entrapment efficiency and controlled drug release properties [9].

This chapter is divided into two main parts: the first part discusses different nanoformulations that were developed to improve curcumin bioavailability with special concentration on polymeric nanoparticles using alginate as the matrix polymer. The second part addresses different systems that use polymer-clay nanocomposites for oral controlled drug delivery. This part focuses on alginate montmorillonite nanocomposites that are used for different drug moieties to improve their pharmacological and/or pharmacokinetic properties.

2.2 Curcumin Nanoformulations

The use of nanoformulations in drug delivery in general can be effective due to the small particle size of the drug carrier which can improve solubilizing in addition to the circulation and permeation of the loaded drug in the body [7]. Consequently, nanoformulations can enhance the bioavailability of drugs in addition to drug targeting to specific tissues. The advance in using nanotechnology in drug delivery systems has been applied to develop curcumin loaded nanocarriers to alleviate the therapeutic limitations of curcumin. Curcumin nanoformulations aim to improve its water solubility, protect it from rapid metabolic degradation and increase its targeting to site of disease [1], [5], [7]. Liposomes, polymeric nanoparticles and micelles, cyclodextrin inclusion, nanoemulsions and solid dispersions are most commonly used in curcumin nanoformulations.

2.2.1 Solid dispersion

Solid dispersion is the dispersion of active ingredients in a hydrophilic matrix using either solvent evaporation or fusion methods, and in some cases both methods are used [3], [6]. This technique helps reduce drug particle size which improves its wettability and solubility. Additionally the rapid dissolution of the carrier materials in aqueous media allows the rapid release of the loaded drug in the form of fine particles which improves its dissolution and absorption [39]. Different synthetic polymers have been used for the development of curcumin solid dispersion with improved solubility, dissolution and bioavailability. Of these polymers, polyvinypyrrolidone K-30(PVP K-30) was used by Nattha et al in 2011 to prepare curcumin solid dispersion with improved dissolution rate [39]. Curcumin : PVP K-30 samples were prepared in different weight ratios using solvent evaporation and the effect of increasing the polymer weight

ratio on curcumin dissolution and solubility was studied. Solubility tests indicated that changing the curcumin : PVP K-30 ratio from 1:2 to 1:6 and from 1:2 to 1:8 increased the solubility in simulated intestinal fluid (SIF) without pancreatin 4 and 5 folds respectively. The same trend was observed in simulated gastric fluid (SGF) without pepsin with the solubility increasing 16 and 26 folds at 1:6 and 1:8 ratio respectively compared to 1:2 curcumin : PVP K-30 solid dispersion. The authors attributed this improvement in solubility to the formation of a soluble complex between the curcumin and PVP K-30 as indicated by FTIR results. This led to the change of curcumin from the crystalline structure to amorphous form as indicated by the disappearance of the characteristic XRD peaks of curcumin. The authors also indicated that there was an increase in the dissolution rate of curcumin in both SGF without pepsin and in SIF without pancreatin for the solid dispersion with higher polymer concentrations. However, this increase in dissolution rate became insignificant as the cur:PVP K-30 ratio was increased from 1:6 to 1:8 [39].

In 2013, Kumavat et al studied the formulation of curcumin solid dispersion by fusion using different ratios of polyethylene glycol (PEG 4000 and PEG 6000) instead of PVP K-30 and came out with similar results [40]. The authors indicated that the preparation method and materials produced curcumin solid dispersions with high drug contents ranging from 96.13 to 99.9%. There was a noticeable increase in curcumin solubility in both water and 0.2 M HCl buffer with a linear relationship between the increase in solubility and polymer concentration. However, PEG 4000 demonstrated a better solubilizing effect than PEG 6000 which was attributed to improved interactions between curcumin and PEG 4000 resulting from the lower molecular weight of the latter as compared to PEG 6000. This enhanced the wettability of curcumin. In consequence, marked enhancements in the dissolution of solid dispersions and physical mixtures relative to the pure curcumin were observed. FTIR studies confirmed the presence of hydrogen bonding between curcumin and PEG [40].

2.2.2 Liposomes

Liposomes are lipid based spherical particles consist of phospholipid that are self-associated in the form of bilayer vesicles when hydrated in aqueous media [2], [3], [5]–[7]. This behavior originates from the amphiphilic nature of phospholipids which cause them to shield their hydrophobic groups from aqueous media while using their hydrophilic ones in interaction with

aqueous phase. The liposomal structure makes them suitable for encapsulation of both hydrophobic and hydrophilic drugs by inserting them in either the lipid bilayer or aqueous interior respectively [2], [6]. They can be used for both parenteral and oral drug delivery especially for lipophilic chemopreventive drugs such as curcumin, resveratrol, and oryzanol [2]. Orally administered liposomes provided protection for many pharmaceutical drugs such as insulin, calcitonin, cyclosporine and peptides against enzymatic degradation in addition to efficient delivery to blood stream, i.e. good bioavailability. However, conventional liposomes suffer from gastrointestinal instability as they are easily undergo degradation by bile by salts. Consequently, many attempts are evoked to eliminate this drawback such as using chemically modified phospholipids or surface coated liposomes [41].

Curcumin loaded liposomes are investigated for curcumin delivery by many routs of administration such as parenteral, oral, and transcutaneous. Several curcumin loaded liposomes are prepared for oral administration with concentration on modified liposomes to avoid drawbacks of conventional ones. Chen et al prepared N-trimethyl chitosan-(TMC) coated liposomes for oral delivery of curcumin by thin layer dispersion method using soybean phosphatidylcholine (SPC) as the main phospholipid [41]. The authors prepared different formulations using various components to compare their effect on drug loading and entrapment efficiencies. The addition of cholesterol showed enhancement in both drug entrapment and loading and this was attributed to its ability to retard the fluidity of the lipid bilayer and consequently decrease drug leakage from the liposomal structure. D-α-tocopheryl polyethylene glycol 1000 (TPGS) also significantly improved the drug entrapment and loading efficiencies relative to Pluronic F127 containing formulation. This findings was prone to the lower critical micelle concentration and more bulky lipophilic structure of TPGS than those of PF127 which led to stronger hydrophobic interaction between the drug and lipid bilayer. For liposome coated structure, the authors reported that using 0.5% w/v TMC and incubation time of 3 hours will produce no aggregation due to complete coating of the liposomes. At lower TMC concentration and shorter incubation time liposomal aggregates occur. TMC coated liposomes showed larger particle size (657.6 nm) than uncoated liposomes (221.4 nm). The release of curcumin from both coated and uncoated liposomes showed initial burst release after 8 hours followed by slow sustainable release. The cumulative amount of curcumin released after 48 hours was 77% and 74% from TMC coated and uncoated liposomes. This insignificant difference between coated

and uncoated liposomes is attributed to weak electrostatic interaction between the polymer and liposome surface and the dissolution of the polymer layer in water. These two factors led to relatively loose coating layer and consequently insufficient retardation of curcumin release. However, the pharmacokinetic study done in male Wistar rats revealed that TMC-coated liposomes improved the oral bioavailability of curcumin compared to uncoated liposomes. This is demonstrated by longer elimination half-life of coated formulation (12.05 hours) than uncoated one (9.79 hours). Additionally, the area under the concentration-time curve $(AUC)_{\infty}$ was found to be 416.58 µg/L.h. and 263.773 µg/L.h in case of coated and uncoated liposomes respectively which suggests that TMC coating increased curcumin bioavailability. This result suggests that TMC prolonged the drug residence time due to the adhesion properties of TMC polymer and protected the liposomal structure from disruption by the gastrointestinal media. Moreover, TMC enhanced curcumin absorption by facilitating the paracellular transportation [41].

Karewicz et al used other chitosan derivatives, cationic, hydrophobic and cationic-hydrophobic derivatives, to produce more stable liposomes as curcumin carrier [42]. Of the prepared chitosan derivatives coatings, cationic-hydrophobic derivative is suggested as the most promising one for curcumin containing liposomes. Chitosan derivative containing both quaternary ammonium and N-dodecyl group (cationic-hydrophobic) could provide both enhanced stability and improved membrane penetration for curcumin containing liposomes. Compared to the TMC-coated liposomes prepared by Chen et al, cationic-hydrophobic chitosan coated liposomes prepared by Karewicz et al showed no burst release. Its release profile is practically linear up to 90 mints and plateau is reached plateau after 10 hours. Cellular uptake studies using murine melanoma B16F10 cells demonstrated maximum penetration for coated liposomes into cells after 90 mints, while free curcumin showed much weaker cell penetration properties. Cytotoxicity studies demonstrated no toxic effect for both the coating polymer and the empty coated liposomal structure on both murine melanoma B16F10 and murine fibroblast NIH3T3. However, curcumin containing coated liposomes showed high toxicity to murine melanoma B16F10 in a very low concentration 2.5µM curcumin. On the other hand, curcumin loaded coated liposomes had no influence on normal murine fibroblast NIH3T3 cells even at concentration up to 20 µM curcumin. Moreover, liposomal form of curcumin exerts cytotoxic effect on cancerous cells at much lower concentration (2.5 µM) than free curcumin which can be tolerated in concentration

up to 10 µM. The increased cytotoxicity of liposomal formulation toward cancerous cells compared to normal ones is explained by higher uptake of liposomal curcumin by cancerous cells than normal ones. In addition to the ability of curcumin to suppress the NF-κB-regulated genes which produce the factor mediating the survival of tumor cells.

Li et al investigated the silica coated flexible liposomes as a promising carrier for curcumin. Flexible liposomes are lipid vesicles composed of phospholipids and surfactants such as bile salts, they have better membrane flexibility and permeability compared to conventional ones due to the presence of bilayer softening component [43]. The presence of bile salts make them brilliant carriers for drugs of poor water solubility. However, flexible liposomes (FL) suffer from poor stability and structural deformability upon oral administration. Thus, surface modification is proposed to enhance its structural stability. Silica coating is considered a promising coating to FL as it is biocompatible and inexpensive, in addition to its protective effect against acidic environment of the stomach. Curcumin loaded FL had smaller particle size (91 nm) than silica coated liposomes (157 nm). The encapsulation efficiency of FL was 93.28% while that of silica coated one was 90.62% (based on curcumin value in FL). According to the authors silica coated liposomes showed more sustained release in intestinal environment than uncoated ones. In addition to greater decrease in the amount released in gastric media due to protective effect of silica coating. Silica coating also increased the stability of liposomes as indicated by less increase in particle size after storage at room temperature and at 4 °C relative to the high increase in FL particle size under the same conditions. Bioavailability studies demonstrated delayed peak of curcumin plasma concentration of silica coated liposomes compared to uncoated FL (3 hours versus 0.75 hour). Silica coated FL revealed higher plasma concentration (446.66 ng/L) than uncoated FL (128.78 ng/L) [43].

2.2.3 Polymeric Nanoparticles and Micelles

Biodegradable polymers, both synthetic and natural, have been widely applied in drug delivery systems due to their biocompatibility, high drug loading capacity and versatility of their physicochemical properties. Additionally, polymeric nanoparticles have the ability to provide both systemic and localized drug delivery. In consequence of these properties, many polymers have been used to improve the therapeutic properties of different drug moieties such as curcumin. Chitosan, alginate, starch and gums are natural polymers that have been studied for

the preparation of curcumin oral dosage forms, while polyvinyl alcohol and poly(lactic-co-glycolic acid) are synthetic biodegradable ones that have been used in formulation of curcumin loaded polymeric nanoparticles. Some studies have used blends of natural and synthetic polymers to improve their drug delivery properties such as the study by Umesh et al in 2011 in which chitosan-PVA blends together with Cloisite 30B were used to prepare curcumin controlled release system [44]. The polymers blended film was prepared by solvent casting using different ratios of the polymers while the curcumin loaded polymer/clay nanocomposite was prepared by emulsion/solvent evaporation using different curcumin concentrations. The effect of pH on the percentage cumulative release of curcumin from chitosan/PVA blends with 2.5% Cloisite 30B was investigated. The study revealed that increasing pH from 1.2 to 7.4 increased the percentage of drug released. Additionally, increasing drug contents could increase the percentage of drug released in pH 7.4 media. In another study in 2011, Anitha et al used a blend of chitosan and dextran sulfate polymers to overcome the pharmacokinetic obstacles of curcumin [45]. The nanoparticles were prepared by co- acervation technique that involves the interaction **be**tween the oppositely charged polymers to allow the adjustment of the nanoparticles size and surface charge by changing the polymers concentration and reaction conditions. This system could produce nanoparticles with 74% entrapment efficiency and 4.4% loading efficiency. The drug release study showed a burst release in the first 3 hours at both pH 5 and pH 7.4, however the release was faster in acidic one [45]. Although the rapid release in acidic media seems beneficial for the accumulation of the drug in tumors which mostly have microenvironment of acidic pH, this would represent a disadvantage for orally administered formulations. These need to be delivered to the intestine where they are to be absorbed, or where they would exert their effect, needing protection from the acidic stomach medium.

According to Weitong et al, curcumin loaded on chitosan (CS) nanoparticles were prepared by using modified ionotropic gelation [46]. Sodium tripolyphosphate (TPP) was used as the cross-linking polyanion. The authors adjusted the CS:TPP ratio to 3:1 and the drug : carrier ratio to 1:8 to get the maximum entrapment efficiency of the system. At these ratios the EE was 84.2±2.5% and the drug loading was 13.7±0.12%. The release study was carried out under sink condition using a phosphate buffered saline solution of pH 7.4 and sodium dodycyl sulfate (SDS) as a solubilizing agent for curcumin. This study revealed a double phase

release pattern in which 50% of the drug was released during the first 2 hours followed by a slower release plateau during the subsequent 8 hours (2-10hours) with 99% of the drug released by the end of this time period. The release during the first 2 hours was attributed to unloaded drug molecules on the surface of the nanoparticles and the leakage of the drug through the netted-porous structure of the system. Applying mathematical modelling, it was found that the controlled release was achieved by both diffusion and solubilization of the cross-linked system [46].

Natthakitta et al reported the loading of curcumin on the monoplymeric system of ethycellulose (EC) and the dipolymeric system of EC and methylcellulose (MC) by using the solvent displacement technique [47]. The two systems demonstrated high entrapment efficiency (EE), 91.2 ±1.7% and 95.4% ±2.9% for curcumin-ethylcellulose (C-EC) and curcumin-ethylcellulose/meyhylcellulose (C-ECMC) respectively. Additionally, the two systems demonstrated very high loading capacity ranging from 47.7 to 48.8%. The authors mentioned that using MC in ratios less than 50% would not affect either EE or loading capacity significantly. Additionally, the particle size of the dipolymeric conjugate (117.1±92.5 nm) was found to be less than that of monopolymeric conjugate (281.2±92.9 nm) as measured by SEM. The release studies for the two systems were done in both (simulated gastric fluid (SGF) (pH1.2) and simulated intestinal fluid (SIF) (pH 6.8) and the amount released was less than 10% indicating that the curcumin structure was not altered and retained its insolubility in aqueous media. However, in SGF, the release was faster for C-ECMC than C-EC [47].

In 2009 Anindita and Jamboor formulated curcumin loaded poly (lactic-co-glycolic acid) nanospheres by solid/oil/water solvent evaporation [48]. The optimized formulation resulted in nanospheres of particle size ranging from 35 to 100 nm, a percentage yield of 92.01±0.14% nm and an encapsulation efficiency of 90.88±0.14%. The TEM images depicted spherical and smooth nanospheres with a uniform size distribution. The authors used the confocal laser scanning microscope to evaluate the drug distribution within the nanospheres and the images demonstrated uniform distribution. The release study was carried out over a period of 10 days in phosphate buffer (pH 7.4) and resulted in an initial release of curcumin (13%) within the first

hour followed by slow controlled release with a total amount of 65% during the whole period of study [48].

2.2.3.1 Alginate Based Curcumin Nanoparticles and Micelles

One of the widely used polymers in the preparation of novel drug delivery systems is alginate because it is a hydrophilic biocompatible and biodegradable polymer. It consists of alternating blocks of β-D-mannuronic acid and α-L-guluronic acid in addition to regions of alternating units of the two monomers. The polymer units are connected to each other with 1-4 glycosidic linkage. Alginate can be used alone, in conjugation with other polymers and/or with other nanomaterials such as clay in the preparation of drug delivery systems [15], [16], [20]. In this section the use of alginate either alone or with other polymers for the development of curcumin loaded oral formulation will be discussed. The use of alginate with clays in general and montmorillonite particularly for the loading of different drugs moieties for oral administration will be discussed in the next section.

Dey and Sreenvasan developed alginate-curcumin (Alg-Cur) conjugate via an esterification reaction, after the activation of the C-6 carboxylate group of the hydrophilic alginate by 3-dicyclohexylcarbodiimide (DCC) and 4-dimethylaminopyridine (DMAP) to allow it to interact with the hydrophobic curcumin molecules [49]. The conjugate demonstrated self-assembly activity and formed nanosized micelle structure with improved curcumin solubility and potential cytotoxicity. The formation of Alg-Cur conjugate was demonstrated by IR studies which revealed the appearance of sharper and shifted O-H stretching vibration at 3441 cm^{-1} in the conjugate spectrum compared to that of alginate O-H stretching vibration which occurs at 3421 cm^{-1} due to the presence of phenolic OH of curcumin. The conjugate spectra also showed the stretching vibration of the curcumin enol group at 1617 cm^{-1}. The formation of ester linkage in the conjugate is verified by the appearance of the two stretching peaks at 1658 and 1217 indicating C=O and C-O bonds respectively. The TEM images demonstrated spherical particles with an average diameter of 62.5 nm. The curcumin content of the conjugate was presented as the degree of substitution which is the number of curcumin ester linked to hexuronic acid residues of alginate and it was 0.5%. Conjugate aqueous solubility was found to be more than 10 mg/ml, indicating a curcumin solubility of 109µg/ml. Additionally the conjugate demonstrated an improvement of curcumin stability in phosphate buffer compared to pure curcumin. This was

explained as due to the inclusion of curcumin in the core of the conjugate micelles protected by the alginate shell from the hydrolytic degradation [49].

In 2013 Alessandro et al formulated polyelectrolyte complexes of alginate and two types of N-trimethyl chitosan, of different quaternization degrees (DQ) [50]. This was carried out at pH values of 2, 7 and 10. The polyelectrolyte complex (PEC) between the alginate and the N-Trimethyl chitosan with a DQ of 20 mol% at pH 2 lead to the formation of beads of an average diameter of 0.1-0.2 mm (TMC20/Alg). The formed beads were used for curcumin loading by dispersion in a curcumin solution. The curcumin was believed to have transformed with loading from the crystalline to the amorphous or disordered crystalline phases. This transformation indicated the well dispersion of curcumin in the beads, which in consequence slowed down its degradation and enhanced its bioavailability. The loading efficiency of the beads was claimed to be 82% and about 80% of the loaded amount was released during the first hour in SIF, without enzymes, while 21.6% only was released during the same time period in SGF, without enzymes. The release study showed a burst release of curcumin in both media during the first 15 mints (19.4% in SGF and 36% in SIF), which was attributed to the adsorbed curcumin on the surface, as well as the increased dissolution rate of the polymers near the surface leading to release of the entrapped curcumin. This was supported by the swelling of the beads in the release media due the hydrophilicity of the alginate polymer. The total amounts released in 24 hrs were 100% and 30% in SIF and SGF respectively [50].

In 2011, Song et al investigated the effect of the type and amount of food emulsifiers on the loading and release of curcumin from calcium alginate beads [51]. The study used two sets of food emulsifiers: Span-80 and Tween-80 on one hand and Q-12A and F-18A on the other hand. Generally, the loading efficiency and release profile could be controlled by controlling the emulsifiers' ratio in case of Tween-80/Span-80 systems, in contrast to Q-12A and F-18A systems where this was not the case. This was attributed by the authors to the stronger interaction between alginate and Q-12A and F-18A systems and as indicated by FTIR studies. The authors could decrease the burst release of curcumin from Alginate/Span-80/Tween-80 (A/S/T) beads from 28.8% to 6.9% by increasing the amount of Span-80 from 0.2% to 0.6% at constant concentration of Tween-80. Additionally, the increase in Span-80 concentration led to the prolongation of the release time and the increase of the total amount of released curcumin to be

about 100%. At 2% Tween-80 and 0.6% Span-80 the loading efficiency was maximum (91.69%) and the beads structure was smoother and denser in SEM images [51].

Alginate was used, together with chitosan (CS) and Pluronic F127 (PF 127), in a tripolymeric composite by Utpal et al for the encapsulation of curcumin with the aim of improving its encapsulation efficiency and release kinetics [52]. The composite was prepared by ionotropic pre-gelation followed by polycationic cross-linking and the composite's parameters were compared to those of the dipolymeric composite of alginate and chitosan. An enhancement in encapsulation efficiency of 5 to 10 folds was observed by the addition of pluronic F127. In contrast to the tripolymeric system, which demonstrated an increase in encapsulation efficiency with increasing curcumin concentrations, the dipolymeric system showed a decrease in encapsulation efficiency with increasing curcumin concentrations. However, the increase in encapsulation efficiency in the tripolymeric system was reversed at a curcumin concentration of 1mg. Additionally, the use of pluronic F127 led to a uniform size distribution of the nanoparticles with a mean size of 100±20 nm. As for release, the tripolymeric system showed slow release for 96 hours as well as controlled release pattern: 36% was released during the first 12 hours then this increased to 51% in 24 hours and ended up with maximum of 75% released after 96 hours. This prolonged release period is claimed to be effective for passive targeting of cancerous tissues by extending the time of drug in circulation. The release mechanism was described by the power law model, indicating diffusion controlled and swelling controlled drug release mechanisms for the tripolymeric system. Replacement of pluronic F127 with carrageenan, a hydrophilic polysaccharide, was carried out by Diana et al in order to enhance curcumin aqueous stability [53]. The investigators tested the effect of carrageenan on the morphology and curcumin release from chitosan/alginate microparticulates and the effect of drying methods on these parameters. The addition of carrageenan was found to produce less compact microparticulates due to its weaker ability to form cross linked network compared to alginate. This weakness in network led to the increase of curcumin amounts released from the tripolymeric system as compared to the alginate system: the replacement of 50% of alginate by carrageenan increased the amount released from 38% to 96% in case of freeze-dried samples and from 39% to 48% in case of air-dried samples. The enhancement of the amount of curcumin released from air-dried samples was less than that from freeze-dried samples due to the higher compactness of the microparticulates produced by the former method. For the freeze-dried

sample that contained 50% carrageenan, a complete erosion of the microparticulates after 7 hours in SIF was observed. This suggested that the release was controlled by matrix degradation rather than matrix swelling [53].

Comparing the two polymeric systems of Utpal et al and Hugh et al reveals that the use of pluronic F127 with alginate and chitosan would produce nanosized particles with more prolonged release pattern, while using carrageenan with alginate and chitosan produces larger particles (microparticles) with higher release (freeze dried samples) in a shorter time span. Pluronic F127 showed diffusion and swelling release mechanisms while carrageenan demonstrated drug release by matrix erosion and hydrogel degradation.

2.3 Biopolymer-Clay Nanocomposites

For decades biopolymers and clay minerals have been used separately in pharmaceutical industry and played many roles in drug delivery systems. However, development of new systems that are capable of delivering adequate amounts of the drug to the specific site of action during the whole period of treatment could not be achieved using only one type of material. Consequently, the combination of two materials or more was used for the improvement of physicochemical properties in order to meet the needs of new drug delivery systems. Of these combinations, biopolymers and mineral clays are considered strong candidates to develop successful controlled drug delivery system. The addition of clay to biopolymers could improves the latter's bio adhesion, swelling, rheological and mechanical properties. On the other hand, biopolymers can enhance the clays' dispersion, stability and drug adsorption capacity [9], [12], [25].

2.3.1 Montmorillonite-polymer nanocomposites as drug delivery system

Montmorillonite is a smectite clay composed of an aluminum (Al)-octahedral sheet sandwiched between two silicate-tetrahedral sheets and has net negative charge. MMT has been widely used in pharmaceutical preparation because of it versatile properties. It has large specific surface area, cation exchange capacity and adsorption capacity that make it a good detoxifier, adsorb toxins from the body [31], [54]. Additionally, MMT has good mucoadhesive properties that make it a good drug carrier that allow the drug molecules to pass through the mucus membranes in the gastrointestinal tract and consequently help improve their bioavailability. Moreover, MMT is nontoxic and biocompatible with good drug controlled release properties [54]. MMT has been widely used for modified drug delivery system either alone or with polymers. MMT has been

used for loading of different types of drugs such as ibuprofen, 5-fluorouracil, promethazine chloride and buformin hydrochloride [31].

Salcedo et al (2014) prepared oxytetracycline-loaded chitosan/MMT nanocomposite with improved drug bioavailability [55]. The authors tested the nanocomposite permeability across Coca-2 cell line and the results showed good permeation of the drug molecules in the cells and an increase of the amount permeated along the study time (3hrs) in contrast to the drug alone which shows constant amount permeated at the same time period. This was explained by the ability of the nanocomposite to protect the drug molecules from transport efflux of P-glycoprotein which limit the permeability of drug molecules. Additionally, the oxyteteracycline-loaded chitosan/MMT nanocomposite showed good biocompatibility as evaluated by an MTT test, in which the cell viability is tested by measuring the amount of MTT metabolite. The MTT test showed insignificant difference between control and all tested samples. Thermal analysis of the prepared samples showed improvement of chitosan thermal stability by the formation of polymer clay nanocomposite and this is attributed to the intercalation of the polymer molecules in the clay interlayer that delayed polymer dehydration to above 200 ˚C instead of 120 ˚C. XRD results showed an increase in the MMT basal d-spacing from 12.0Å to 13.2 Å for the unloaded nanocomposite, indicating chitosan intercalation. For the oxytetracycline-loaded nanocomposite, the increase in MMT d-spacing was up to 15 Å indicating the intercalation of the drug molecules in the clay interlayer. These results were further confirmed by FTIR and zeta potential analysis which indicated the presence of electrostatic interaction between the positively charged amine groups of chitosan and the negatively charged sites on the MMT interlayer spaces and the coverage of clay particles with some of the ionized polymer molecules [55].

Anirudhan et al developed MMT/chitosan nanocomposites for the controlled delivery of paracetamol [54]. The authors used chitosan coated magnetic particles to provide magnetic drug targeting and to improve the chemical and physical properties of both the magnetic particles and the polymer. Polymer-coated magnetic particles have good dispersion and high stability against oxidation on one hand and higher drug loading capacity than the polymer on another hand. The authors also improved the solubility of chitosan at neutral and alkaline pH by chemical interaction with succinic anhydride to form N-carboxyacyl chitosan. Consequently, N-carboxyacyl chitosan could be used for the delivery of drugs at neutral and basic environments in

addition to its long-term retention in the body which allow its application in sustained delivery of drugs. The authors first prepared magnetic iron nanoparticles by chemical precipitation then the magnetic particles were coated with chitosan by reverse-dispersion cross-linking. Afterward the outer layer of chitosan molecules was chemically modified by interaction with succinic anhydride. Subsequently, the formed N-(carboxyacyl) chitosan coated magnetic particles were intercalated into the MMT's interlayer spacing to form the nanocomposite that is used for drug loading. The loading process of paracetamol molecules was carried out at different pH values to get the maximum drug loading. The XRD and the FTIR results demonstrated the successful coating of the magnetic particles with the chitosan molecules and then their intercalation into the MMT interlayers. The SEM images also confirmed the formation of the supposed nanocomposite structure. The experiments revealed that the maximum loading was 84.6% at initial concentration of 200 mg/L and 96 % at initial concentration of 100 mg/L and both were achieved at pH 6. These results were attributed to the electrostatic interaction between the drug and the nanocomposites' functional groups at different pH values. Not only the drug loading capacity was found to be pH sensitive but so were the nanocomposite swelling and the drug release properties. The swelling was up to 95% after 3 hrs at pH 7.4 and only up to 58% at pH 1.4. Additionally the cumulative drug release was 85% after 10 hrs at pH 7.4 while at pH 1.4 was only 64%. The release data revealed that the release mechanisms is swelling and diffusion controlled [54].

Shuibo Hua et al. also used chitosan/MMT nanocomposite as carrier system for the antibiotic drug ofloxacine [56]. The authors used solution intercalation for system preparation and studied the effect of increasing the clay content on the entrapment efficiency and drug release. Increasing the amount of MMT from 0g to 5g was found to increase the entrapment efficiency from 31.2% to 83.5%. This improvement in entrapment efficiency was attributed to the intercalation and adsorption of the drug molecules into the clay interlayer spaces and on its surface. This was confirmed by the XRD spectra which revealed an increase in the montmorillonite d-spacing from 1.32 nm to 2.4 nm after the addition of the drug. Additionally, the enhancement of the entrapment efficiency was accounted to the increase of the system viscosity after the addition of the clay and consequently decrease the leakage of drug out to the solution. The release study also showed decrease in cumulative drug release in both simulated gastric and intestinal fluids by increasing the montmorillonite content [56].

The development of orally-controlled release system for propranolol hydrochloride, an antihypertensive drug, would minimize the dosing frequency and improve patient compliance [57]. Consequently, many studies were performed to compensate the short half-life of propranolol and hence maintain the therapeutic concentration through the least dosing frequency. Seema (2013) developed propranolol loaded poly lactic-co-glycolic acid nanoparticles and MMT/poly lactic-co-glycolic acid nanocomposites as controlled delivery systems of propranolol [57]. The authors used emulsion/evaporation for the preparation of two carrier systems and the non-ionic Pluronic F68 co-polymer as emulsifier and stabilizing agent. The authors reported an increase in the percentage of drug encapsulation efficiency from 18% to 77% by increasing the ratio of the drug to clay from 1:1 to 3:1. This increase in drug encapsulation efficiency is explained by electrostatic interaction between the cationic drug and the anionic clay and polymer of the nanocomposite. The XRD results revealed that drug/polymer moiety was intercalated between the MMT interlayer spaces at low drug ratio (1:1 drug to clay) which resulted in increase in d-spacing from 13.6 A° to 21.4 A°. However, at higher drug to clay ratios of 2:1 and 3:1, the XRD spectra demonstrated exfoliation of the MMT layers and this is explained by the increase in drug encapsulation at a higher drug ratio as higher surface area of the MMT was available for drug adsorption The exfoliation of the nanocomposite at high drug ratios was further confirmed by the increase in weight loss during the thermal gravimetric analysis compared to the nanocomposites of low drug ratio as in the latter case the polymer/drug moiety were protected from thermal degradation by the clay ordered lattice. The release study showed that the presence of MMT increased the amount of drug released (up to 72% in case of 3:1 drug to clay ratio) in simulated intestinal buffer pH 7.4 over a period of 8 hours compared to drug-polymer nanoparticles (only 28% were released during the same time period). This was due to the increase of the surface porosity of the system by the presence of clay platelets on the surface of the nanocomposites. [57].

Jain and Datta reported the loading of Venlafaxine, a hydrophilic antidepressant drug, on the same clay-polymer system [58]. They studied the effect of the concentration of both the stabilizing agent (Pluronic F68) and the clay on drug loading and drug encapsulation efficiency and used XRD and TEM techniques for the characterization of the formed nanoparticles and nanocomposites [58]. The drug encapsulation efficiency calculations showed that increasing the PF68 concentration from 0.04mM to 0.12 mM enhanced the EE% from 4% to 85% and this was

attributed to formation of more stable emulsion due to the increase in surfactant concentration. However, a further increase in the surfactant concentration up to 0.24 mM decreased the EE% to 75%. Additionally, increasing the MMT concentration from 5 to 10 mg increased the EE% from 12.38 to 88.8%. However, increasing the clay content above 10 mg showed a decrease in EE% and this was attributed to the decrease in the surfactant concentration by interaction with the platelets of the clay leading to the leakage of the drug to the outer aqueous layer. Regarding the characterization of the formed nanoparticles and nanocomposites, the XRD spectra revealed the increase in the d-spacing of clay interlayer which was attributed to the intercalation of the drug-polymer moiety. Additionally, the XRD spectra of the nanocomposites confirmed the presence of the drug and polymer by the appearance of the sharp peaks of crystalline drug and broad hump in the region of 2θ from 10.5° to 25° of the polymer. The in vitro release study indicated that the presence of the MMT can effectively decrease the initial drug burst release (within 0.5 hr.) and provide a longer cumulative drug release period in both the gastric pH 1.2 and intestinal pH 7.4 media for 27 and 12 hrs respectively. The authors suggested that MMT layers provide a longer path for the drug to come out of the nanocomposite structure leading to the decrease in the initial burst and to longer drug release pattern [58].

Venlafaxine was also loaded on MMT by the ion exchange method and then coated by polyvinylpyrollidone as reported by Patel et al. in 2011 [59]. The authors confirmed the entrapment of the drug and polymer molecules into the clay interlayers through XRD analysis, which revealed an increase in the clay d-spacing. The in-vitro release study showed a higher increase in the percentage of drug released in simulated intestinal fluid compared to simulated gastric fluid for both polymer coated and uncoated samples [59].

2.3.2 Alginate Montmorillonite Nanocomposites

The combination of alginate as a polymer matrix and montmorillonite (MMT) as a nanosized filler material was used by numerous pharmaceutical researchers**,** due to the ability of this nanocomposite to enhance both the physicochemical properties of the carrier substances and the therapeutic and pharmacokinetic properties of the loaded drugs. Many studies were conducted to formulate drug loaded alginate/montmorillonite nanocomposites with the aim of investigating the effect of the formulation variables on both the drug loading efficiency and the drug release kinetics.

In 2010 Kevadiya et al formulated diclofenac sodium loaded alginate MMT nanocomposites and studied the effect of increasing MMT content on beads diameter, encapsulation efficiency and total amount of drug released in SIF (pH 7.4) and SGF (pH 1.2) [60]. Increasing the MMT content led to the increase in beads diameter up to 0.85 mm and encapsulation efficiency to 82.84%. The latter was explained by the increase in hydrogen bonding between diclofenac sodium and hydroxyl groups of MMT. For the release profile in SGF (pH 1.2) only 1-2% diclofenac sodium was released from all formulations after 8 hours. On the other hand, the total amount of diclofenac sodium released in SIF (pH 7.4) increased with increasing MMT content. The maximum amount released in SIF was 62.49% within a period of 8 hours, while in case of diclofenac sodium alginate beads (with no MMT) the maximum amount released was 17.7% after the same time period. The negative charge on both diclofenac sodium and MMT led to weak interaction between them and a consequent increase in the rate of diclofenac sodium release in case of high MMT content [60]. Kevadiya et al also reported the loading of an antiarrhythmic local anesthetic drug, Lidocaine HCl, on MMT only and alginate/MMT nanocomposite [61]. This demonstrated the efficacy of nanocomposites in improving the release kinetics of the drug. XRD spectra indicated the intercalation of the drug into the MMT interlayer spaces, with an increase in the d-space from 1.18 nm for the MMT to 1.80 nm for the drug/MMT hybrid. The rate of drug release after both 10 and 20 hours improved: for the first 10 hours the total amount released was 83%, 60% and 37%, while after 20 hrs the total amount released were 83%, 65% and 49% for the free drug, drug/MMT hybrid and drug/MMT- alginate nanocomposite respectively. Additionally the release plateau was achieved more rapidly in case of the drug/MMT hybrid than in case of the drug/MMT-Alginate nanocomposite [61].

One of the promising applications of alginate/MMT nanocomposites is their potential for the oral delivery of intact proteins to the intestine without degradation by the acidic environment of the stomach. Consequently, many attempts were carried out to load proteins on this system. Kaygusuz et al encapsulated bovine serum albumin as a model protein in alginate/K10 MMT (synthetic MMT activated with mineral acid) nanocomposites in 2013 [11]. The intercalation was achieved by simple stirring of the protein in the clay suspension, and was indicated in an increase in d-space of the MMT from 12.8nm to 32.2 nm in XRD spectra. Morphologically, the addition of MMT to alginate could maintain the spherical shape of the beads after drying rendering them denser, rougher and without gaps on the surface. These changes in bead

morphology explained the improvement in the entrapment efficiency and release kinetics for the alginate/MMT nanocomposites compared to beads of pure alginate. An increase of protein encapsulation efficiency-from 40 to 78% with the increase in MMT content from 0 to 2% was observed. For the release in SGF without pepsin immediate release of up to 27% of the protein was observed for the alginate beads after 90 minutes. On the other hand, the release from the nanocomposite started after 90 minutes and the maximum amount released after 2 hours was 13%. This slower release was explained by the interaction between the protein and the MMT which controlled the rate of release rather than the swelling ratio. In SIF, protein release from all types of beads was very high due to the high swelling of alginate polymer in basic media but the rate of release from nanocomposites was slower than that from alginate beads due to the interaction between the protein and MMT. According to the authors, the release kinetic of the protein could be explained by the Ritger and Peppas model, indicating that the release of bovine serum albumin from the nanocomposite was by both diffusion and erosion mechanisms (non-Fickian transport) while the release from pure alginate beads was only due to an erosion release mechanism [11].

Improvement of the pharmacokinetic properties of chemotherapeutic and chemopreventive drugs through loading on alginate/montmorillonite systems is of one of the promising applications of nanocomposites. Consequently, many studies have been conducted to achieve this goal such as the study done by Iliescu et al to prepare irinotican loaded MMT/Alginate nanocomposites [62]. Iliescu et al prepared the irinotican loaded system to be used intra-operatory chemotherapy colorectal carcinoma after cytoreductive surgery. The characterization of the formed nanocomposites by XRD and FTIR revealed the intercalation of the drug molecules into the clay interlayer with some of drug adsorbed on the surface of the clay lamella. However, the alginate molecules are shown to interact with the clay surface through hydrogen bonding and electrostatic interaction. The authors tested the effect of the drying technique on the beads morphology through scanning electron microscopic imaging. The SEM images revealed that freeze drying technique protected the beads from shrinkage and consequently the size of beads is the same as before drying. Additionally, the freeze drying technique retained the uniform spherical shape of the beads and gave them a stratified surface. The freeze drying process formed cell-like structured beads that have better swelling capacity and slower drug release rate. The migration of drug molecules to the beads' surface is hindered by freeze drying. The in vitro release study

showed decrease in the amount and rate of drug released in simulated intestinal fluid in both irinotican/montmorillonite hybrid and irinotican/montmorillonite/alginate nanocomposites compared to the pure drug. However, the nanocomposite demonstrated slower rate of drug release than the hybrid which is attributed to the electrostatic and intermolecular hydrogen bonding between alginate and the clay in the hybrid, in addition to the drug intercalation into clay inter layer [62].

Procainamide is an antiarrhythmic drug that has short life time in vivo and to attain the therapeutic level it should be administered 3 to 4 times daily. This high dosing rate is against patient compliance and consequently preparation of controlled release formulation is highly recommended. Kevadiya et al addressed this issue by intercalating Procainamide into MMT followed by compounding the formed hybrid with alginate and coating the resulting beads with chitosan [10]. The prepared nanocomposite decreased the drug release in gastric environment from 38% for the Procainamide/MMT hybrid to 11% for the chitosan-coated alginate nanocomposite and allowed the controlled release of the drug in an intestinal environment. The maximum amounts of drug released were 31% and 25% after a time period of 70 hours from the Procainamide/MMT hybrid and the chitosan-coated alginate nanocomposite respectively. Applying different kinetic models to the release study results revealed that the drug release from the chitosan-coated alginate nanocomposite was by anomalous diffusion, while its release from the MMT interlayer was diffusion controlled. The authors studied the effect of different preparation parameters on the drug encapsulation efficiency such as the interaction time, pH, temperature and the drug concentration. The optimum interaction time was 3 hours to get a maximum of 24.4% of the drug intercalated into the clay interlayer while the reaction temperature insignificantly affected drug intercalation. The Procainamide intercalation into the clay interlayer followed an ion exchange mechanism, so changing the drug charge would affect the intercalation process. Consequently, the pH of drug solution had a crucial role in drug intercalation. At a pH range of 4 to 9 the amount of intercalated drug remained constant and decreased out of this range. The authors explained the decrease in drug intercalation at pH below 4 by the competition between cationic drug and H^+ for the MMT cation exchange sites, while at pH above 9 the intercalation decreased due to the increase in the number of uncharged species of procainamide. Additionally, the drug concentration played a role in drug intercalation, reaching an equilibrium at a concentration of 244 mg of Procainamide per one gram of MMT [10].

3 Theoretical background

3.1 Spectroscopy

Spectroscopy refers to the interaction of investigated material with electromagnetic radiation. Different classifications are used to describe this interaction, such as atomic and molecular spectroscopy, and which depend on the nature of the investigated material. Spectroscopy techniques are also described based on the change monitored during the process, leading to absorption and emission spectroscopic techniques [63]. Figure 3-1 summarizes the different spectroscopic techniques typically used.

The following two sections will address both visible and infrared spectroscopy. Visible spectroscopy is applied throughout the work to measure the amount of curcumin loaded and/or released while infrared is used to identify and confirm the interaction between the different components of the prepared system.

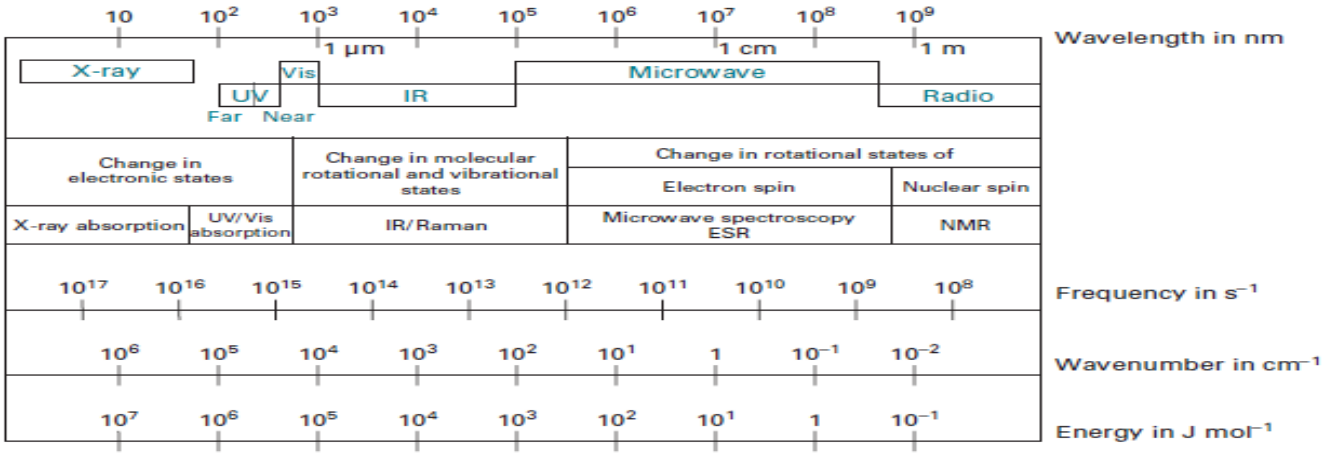

Figure 3-1: Different spectroscopic techniques and the corresponding energy changes occurring along the electromagnetic spectrum. [63]

3.1.1 Visible Spectroscopy

The absorption of visible electromagnetic radiation leads to electronic excitations and the change in the electromagnetic radiation after passing through the test sample is described by two terms, transmittance and absorbance. Transmittance is defined as the ratio between the power of radiation coming out of the sample (P_T) and that of the radiation source (P_0). Multiplying this ratio by 100 gives the % transmittance as shown in equation 3-1.

$$\%T = \frac{P_T}{P_0} \qquad \text{Equation 3-1}$$

The amount of absorbed radiation, as measured by Absorbance (A), is linearly dependent on the concentration of the absorbing species in a sample, and is calculated from the % transmittance according to equation 3-2.

$$A = -\log \%T = -\log \frac{P_T}{P_0} \qquad \text{Equation 3-2}$$

Absorbance is used to quantitatively determine concentration of the measured sample according to the Beer Lambert law expressed in equation 3-3.

$$A=abc \qquad \text{Equation 3-3}$$

where A is the absorbance, a is the molar absorptivity of the sample (a constant for each substance), b is the path length of the beam through the sample cell and c is the sample concentration. The linearity between Absorbance and concentration is true within a limit of concentration. It can be used to determine unknown concentrations based on pre-constructed calibration curves[64].

3.1.2 Infrared spectroscopy

Infrared (IR) spectroscopy is used in structural determinations of compounds. For a given species to absorb IR radiation, the radiation would need to lead to a vibrational excitation resulting in a change in the dipole moment of the species. Different vibrational modes can occur in a species, categorized into stretching and bending modes. A stretching vibration encompass continuous change in the distance between the centers of two atoms along the axis of the bond between them and it can symmetric or asymmetric vibration. On the other hand, bending vibration involves changes in the bond angle and sub divided into scissoring, rocking, wagging, and twisting vibrations [65].

Considering the vibration motion as harmonic oscillator, the vibrational energy of any molecular vibration can be expressed by equation 3-4.

$$E = (v + 1/2)\,(h/2\pi)\,\sqrt{k / (m1m2/m1 + m2)} \qquad \text{Equation 3- 4}$$

Where: v = vibrational quantum number (positive integer values, including zero, only), h = Planck's constant, k = force constant of the bond, and m1 and m2 = masses of the individual atoms involved in the vibration.

Accordingly, the vibrational energy is directly proportion to bond strength and inversely to the mass of the individual atoms/functional groups involved in the vibrational motion.

The absorption of IR radiation would take place if it results in a change of vibrational modes with a subsequent change in the dipole moment of the species. This would appear on a IR spectrum as an absorption peak occurring at the frequency value corresponding to this vibrational mode. Analysis of a spectrum with the different absorption peaks gives indications of the different functional groups present in a species, thus providing valuable structural information. Shits in frequency values of vibrational modes can indicate interactions between functional groups present in a sample [65].

3.2 X-Ray Diffraction

X-ray is an electromagnetic radiation with short wavelength ranging from 1^6 nm to 10 nm and high energy that is used in X-ray diffraction (XRD) for the determination of the crystal structure parameters such as the measurement of the unit cell dimensions. X-ray is produced when high energy electrons hit a target metal such as copper and remove an electron from its inner shells. Accordingly, an electron from the outer shells drops down to occupy the vacancy and this movement is accompanied by emission of x-ray radiation that is characteristic for the target metal. The wavelength of X-ray radiation is almost equal to the spacing between atoms or molecules that are arranged into a crystalline structure and consequently can be diffracted upon hitting them. The diffracted beams can interact either constructively or destructively. Constructive interference occurs if Bragg's law is satisfied. Bragg's law correlate the angle of the incident beam to the wavelength of that bean and the interlayer spacing according to equation 3-2 [66].

$$n\lambda = 2d \sin\theta \qquad \text{Equation 3-5}$$

where n is an integer number, λ is the wavelength of the incident x-ray beam, θ is the angle of the x-ray beam with respect to certain plane of the crystal, and d is the interlayer distance. According to equation 3-5, constructive interference between the diffracted x-ray beams from different planes of a crystal at angle θ only if the distance between the crystal's planes equal or

integer number of the wavelength of the incident beam (Figure 3-2). Upon applying Bragg's law, the distance between the crystal planes can be calculated if the wavelength of the used X-ray radiation and the angle of diffraction (equal to the incidence angle) are known.

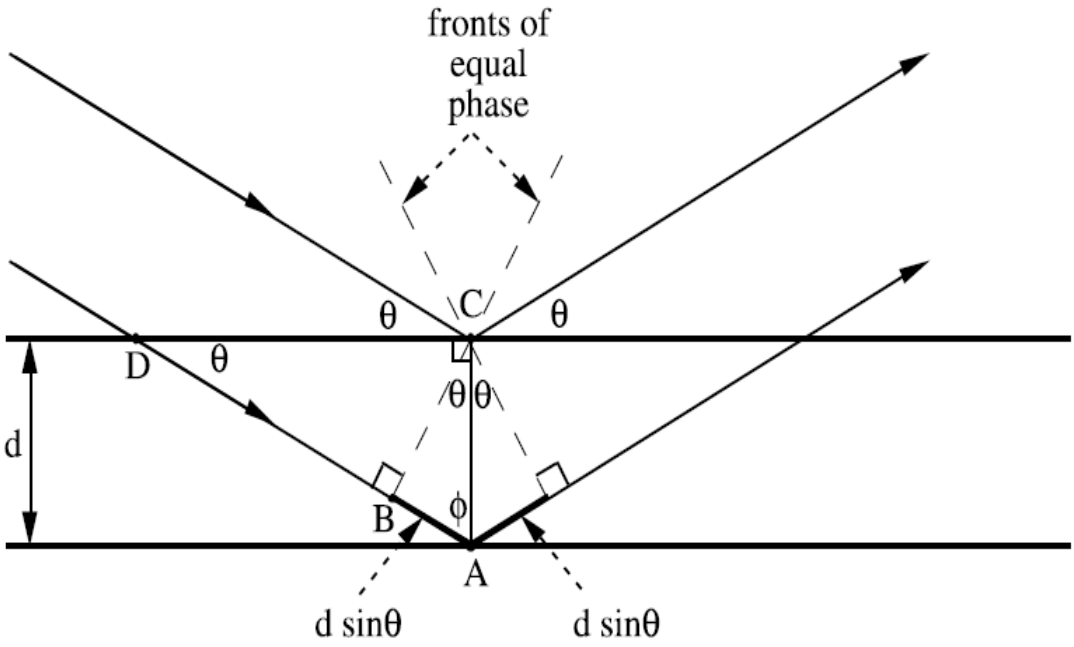

Figure 3-2: X-ray strikes crystal planes at θ and diffraction occurs when Bragg's law is satisfied. [66]

4 Material and methods

4.1 Materials

Cloisite NA+ (montmorillonite) was purchased from Southern Clay Products, INC. Alginic acid sodium salt (from brown algae -low viscosity), curcumin (from Curcuma longa-Tumeric-powder), maleic acid (purity ≥99%), sodium hydroxide (98% purity), sodium chloride (99.5% purity), potassium bromide (99.5% purity) and acetic acid (purity ≥99.8%) were purchased from Sigma-Aldrich. Calcium chloride anhydrous (approx. 95% purity) and absolute ethanol were purchased from Scharlau and Carlo Erba respectively. SIF Powder Original and SIF powder FaSSIF were obtained from biorelevant.com.

4.2 Equipment

A D8 Bruker X-ray powder diffractometer was used to obtain XRD patterns for the samples. A Thermo-scientific Nicolet 380 Fourier Transform Infrared spectrometer was used for the infrared spectra of samples, and a Spectronic 20D+ spectrophotometer was used for solution Absorbance measurements. Reciprocal shaking bath (Model 25) from Precision scientific Instruments, Inc., USA, was used for conducting the release studies. Heratherm Oven, centrifuge (Centrific) and pH meter (Accumet AR10) were obtained from Fischer scientific, UK. Sonicator (150HT) and Stirrer (VWR) were obtained from ETL testing laboratories, INC., USA.

4.3 Preparation of exfoliated Montmorillonite

About 5 g of the pristine clay were added to 250 ml ultrapure water and different conditions of stirring at 500 rpm or sonication were conducted in order to identify the best conditions leading to the exfoliation of the montmorillonite (MMT) clay. This was identified by the decrease of the d_{001} XRD peak of the clay, occurring at 7.1° two-theta [67]. The different conditions investigated are listed in Table 4-1.

Processed MMT clays (by stirring or sonication in water) were then filtered from the suspension in the solvent, using Whatman filter papers no. 42. The clays were then oven dried at 70°C till constant weight. The dried powder was then ground and sieved through sieve no. 45 (355 μm opening size).

Table 4-1: Conditions investigated for obtaining exfoliated MMT in water at 25 °C

Process	Time (hrs)
stirring	4
stirring	24
stirring	48
Sonication	1
Sonication	2
Sonication	3

4.4 Drug Loading in Exfoliated Montmorillonite

In order to determine the conditions for highest curcumin loading, about 5 g of the pristine and exfoliated clay was dispersed in 100 ml of drug solutions (1 mg/ml) in absolute ethanol. This was conducted at room temperature (25°C) and stirring was carried out for different times at 500 rpm. According to the result, exfoliated clay was used to determine the best loading conditions (stirring time, concentration of drug solution, and amount of clay relative to volume of drug solution). Figure 4-2 lists the conditions investigated for loading.

After stirring, the suspensions were then centrifuged for 10 mins at 700 rpm using Centrific^{TM} centrifuge, and the curcumin-loaded clay was collected after decantation of the supernatant curcumin solution, and dried for 24 hours at 50°C to produce the clay-curcumin hybrid samples. The dried hybrid samples were then sieved through sieve no. 45 (355 µm pore size).

The amounts of curcumin loaded onto the MMT clays (i.e. the amount present in a hybrid clay-curcumin sample) were determined by the difference in concentration of the curcumin solutions before and after stirring and separation of the clay, as indicated by the change in Absorbance at λ_{max} = 425 nm. A calibration curve for curcumin in absolute ethanol was used (Appendix II).

Table 4-2: Conditions investigated for loading curcumin in MMT clay at 25 °C

Stirring Time (hrs)	Curcumin Solution Concentration (mg/ml)	Amount of clay to curcumin solution (%W/V)
1	1.00	5
2	1.00	5
3	1.00	5
1	1.00	5
1	0.10	5
1	0.05	5
1	1.00	1
1	1.00	3
1	1.00	5
1	1.00	10

Entrapment efficiency was calculated by based on the amount of curcumin loaded onto the exfoliated clay according to equation 4-1:

$$EE = (Ci - CF)/Ci * 100 \qquad \text{Equation 4-1}$$

where C_i is the initial concentration of curcumin solution used for drug loading, C_f is the concentration of curcumin into the filtrate after the separation of loaded clay.

4.5 Preparation of Alginate/Hybrid Nanocomposites

Different samples of alginate/clay hybrid were prepared with variable ratios of clay hybrid to alginate solution. Generally, an alginate aqueous solution, prepared by dissolving about 2 g of alginate in 100 ml ultrapure water (2% w/v), was used to disperse a known weight of the clay hybrid (Table 4-3 lists the different alginate/clay hybrid used). The mixture was stirred at 25°C for 1 hour at 1000 rpm to ensure homogenous dispersion. The suspension was then added to a

$CaCl_2$ solution (3 g $CaCl_2$ dissolved in 100 ml of ultrapure water) using syringe with 1.5 mm opening, and MasterFlex L/S peristaltic pump with a flow rate 1ml/min. The reaction between the alginate and the $CaCl_2$ led to the formation of beads, composed of cross-linked alginate polymer containing clay hybrids. The formed beads, were allowed to cure in the $CaCl_2$ solution for 30 mins, and were then washed three times with ultrapure water. The Absorbance of the $CaCl_2$ solution was measured at λ_{max} = 464 nm at the end of the curing period and the concentration of curcumin lost in the $CaCl_2$ determined from a calibration curve for the Absorbance of curcumin in $CaCl_2$ solution. The difference between the amount of curcumin loaded on the used mass of clay hybrid (which was dispersed in the alginate solution) and that present in the $CaCl_2$ solution was considered the amount of curcumin loaded in the formed beads, as expressed by equation 4-2.

$$C_{beads} = C_{hyb.} - C_{Ca} \qquad \text{Equation 4-2}$$

where C_{beads} is mg of curcumin loaded on known weight of beads, $C_{hyb.}$ is the amount of curcumin loaded on the amount of hybrid used for the preparation of this weight of beads, and C_{Ca} is the amount of curcumin lost in calcium chloride solution during the process. However, the amount lost in $CaCl_2$ solution was less the limit of detection of the method (LOD) as calculated by equation 4-3, and using the calibration curve of curcumin in $CaCl_2$ solution. Therefore the amount of curcumin loaded into the nanocomposites was assumed to be the same as that loaded into the amount of hybrid used for the preparation of the nanocomposites.

$$LOD = (3.3 \times SD) \div b \qquad \text{Equation 4-3}$$

Accordingly, the preparation of curcumin loaded alginate/montmorillonite nanocomposites can be described through the following schematic diagram Figure 4-1

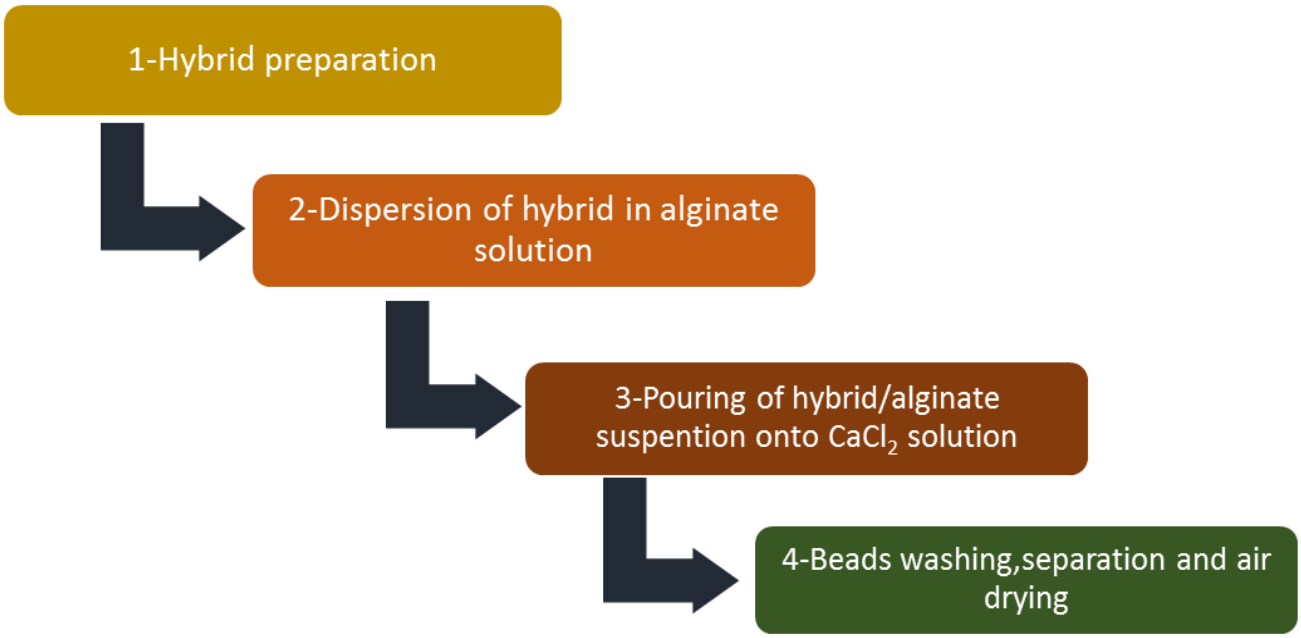

Figure 4-1: Schematic diagram representing the preparation steps of curcumin loaded MMT/Alginate cross-linked beads

Table 4-3: Prepared nanocomposites with different hybrid/alginate ratios

Hybrid/Alginate Ratio (weight/weight)	***Sample Code***
1:20	NC 1
1:10	NC 2
1:5	NC 3
1:2	NC 4

4.6 In Vitro Release Experiments

In vitro release tests were conducted using ready to use biorelevant media prepared according the manufacturer instructions (included in Appendix I). Three release tests were conducted, as follows:

- Fast State Simulated Gastric Fluid (Fast-SSG): 0.06 g of FaSSIF-original powder (previously known as SIF original) were dissolved in 1L NaCl/HCl solution of pH 1.6.
- Fast State Simulated Intestinal Fluid (Fast-SSIF): 1.79 g of FaSSIF-V2 (previously known as SIF FaSSIF-V2) by dissolving it in 1L maleate buffer of pH 6.5.
- Fed State Simulated Intestinal Fluid (Fed-SSIF): 11.2 g of FaSSIF-original powder (previously known as SIF original) were dissolved in 1L acetate buffer of pH 5.0.

The λ_{max} of curcumin in each medium occurred at different wavelength values, as listed in Table 4-4.

Table 4-4: list of λmax for curcumin in each media

Media used	***Corresponding λ_{max}***
Fasting state simulated gastric fluid	425 nm
Fasting state simulated intestinal fluid	418 nm
Fed state simulated intestinal fluid	424 nm

To ensure sink conditions (in which the saturation solubility of the drug in the dissolution medium is at least three times more than the drug concentration) [68] throughout the curcumin release runs, the maximum solubility of curcumin in each media was first determined. Maximum solubility of curcumin in each media is measured by dispersing excess amount of curcumin powder (5 mg) in known volume of the media (20 ml) and shaking the suspension in water bath shaker for 24 hours at 100 stroke/min and at 37°C. Afterwards the suspension is centrifuged for 15 min at 700 rpm. The absorbance of the supernatant is measured at the corresponding λ_{max} of curcumin in each media. The concentration is calculated based on the calibration curve constructed for curcumin in each media**.** The maximum possible amount of curcumin in any of the samples (this was in sample NC4) was used for the determination of the total volume needed for each of the release media to ensure sink conditions for a given mass of alginate beads containing the clay hybrid. Accordingly, 0.16 g of beads containing 45µg, 81µg, 147 µg and 307µg in case of NC 1, NC 2, NC 3 and NC 4 respectively were dispersed in 10 ml FaSSIF media and were shaken for 24 hours at 100 stroke/min, thermostated at 37°C. While 0.103 g beads containing 26 µg, 54 µg, 95 µg and 198 µg for NC 1, NC 2, NC 3 and NC 4 respectively

were dispersed in 10 ml FeSSIF media and were shaken for 24 hours at 100 stroke/min, thermostated at 37°C. At time intervals of 1, 2, 4, 8, 12 and 24 hours, a sample of the solution was drawn and its absorbance measured so as to determine the amount of curcumin released in the medium at the value of λ_{max} for this medium. For Fast-SSGF, with lower curcumin solubility, 0.022 g of beads containing 6µg, 12 µg, 20 µg and 42 µg in case of NC 1, NC 2, NC 3 and NC 4 respectively were dispersed in 10 ml of the medium and shaken at 100 stroke/min, thermostated at 37°C. As the average residence time of foods and drugs in the stomach is about 2 hours [69], samples of the solution were drawn at time intervals of 1, 2, and 4 hours and Absorbance measured so as to determine the amount of curcumin released in the medium at the corresponding value of λ_{max}.

4.7 Characterization

Powder x-ray diffraction (XRD) and Fourier Transform Infrared (FTIR) spectroscopy were used for the characterization of the clay, curcumin and alginate before and after every preparation step to estimate the effect of processing on their structure and interaction. UV-Vis spectroscopy, on the other hand, was used for the quantification of the amount of curcumin loaded on and released from the prepared systems.

4.7.1 Powder X-ray Diffraction

The diffractometer was run using Cu target with Kα, $\lambda = 0.1542$ nm and operated at 40 KV and 30mA. The two-theta range was between 3 and 80 degrees with step size 0.03 degrees and step time 3 seconds for all samples.

4.7.2 Fourier Transform Infrared Spectroscopy

Infrared spectra for samples were presented as plots of wave number (400500 cm^{-1}) against % transmittance. The KBr method was used where 0.2 g of KBr were thoroughly mixed with 0.002 g of sample, followed by vacuuming while subjecting the mixture to1400 kPa for 20 mins.

4.7.3 Ultraviolet-Visible spectroscopy

Absorbance measurements carried out were translated to solution concentrations using calibration curves of curcumin in the different solvents used, namely ultrapure water, absolute ethanol, $CaCl_2$ aqueous solution, and the simulated gastric and intestinal fluid solutions.

5 Results and Discussion

5.1 The exfoliation of Montmorillonite clay (E-MMT)

Pristine MMT shows XRD characteristic intense peak of (001) plane at 2theta 7.1 degree, corresponding to a d-spacing of 12.44 Å (Figure 5-1). Upon dispersing MMT in water and stirring for different time intervals different structural changes occurred as can be deduced from the XRD patterns (Figure 5-1). Stirring of MMT aqueous suspension led to changes mainly in peak's intensity of MMT and less changes in peak's position as demonstrated in Table 5-1. Stirring for 4 hours showed great decrease in (001) peak's intensity which was attributed to the exfoliation of the clay particles. However, there is slight increase in the 2 theta which may be attributed to the formation of clay aggregates with smaller interlayer spaces[70], [71]. Stirring of MMT for 24 hours led to an increase in d-spacing as well as a development in peak intensity compared to raw MMT. Increasing the stirring time up to 48 hours led to a further downshifting of the peak position to correspond to d-spacing of 15.01 Å, with a noticeable increase in peak intensity. The increase in the d spacing is probably due to the intercalation of water molecules, leading to clay "swelling". The increase in peak intensity reflects an increase in the order of clay layers. This may be attributed to the some re-stacking of MMT layers due to the presence of intercalated and absorbed water molecules, leading to increased hydrogen bonding between the water and clay layers. According to Faheem Uddin and Katti et al, increasing clay hydration leads to breakdown of clay particles followed by rearrangement of the clay platelets and this is accompanied by change in the silicate (Si-O) stretching region (1150-950 cm^{-1}) in the FTIR spectrum [30][72].

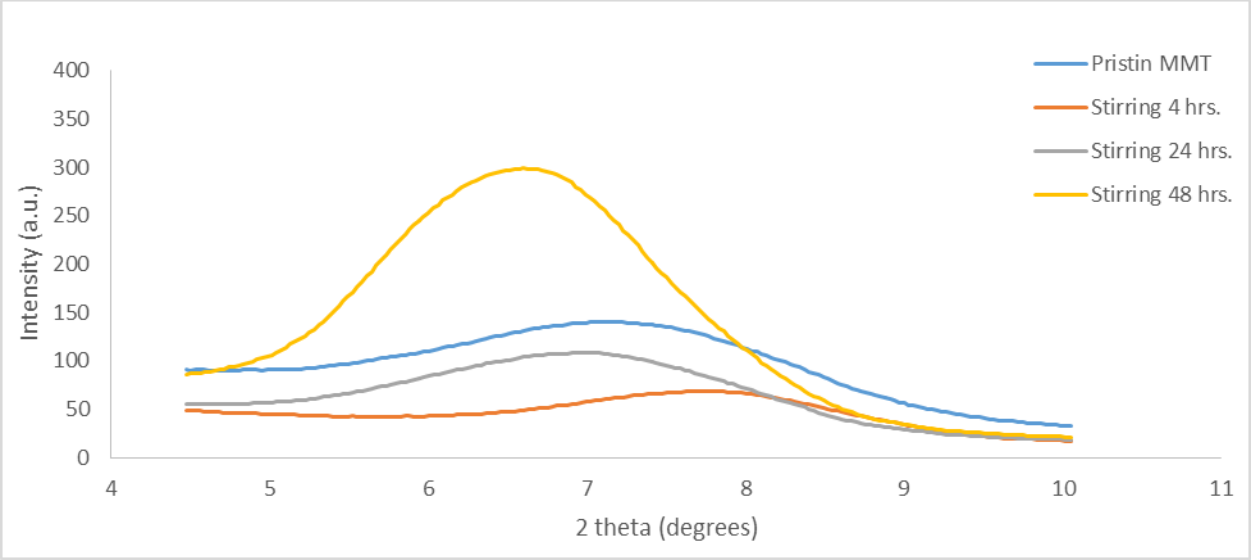

Figure 5-1: Effect of stirring time on XRD pattern of MMT suspension in water at room temperature

Table 5-1: Peak parameters of MMT after stirring in water for different time intervals

Sample	Peak position (2theta)	d-spacing	Peak intensity
1 (stirring 4 hrs.)	7.26	12.16	98
2 (stirring 24 hrs.)	6.15	14.37	137
3 (stirring 48 hrs.)	5.85	15.01	350

Sonication of MMT aqueous suspension for different time intervals (1, 2, and 3 hours) showed high degree of clay exfoliation as indicated by the great decrease in intensity of plane (001) peak in XRD pattern (Figure 5-2), together with the shift of the (001) peak intensity to lower 2theta values. This was reported previously. For example, Morgan et al achieved a complete exfoliation of MMT layered structure upon applying sonication to organic MMT suspension [73] As seen in Figure 5-2, sonication for one hour led to larger decrease in the peak intensity than two hours sonication, this may be explained by the delamination of MMT layers during the first hour followed by agglomeration of some of the dispersed layers due to the attained high surface energy by sonication. Similar observations were made for the sonication of kaolinite by Franco et al and this was explained by agglomeration of colloidal particles upon prolonged sonication [74], [5]. On the other hand, 3 hours sonication could overcome the surface energy of MMT

layers leading to further exfoliation of clay layers, as shown by an almost disappearance of the (001) peak.

It is interesting to report the difficulty in filtration of the resulting suspension by Whatman filter paper No. 42 due to the passage of the particles through the pores of the filter paper, which led to high loss of the powder into the filtrate. The passage of the clay particles through the filter paper pores may be attributed to the reduction of the particles size of clay particles due to the sonication [74].

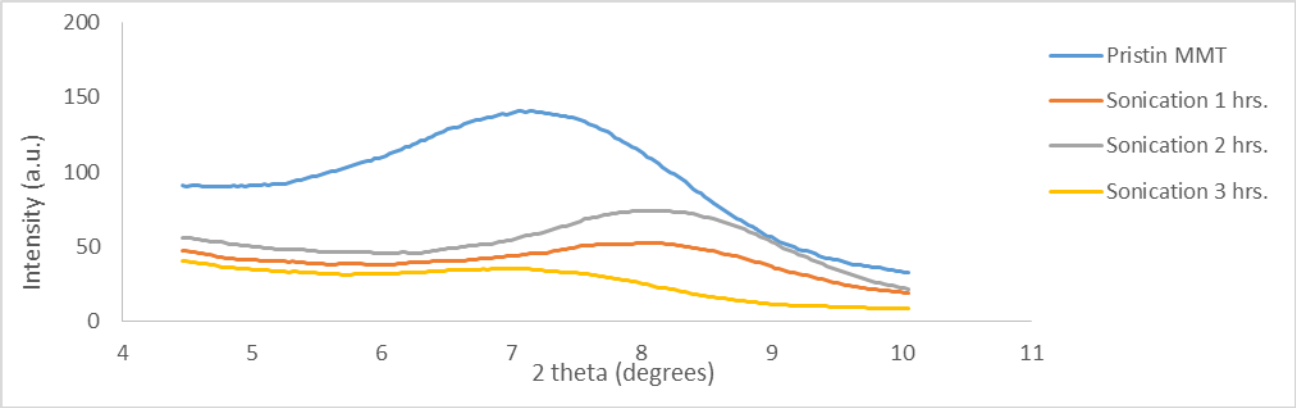

Figure 5-2: Effect of sonication for different time intervals on XRD pattern of MMT

Because of the hydrophobic and weak acidic properties of curcumin, cationic intercalation of curcumin into MMT is difficult to achieve, and thus cannot be ideally used for drug loading. However, finely dividing curcumin onto the hydrophilic large surface area of MMT is assumed to enhance its wettability and accordingly its dissolution rate. According to Aguzzi et al, smectite clays can enhance the dissolution of hydrophobic weak acidic drugs [22]. Different water insoluble drugs demonstrated enhancement in dissolution rate upon adsorption onto MMT surface such as indomethacine [22], phenytoin [76] and griseofulvin [77]. Consequently, stirring for 4 hours at 500 rpm in water was applied to obtain exfoliated MMT, with a high surface area and suitable adsorption sites for curcumin loading by adsorption. Kittinaovarat et al reported an increase in the adsorption rate of reactive red 120 acidic dye from aqueous solution by the use of chitosan/modified MMT beads due to the formation of disordered or almost exfoliated MMT structurture [78]. Similarly, the adsorption of methylene blue dye onto Na-MMT was higher than onto copper exchanged MMT due to the larger surface area of the Na-MMT that provided more adsoption sites [79]. Additionally, anionic forms of curcumin may be present due to the weak

acidic properties of curcumin and these species would be adsorbed onto the surface of exfoliated MMT through different mechanisms [80]. According to Epstein et al [11], broken bonds at the edges of clay layers are considered the principle sites for adsorption of anionic molecules through different mechanisms such as anion exchange in which organic anions replace exposed OH group, formation of hydrogen bonds between the anions of weak organic acids and the exposed OH group, or by coordination with polyvalent cations such as Al^{+3}.

5.2 Curcumin loading

Different parameters were investigated to ensure curcumin maximum loading, including clay exfoliation, curcumin solution concentration, time of mixing, and ratio of clay to curcumin solution (W/V %).

5.2.1 Clay exfoliation and drug loading

Exfoliation of clay showed increase in loading more than pristine clay, this is expected due to the higher surface area available for drug adsorption on the clay surface in case of exfoliated clay [57]. The amount of curcumin loaded is 3.5 mg and 6.5 mg per one gram of pristine and exfoliated clay respectively under the same conditions. This also suggests that the mechanism of clay drug interaction is by surface adsorption rather than ion exchange and intercalation, consequently in case of pristine MMT, lower amount of curcumin was loaded due to the smaller surface area available for adsorption compared to exfoliated clay. This is in agreement with the study done by Seema in 2013 in which increasing the drug (propranolol hydrochloride) to clay ratio increased the drug loading efficiency due to the exfoliation of the clay layers and changing the interaction of the clay with the drug-polymer moiety from intercalation to surface adsorption. The author suggested that the drug encapsulation is proportional to the degree of clay exfoliation. However after saturation of all clay surface sites there was no increase in drug loading [57]. This is also confirmed by the XRD spectra of both hybrids in which the pristine MMT demonstrated some degree of exfoliation after curcumin loading. Curcumin-loaded exfoliated MMT demonstrated a decrease in peak intensity compared to exfoliated MMT which refers to delamination of any stacked or agglomerated layers by the adsorption of curcumin into the clay surface (Figure 5-3).

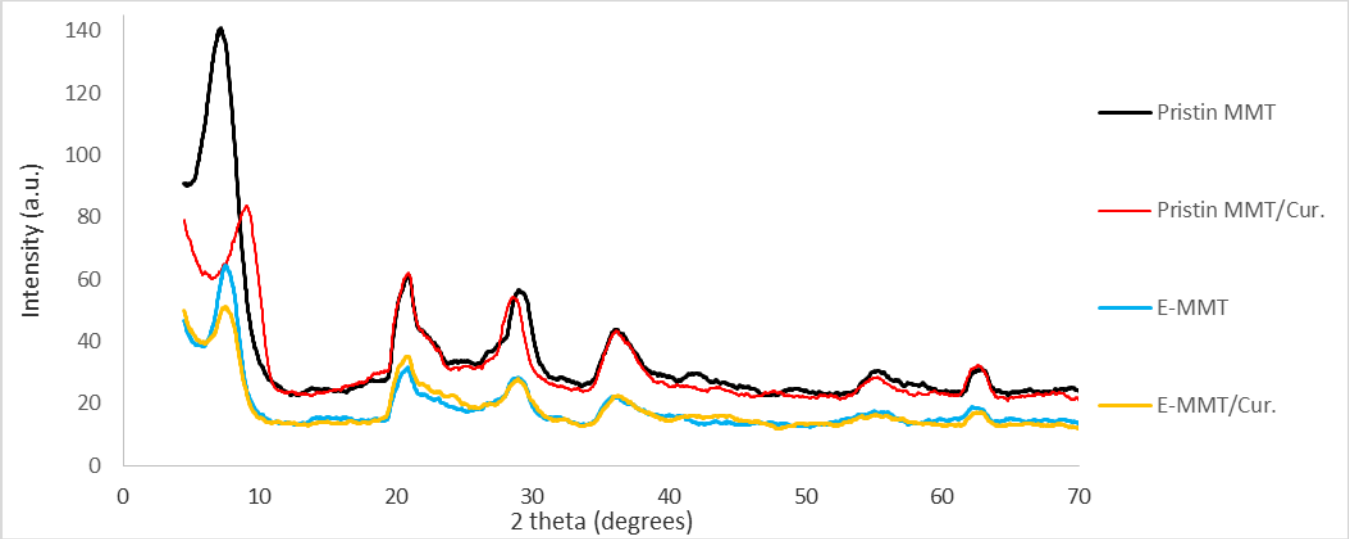

Figure 5-3: XRD spectra of curcumin loaded MMT (pristine and exfoliated)

5.2.2 Curcumin concentration and drug loading

Increasing the curcumin concentration up to 1 mg/ml demonstrated an increase in the amount loaded up to 6.5 mg curcumin per 1 g MMT, while in case of lower curcumin concentrations, 0.1 mg/ml and 0.05 mg/ml, the amount loaded decreased to 1.19 mg and 0.56 mg curcumin/ 1 g MMT respectively as shown in figure 5-4. However, the increase of the amount of drug loaded was limited by the maximum solubility of curcumin in absolute ethanol, which is 1mg/ml. This is significantly lower than the loading capacity of other drugs on MMT, such as timolol maleate (217mg/1g MMT), tamoxifen citrate (397 mg/g MMT), 5-fluorouracil (87.5 mg/g MMT), and procainamide (244 mg/g MMT) [10], [31], [81], [82]. According to Joshy et al and Kevadiya et al, the initial increase in the amount loaded is attributed to the high concentration gradient between the drug solution and the adsorption sites on the dispersed clay layers. After reaching equilibrium, the amount loaded remains constant due to the saturation of adsorption sites [78], [57] .

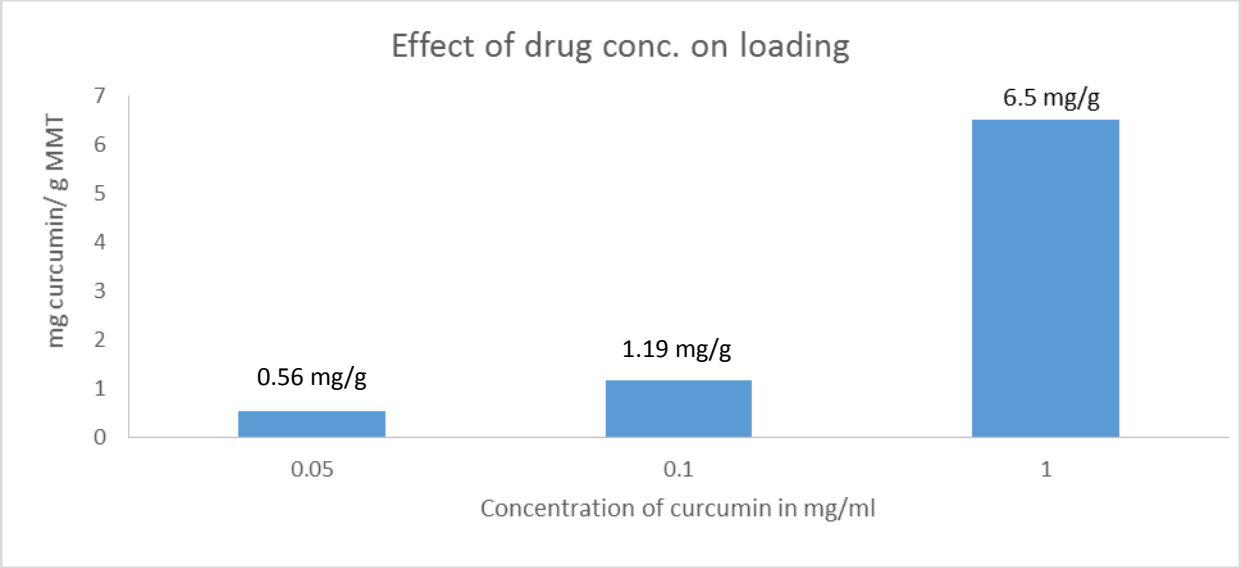

Figure 5-4: Effect of curcumin concentration on amount loaded per gram MMT

5.2.3 Stirring time and drug loading

Regarding the stirring time, there was no noticeable increase in the amount of curcumin loaded by increasing the stirring time from one to two or three hours (Figure 5-5). This is consistent with the results obtained by Joshi et al for the intercalation of timolol maleate into MMT. They reported that 17% of timolol was intercalated into the MMT interlayer within one hour and this amount remained constant after 15 hours [31].

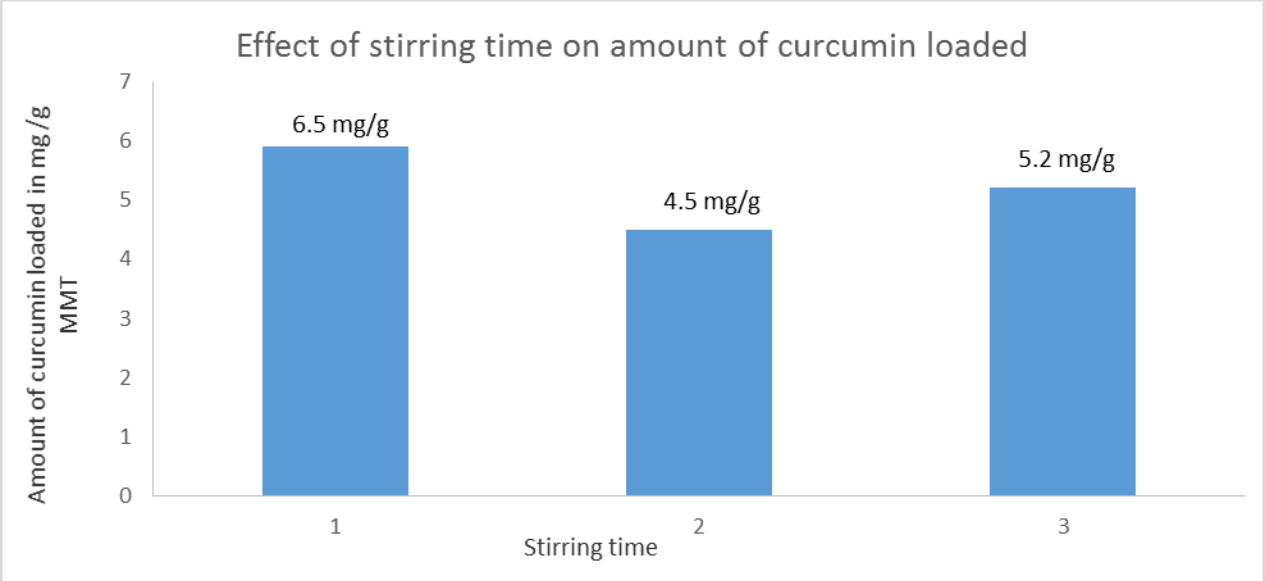

Figure 5-5: Effect of stirring time on amount of curcumin loaded onto clay

5.2.4 The amount of clay and drug loading

For the ratio of MMT powder to the curcumin solution, increasing the amount of MMT added to curcumin solution (of concentration 1mg/ml) from 1 to 5% W/V showed an increase in the amount of curcumin loaded. However further increase in the amount of MMT ratio to 10% W/V showed a decrease in the loaded amount (Figure 5-6). This first increase in amount of curcumin loaded is attributed to the increase of the surface areas of clay available for drug adsorption by increasing the amount of clay. On the other hand, increasing the amount of clay up to 10% probably led to an agglomeration of the clay layers and consequently decreased the surface area available for drug adsorption. In their work on the preparation of polystyrene/clay (either MMT or fluorinated synthetic mica) nanocomposites using solvent blending and sonication, Morgan and Harris reported that using clay concentrations between 2-3% allowed the polymer and clay to freely interact and form well exfoliated clay, while at higher concentrations, clay layers re-aggregate back to larger tactoids [73]. In other words, the critical coagulation concentration of Na-MMT depends on its content in the solution [83]. Additionally, alcohol would decrease the critical coagulation concentration of MMT [83], [84]. In the light of these facts, increasing the amount of MMT into the curcumin ethanoic solution may lead to aggregation of clay particles due to the increase of the clay content.

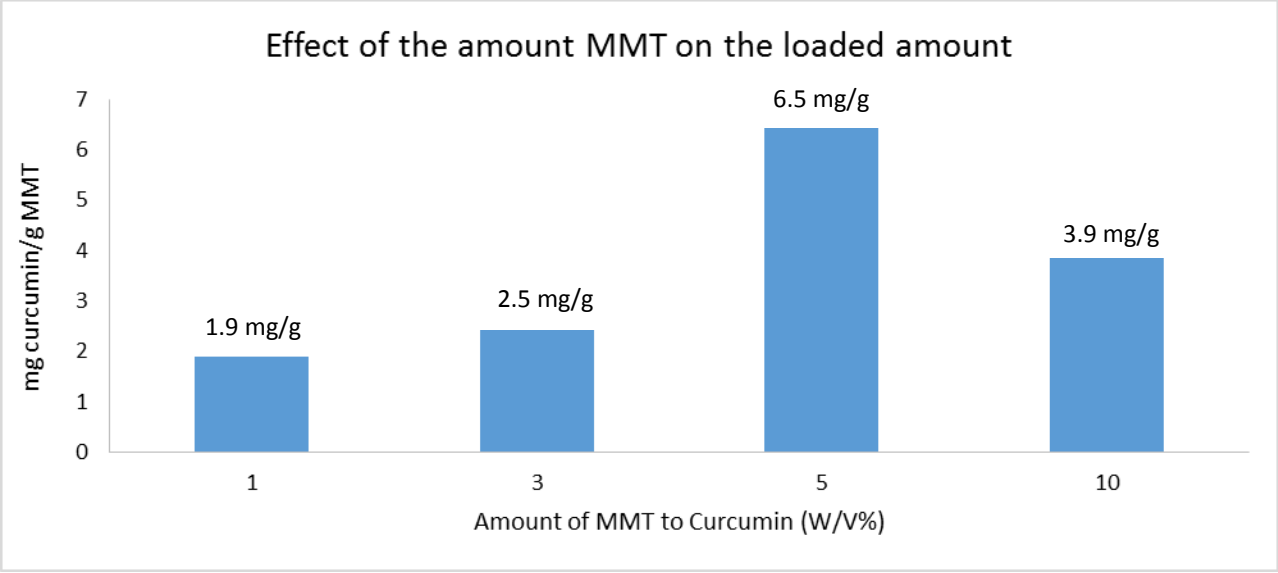

Figure 5-6: Effect of MMT amount on the amount of curcumin loaded

5.2.5 Conclusion

According to the above discussion, dispersing 5 g of e-MMT in 100 ml curcumin solution (1mg/ml) with continuous stirring for 1 h at 500 rpm produced curcumin/clay hybrids with a maximum loading of 6.5 mg curcumin/ g e-MMT. Consequently, these are the conditions used for the preparation of curcumin/clay samples to be encapsulated by the alginate biopolymer. These curcumin/clay samples are also characterized by XRD and FTIR for the elucidation of their structure and the investigation of the clay/drug interaction.

5.3 Characterization of hybrid and nanocomposite samples

5.3.1 FTIR results

E-MMT showed the same characteristic peaks of pristine MMT as demonstrated in Figure 5-7, the interlayer Al-OH and Si-OH groups show vibrational peak 3630 cm^{-1} [56] while Al-Al-OH and Al-Fe-OH bending vibrations peaks occurred at 918 cm^{-1} and 876 cm^{-1} respectively [85], [86]. The bending vibration of adsorbed water also occurs at 1637.9 and this is attributed to the firmly held water molecules while OH group of interlayer water demonstrate stretching vibration around 3440 cm-1 (Figure 5-7). Si-O stretching and Si-O-Al bending bands occurred at 1043.3 cm^{-1} and 526 cm^{-1} respectively [71]. However, Si-O-Al bands is less intense and sharp in the exfoliated than pristine clay this may be attributed to destruction of the linkage between octahedral and tetrahedral sheets due to the delamination of the layers [85]. Moreover, the structural change due to destruction of the layered structure of MMT is observed in the diminishing of the 3630 cm^{-1}, 918 cm^{-1} and 876 cm^{-1} bands assigned to the OH groups associated with Al (the central atom of the octahedral sheet). The weakening of these bands indicate either the release of these groups upon clay exfoliation or destruction of some octahedral sheets during stirring. The same observation is reported by Xia et al upon wet grinding of MMT using planetary ball mill and forming disordered layered structure [85]. These results are in agreement with those of XRD analysis, which confirm the formation of exfoliated clay upon it dispersion in water and stirring for 4 hours at room temperature.

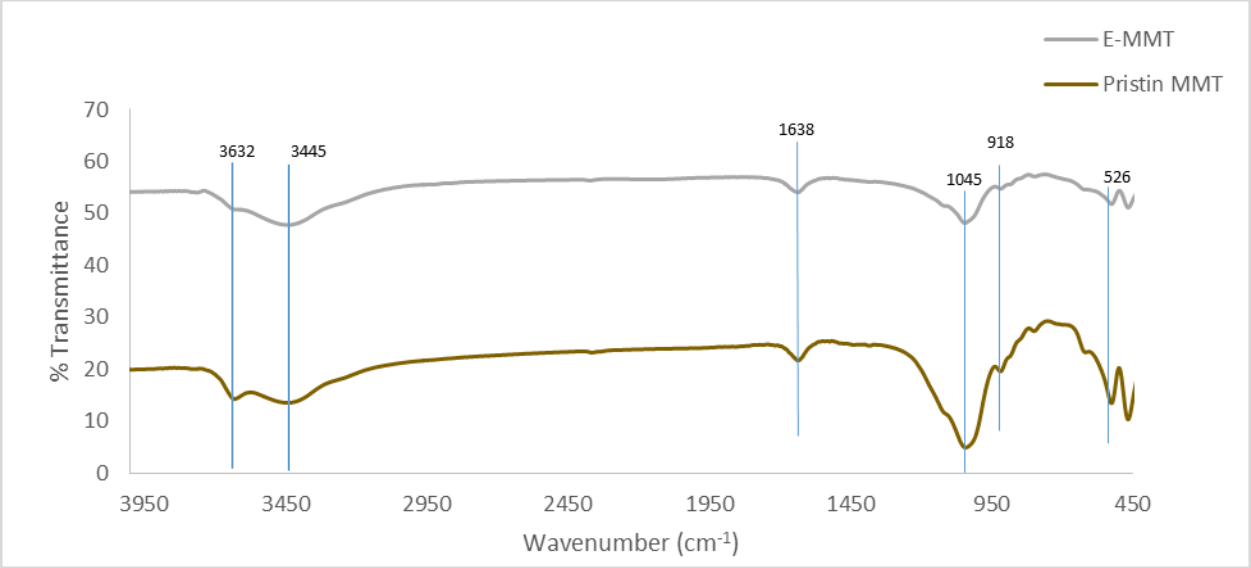

Figure 5-7: FTIR Spectra of pristine and exfoliated MMT

Curcumin demonstrated two broad absorption bands around 3500 cm^{-1} and 3390 cm^{-1} which are attributed to the two phenolic OH groups and two small peaks at 1599 cm^{-1} and 1027 cm^{-1} corresponding to the aliphatic carbonyl group. The aromatic C=C group demonstrate different vibrational bands in the range of 1520-1400 cm^{-1}[87] For the curcumin/E-MMT hybrid, an overlap could be observed between the absorption bands of each components that occurs in the increase in the intensity and sharpness of the characteristic peaks. Additionally the very small amount of curcumin present in the hybrid may account for the disappearance of some of it characteristic bands in the hybrid spectrum, such as the aromatic C=C group bands. This is shown in Figure 5-8 in which there is an intense sharp peak at 3446.1 cm^{-1} that can be assigned to the phenolic group of curcumin in addition to the OH group of Al-OH and Si-OH of the clay layers. The peaks occurred at 1637 cm^{-1} may be assigned to the carbonyl group of curcumin, in addition to the bending vibration of OH of firmly held water molecules of clay. The sharp intense vibrational peak at 1051 cm^{-1} may be attributed to both the stretching vibration of Si-O of the clay and the ketone group of curcumin. The occurrence of the vibrational peaks of both components of the hybrid suggests that the interaction between them is hydrophobic or physical interaction, i.e. via van der Waals bonding, so there is no significant shift in the characteristic peaks. This also may exclude the agglomeration of the clay particles by curcumin adsorption as there is no shift of the clay bands due to the interaction between layers.

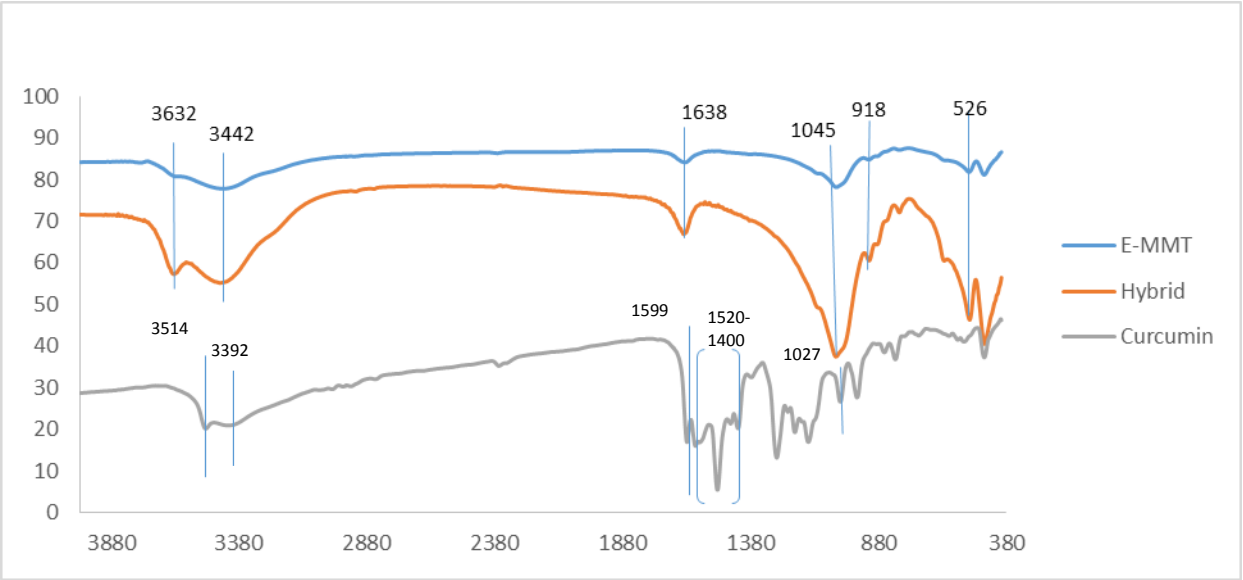

Figure 5-8: FTIR spectra of EMMT, curcumin and curcumin loaded clay (hybrid)

The alginate demonstrated characteristic peaks at 1618 cm^{-1} and 1418 cm^{-1} that are attributed to the asymmetric and symmetric stretching vibration of carboxylate group. The cyclic ether oxygen showed a characteristic stretching peak at 1033 cm^{-1}, while the hydroxyl group is represented by the stretching vibration at 3435 cm^{-1}[61]. The FTIR spectra of all nanocomposites (Figure 5-9) have the same carboxylate peaks of alginate but with pronounced decrease in intensity which may be attributed to the electrostatic attraction between the negative charge of carboxylate and the positive edges of MMT[88][62]. The hybrid demonstrated a band at 3631 cm^{-1} that is assigned to silanol group on the MMT surface. This disappeared in the nanocomposites spectra and this is explained by Kevadiya et al by the hydrogen bonding between the hydroxyl of the silanol group and the carboxyl and/or hydroxyl groups of alginate[60]. Additionally both the cyclic ether oxygen and the Si-O stretching vibrational bands of alginate and E-MMT at 1033 and 1045 cm^{-1} greatly decreased or even disappeared in all NC spectra, indicating the presence of interactions in these samples.

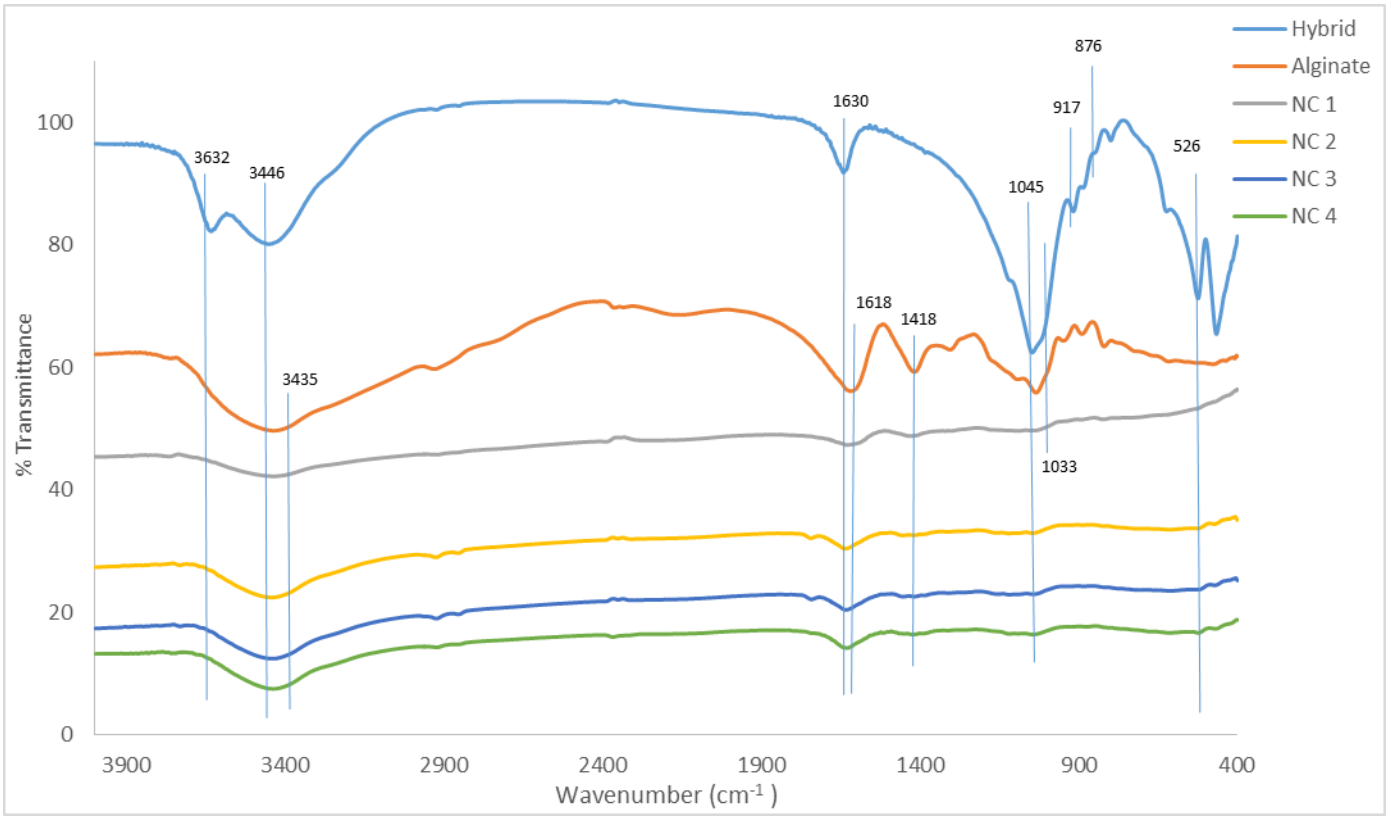

Figure 5-9: FTIR spectra of alginate, hybrid and NC, (a) NC 1, (b) NC 2, (c) NC 3, and (d) NC 4

5.3.2 XRD results

Clay exfoliation and drug loading is further confirmed by XRD analysis. Figure 5-10 includes the XRD patterns of curcumin, and Figure 5-11 shows the XRD patterns of exfoliated clay, hybrid and NC.

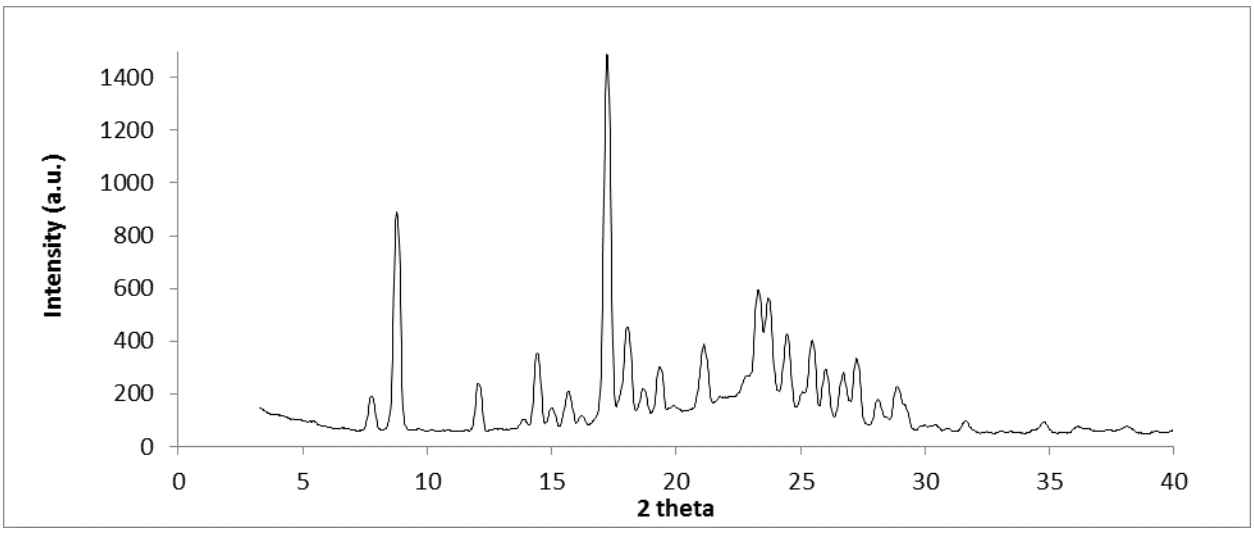

Figure 5-10: Curcumin XRD-spectrum

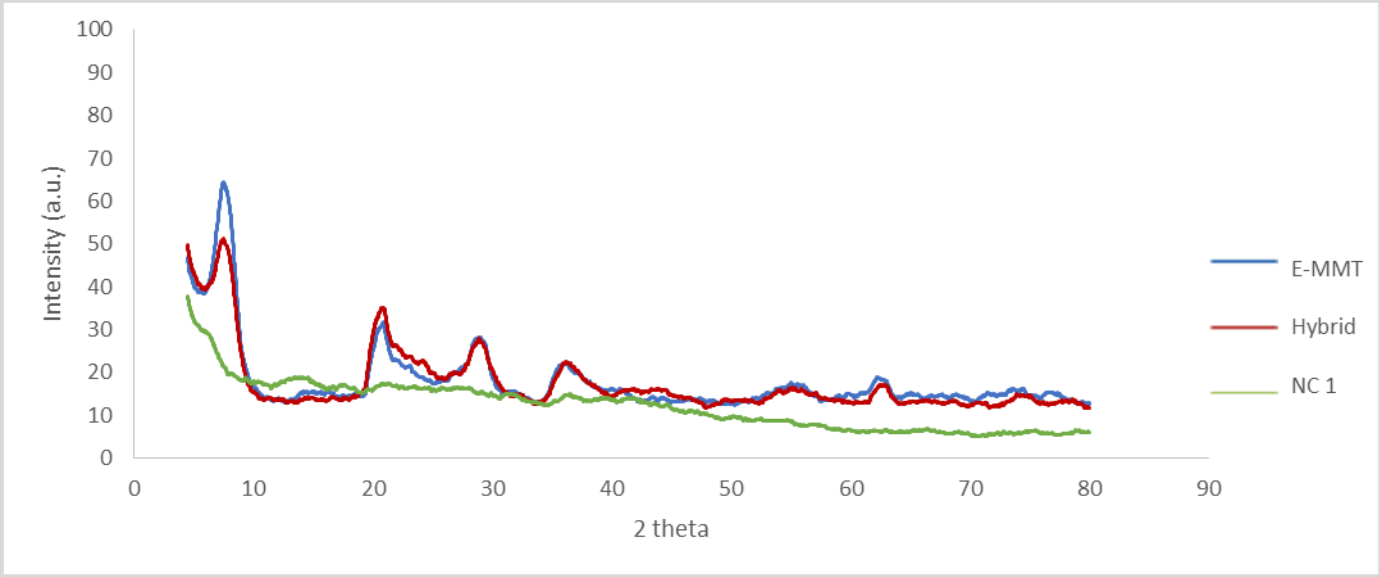

Figure 5-11: XRD spectra of E-MMT, Curcumin loaded clay, NC 1, NC 2, NC 3 and NC 4

The XRD spectrum of the hybrid demonstrated a decrease in the peak intensity of (001) plane relative to the exfoliated clay alone which indicated an increase in degree of exfoliation due to the drug adsorption rather than increasing the interlayer spacing [2], [4], [17]. The decrease in peak intensity indicated the decrease in the number of clay aggregated that have order layered structure with distinct interlayer spacing. Exfoliation of clay by the adsorption of drug molecules was also observed by Datta upon the preparation of propranolol loaded MMT-poly lactic-co-glycolic acid nanocomposites [57].

For the nanocomposite the (001) plane of the clay shows a shift to lower 2 theta value (5.34°) with a great decrease in peak intensity which could be attributed to the intercalation of the alginate molecules into the remaining clay layered structure leading to almost complete exfoliation. This may be attributed to the electrostatic repulsion between the negatively charged alginate and MMT that led to the dispersion of the clay layers into the polymer matrix in disordered manner. Mansa et al reported the decrease in d_{001} diffraction peak of MMT upon preparation of neutral guar-MMT nanocomposites. However, in case of cationic guar-MMT nanocomposites the decrease in the 2 theta value of d_{001} diffraction peak was accompanied with increase of the peak intensity due to the electrostatic attraction between the positively charged polymer and the negatively charged clay [89]. The absence of the characteristic XRD pattern of curcumin in both the hybrid and nanocomposites is attributed to the loss of the crystalline

structure of curcumin upon adsorption on the clay layers' surface. Similarly, Anitha et al reported the disappearance of the characteristic XRD peaks of curcumin after its loading into dextran sulfate-chitosan nanoparticles due to the amorphous or disordered –crystalline nature of curcumin inside the nanoparticles [45]. The disappearance of the characteristic XRD peaks of griseofulvin after adsorption onto MMT surface due to its adsorption in the amorphous phase without mutual association with the clay ions was also reported by Takahashi et al [77].

5.4 Release studies

The release studies were conducted in biorelevant media both intestinal (fed and fasting states) and gastric (fasting state). The different nanocomposite samples demonstrated different release profiles with regard to the site of release (gastric versus intestinal) and to release conditions (fed versus fasting state in the intestine). Additionally, the amount of curcumin released is affected by the ratio of hybrid to alginate, i.e. increasing the amount of hybrid in the nanocomposite generally decreased the amount of curcumin released in different media. Accordingly, NC 1 demonstrated the maximum release percentage in both fasted and fed intestinal media, 71% and 15.5% respectively, while NC 4 exhibited the lowest release percentage in both media, 17.4% and 6.5% respectively. According to Figure 5-12, this effect is more pronounced in the fasted state than in the fed state especially when comparing the decrease in the percentage released in NC 3 and NC 4 (which have higher amount of curcumin than NC 1 and NC 2). In the fed state, the decrease in the percentage released from NC 3 and NC 4 is about 8% while in the fast state is about 39%. This finding may be attributed to the lower solubility of curcumin in the FeSSIF (55.8 µg/ml) than in the FaSSIF (88.2µg/ml), according to the solubility tests carried out before the release experiment, so the decrease in percentage released in case of FeSSIF is related to the limited solubility of curcumin into the medium rather than the MMT effect on alginate swelling capacity. These results may be attributed to the decrease of the swelling capacity of alginate upon increasing the clay content because the latter act as crosslinking agent and consequently increase the hardness of the beads at neutral pH. Upon increasing the swelling capacity of the beads, more curcumin molecules diffuse from them and accordingly the release amounts are enhanced as a consequence to decreasing the clay content. Different clay/polymer systems displayed the same trend such as the bovine serum albumin loaded chitosan/organic rectorite films prepared by Wang et al, in which the percentage of protein release decreased by increasing the clay contents [90]. For chitosan/MMT system prepared by Hua et al, the percentage of

ofloxacin released also decreased by increasing MMT content due to the increase in the hardness of beads due to the crosslinking effect of the clay[56]. Kaygusuz et al reported the same trend in two alginate/MMT systems one of them loaded with bovine serum albumin and the other with vitamin B2. The effect of clay contents on the alginate swelling capacity of polymers was the reason behind the change in the release percentage in all systems [11], [18].

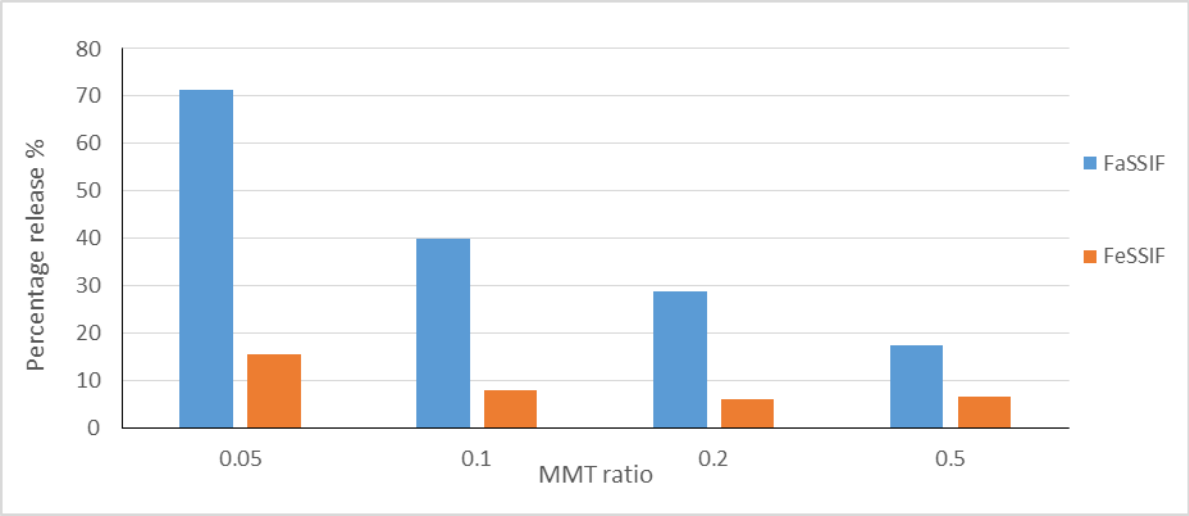

Figure 5-12: Percentage of curcumin released relative to amount of clay in different NC

The release of curcumin in all formulations in the gastric media under fasting conditions was negligible according to the calculation of limit of detection (Equation 4-3) using the calibration curve of curcumin in FaSSG (Appendix II). This is attributed to the very low solubility of curcumin in acidic medium of the gastric (12µg/ml), in addition to the shrinkage of alginate beads at the acidic medium due to the transformation of alginate into alginic acid which, in consequence, hinder the release of encapsulated drugs in general in acidic media [11], [61]. However, at higher pH values, alginate becomes more soluble and the beads start to disintegrate allowing the release of encapsulated drug. Accordingly, the release of curcumin is higher in intestinal media than in gastric medium.

Regarding the release in biorelevant intestinal media, the percentage of curcumin released was higher in the fast state (71% for NC 1 and 15.5% for NC4) than in the fed state (17% for NC 1 and 6% for NC 4) although the later has higher bile salts and phospholipids that could provide higher solubilizing capacity for lipophilic compounds such as curcumin. This behavior may be attributed to a two factors, namely the swelling of alginate and the solubility of curcumin. The

swelling ability of alginate which is pH dependent. Alginate demonstrates an increase in swelling ratio as the pH of the medium increases, due to the loss of divalent cross-linking cations, leading to an increase in drug release [11]. This is indeed observed here, with higher release in the fast state than in the fed state. Similar findings were observed by Oh et al upon studying the effect of the pH on the release of bovine serum albumin from different alginate/bentonite gel. The authors reported an increase in the percentage of drug released as the pH value of the medium increases (the tested pH values are 4.5, 5.2, 7.4 and 9.2) due to the increase of the swelling ratio of alginate at basic pH [91]. It is important to note that though curcumin is a weak acid due to the presence of three acidic protons (one enolic and two phenolic protons), the pKa values for these three protons (7.8, 8.5 and 9 [92]) are all above the highest pH values of the media used here (fast intestinal = 6.5 pH). Consequently, the presence of curcumin in an ionic form at pH = 6.5 is expected to be minimal and would not be playing a significant role in increasing its solubilization. However, this is expected to have a positive effect on the solubility of curcumin, which is higher in the fast than the fed states, which are 88.2µg/ml and 55.8 µg/ml respectively.

The effect of the pH of the medium is reflected in the very low release percentage of curcumin from all nanocomposites in the gastric media in which the amount released was below the detection limits of the methods as calculated by equation 1. Rahman et al reported similar trend for the solubility of curcumin in different media with different pH values and at different concentrations of surfactants [93]. There was increase in the solubility of curcumin as the pH of the solution increases and approaches the pKa values of curcumin. On the other hand, bile salts and phospholipids are known to form micelles and vesicle at physiological concentrations in the intestine and accordingly have solubilizing and stabilizing effects on hydrophobic molecules such as curcumin. Therefore higher release percentage is observed in intestinal media from all nanocomposites (fasting state was 71% 1and fed state wad 15.5% for NC 1) compared to gastric medium as it has very low concentrations of bile salts and phospholipids. Accordingly, curcumin release from different nanocomposites is affected by both the pH of the medium and the concentration of the solubilizing components such as bile salts and lecithin. These findings are supported by those of Zoeller et al who reported higher release percentage of glyburide (weak acid lipophilic hypoglycemic drug with pKa= 5.3) from Euglucon tablets in FaSSIF than in FeSSIF [94]. The solubilizing capacity of both media for was also studied for glyburide by Wei et al and comparable results were reported [95]. The authors confirmed that the solubility of

weak acid lipophilic glyburide is improved due the presence of micelles forming compounds such as bile salts and lecithin in addition to the increase of the pH of the medium. The improvement in the dissolution of weak acid lipophilic drugs as a function of both the pH and the concentration of surfactants that form solubilizing micelles for lipophilic drugs was also reported for piroxicam (pKa =5.6) by Jinno et al [96].

The release of curcumin in fast and fed states intestinal media showed different behaviors that may be attributed to different factors as pH of medium, concentration of bile salts and phospholipids, solubility of alginate and curcumin in different media. Accordingly, different release profiles are noticed as seen in figures 5-13 and 5-14. In the fed state the release of curcumin from different nanocomposites approached a plateau by 8 hours and the release percentage was low for all nanocomposites (maximum percentage is 15.5%, 7.9%, 6%, and 6.6% for NC 1, NC 2, NC 3 and NC 4 respectively). However, they demonstrated sustained release profile during the first 8 hours. On the other hand, the release of curcumin in the fasting intestinal medium was increasing during the experiment time (24 hours) and a higher amount of curcumin is released from all nanocomposites relative to that released in the fed state. Consequently, sustained release of curcumin from all nanocomposites could be attained in the fasting state, with the maximum percentage released from NC 1 (71%) which contains the least amount of hybrid.

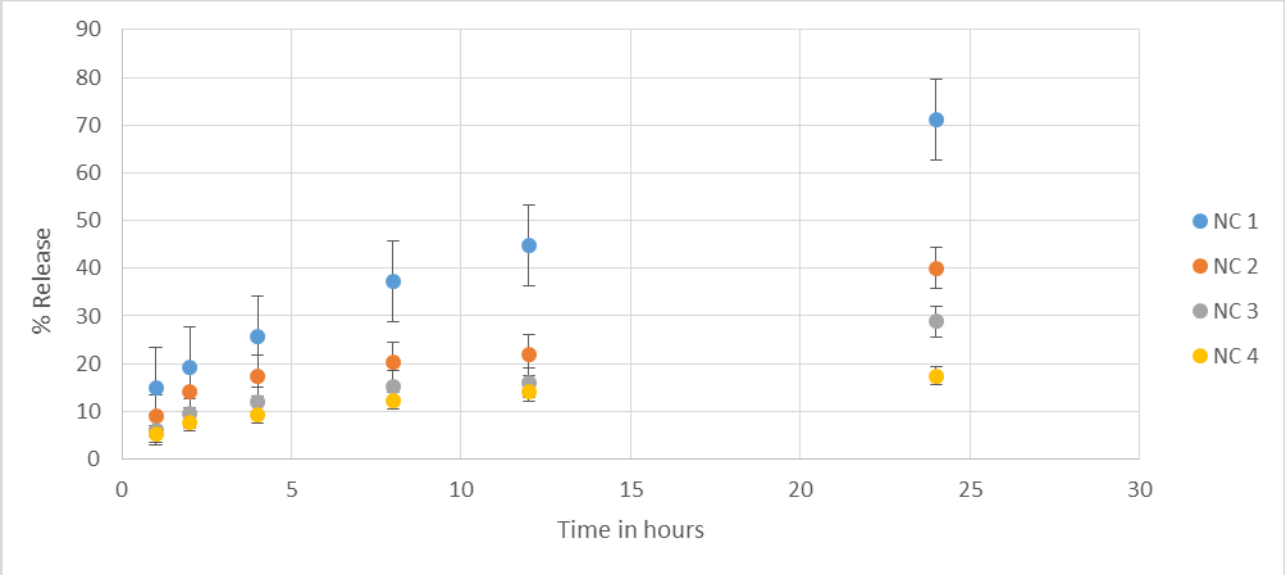

Figure 5-13: Release profile of curcumin from different nanocomposites in FaSSIF-V2

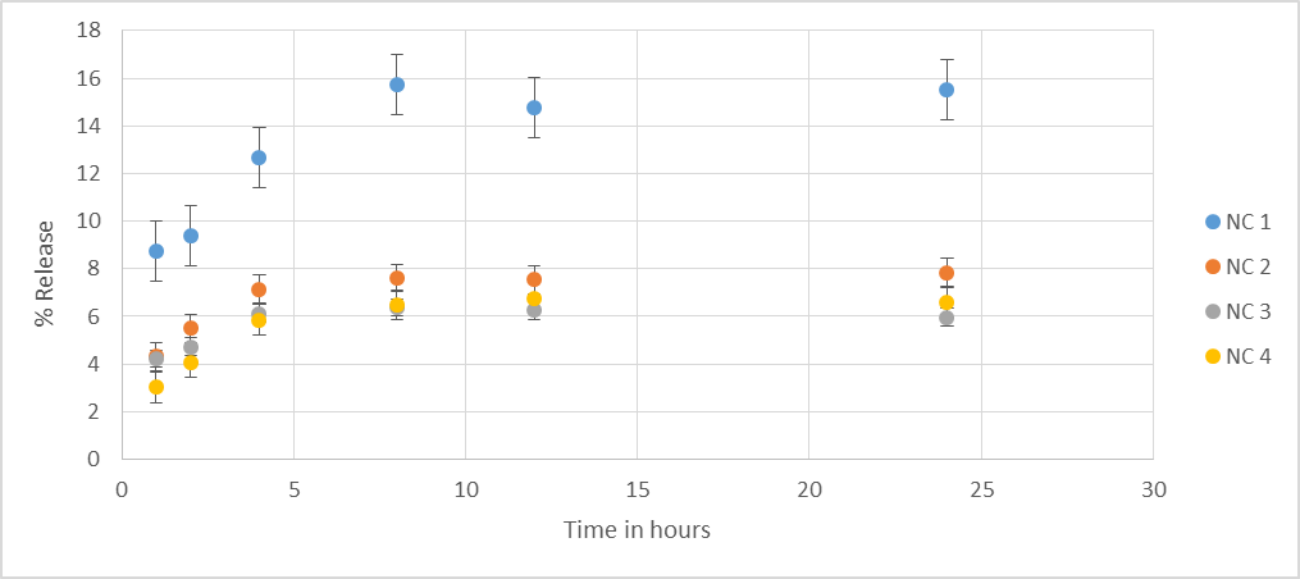

Figure 5-14: Release profile of curcumin from different nanocomposites in FeSSIF-original

The amount of curcumin released from NC 4 is higher (51.7µg) because it contains a higher amount of hybrid. Thus to attain higher concentration of released curcumin NC 4 would be more suitable than NC 1 (29µg is released from the same weight of beads). According to table 5-2, the time required for the release of 50% of the loaded amount ($T_{50\%}$) is more than 24 hours for all formulation except for NC 1 (71% is released after 24 hours) under fasting conditions. However, under fed conditions increasing the release time would not increase the amount released because the release profile approached plateau by 8 hours. According to table 5-2, the amount of curcumin released in both the fasted and fed states is directly proportional to the amount of hybrid used in the nanocomposites preparation. However, the percentage amount released is inversely proportion to the amount of hybrid used. This effect is attributed to the clay effect as it increases the beads hardness by increasing the cross linking between the polymer's chains and accordingly reduced the beads swelling ratio and decreased the amount of drug released. Additionally, the exfoliation of the clay into the polymer matrix provided a tortuous pathway for the drug molecules to move through before being released into the dissolution media and may hinder the escape of the drug molecules out of the polymer matrix.

Table 5-2: Percentage and amount of curcumin released in biorelevant intestinal media after 24 hours

	FaSSIF		FeSSIF	
	Percentage	Amount (μg)	Percentage	Amount (μg)
NC 1	71.2	29.0	15.5	4.0
NC 2	40.0	31.2	7.9	3.4
NC 3	28.8	42.6	6.0	5.6
NC 4	17.4	51.7	6.6	12.2

Many of the clinical trials demonstrated negligible effect in the treatment of colon cancer in doses less than 0.5 g/day for different treatment periods [8]. Accordingly it would be useful to use high doses of NC 4 under fasting conditions as it would produce the highest amount of curcumin compared to other nanocomposites in both fast and fed states. However, this would be accompanied by losing large amounts of the active ingredient as the percentage released after 24 hours is only 17.4%. However, this percentage release is relatively higher than that obtained by Suwannateep et al who reported a release of less than 10% in both gastric and intestinal fluids from both ethyl cellulose and a blend of ethylcellulose and methylcellulose nanoparticles. Additionally, for colorectal cancer treatment, curcumin-loaded alginate/MMT nanocomposites are preferred as they release the loaded drug into the intestinal fluids rather than the gastric fluids in contrast to monopolymeric and dipolymeric nanocarriers prepared by Suwannateep et al [47].

6 Conclusions and Future work

6.1 Conclusions

This study aimed at the preparation of a sustained release delivery system of curcumin using alginate/montmorillonite nanocomposites. Curcumin was first loaded onto exfoliated montmorillonite followed by encapsulation of the obtained hybrid with highest entrapment efficiency, into alginate matrix using different ratios of the hybrid to alginate (W/W). An in-vitro release study was then conducted on these nanocomposite samples, using biorelevant media.

Regarding the release in fast state simulated gastric fluid, the amount released was below the detection limits of the method. This was attributed to both shrinkage of the alginate matrix in the acidic medium and consequently decrease of the drug release through the reduced pore size of the beads, and to the low solubility of curcumin into the acidic pH in general and in the FaSSG (12µg/ml).

For the dissolution in intestinal media, the amount of curcumin released was much higher in both the fed and fast states compared to the gastric medium. These results were consistent with the higher concentration of bile salts and phospholipids in the intestine that provide solubilizing effect to lipophilic compounds such as curcumin (88.2 µg/ml inFaSSIF-V2 and 55.9 µg/ml in FeSSIF). Additionally, the higher pH of both the fast and fed states of the intestine promoted the swelling of alginate beads and consequently increased the percentage of curcumin release. However, fast state simulated intestinal fluids provided higher dissolution rate and release percentage of curcumin from all nanocomposites than fed state simulated intestinal fluid, although the latter contains higher concentrations of bile salts and phospholipids. This finding was attributed to the higher pH of the medium in the fast state, which in consequence increased the swelling ratio of alginate beads and the curcumin's solubility. The release profile was accordingly affected: in the fast state intestinal medium a sustained release profile was observed during the whole experimental time (24 hours) while in the fed state plateau was approached after 8 hours.

Different nanocomposites demonstrated different dissolution rates according to the amount of hybrid encapsulated into the alginate matrix. Increasing the amount of the hybrid in the nanocomposite, led to a decrease in the percentage of curcumin released. This was attributed to

the decrease in the swelling ratio of alginate beads due to the cross-linking effect of clay layers that increased the hardness of the beads. For the nanocomposites containing 1:20 hybrid to alginate (W/W) ratio, the release percentage was 71.2% in the FaSSIF and 15.5 in FeSSIF. Increasing the hybrid to alginate ratio up to 1:2 demonstrated noticeable decrease in the percentage released in both media and became 17.4% in FaSSIF and 6.6% in FeSSIF. The decrease in percentage released in the FaSSIF was more pronounced than in the FeSSIF and this was due to the lower solubility of curcumin in the FeSSIF than in the FaSSIF rather than the effect of clay on the polymer swelling.

The actual amount of curcumin released increased as the ratio of hybrid to alginate increased due to the increase of the amount of curcumin loaded. Accordingly, the nanocomposite with the lowest percentage release, resulted in the largest curcumin amount released, and this might be much better from the therapeutic point of view as large concentrations of curcumin are needed for different therapeutic applications such as colon cancer and Alzheimer.

6.2 Future work

Future work should focus on the following aspects:

- The use of organically modified montmorillonite clays for the intercalation of curcumin. This would significantly affect the amounts of curcumin loaded, as well as the release mechanisms.
- The study of the kinetics of release of curcumin from different Alginate/MMT nanocomposite formulations.
- Conducting stability and solubility tests of curcumin loaded into the alginate/MMT nanocomposites under different conditions.
- Carry out in vitro-in vivo correlation study to estimate the in vivo bioavailability of curcumin after oral administration of curcumin loaded alginate/MMT nanocomposites and compare it to that of the pure curcumin.
- Extending the study to different clay-polymer nanocomposites.

7 References

[1] R. a. Sharma, a. J. Gescher, and W. P. Steward, "Curcumin: The story so far," *Eur. J. Cancer*, vol. 41, no. 13, pp. 1955–1968, 2005.

[2] Bansal, Shyam S., M. Goel, A. Farrukh, M. V. Vadhanam, and R. C. and Gupta, "Advanced drug delivery systems of curcumin for cancer chemoprevention," *Cancer Prev. Res.*, vol. 8, no. 4, pp. 1158–1171, 2011.

[3] S. Wang, M. Tan, Z. Zhong, M. Chen, and Y. Wang, "Nanotechnologies for curcumin: An ancient puzzler meets modern solutions," *J. Nanomater.*, vol. 2011, 2011.

[4] P. Anand, A. B. Kunnumakkara, R. A. Newman, and B. B. Aggarwal, "Bioavailability of curcumin: Problems and promises," *Mol. Pharm.*, vol. 4, no. 6, pp. 807–818, 2007.

[5] N. Ghalandarlaki, A. M. Alizadeh, and S. Ashkani-Esfahani, "Nanotechnology-applied curcumin for different diseases therapy," *Biomed Res. Int.*, vol. 2014, 2014.

[6] O. Naksuriya, S. Okonogi, R. M. Schiffelers, and W. E. Hennink, "Curcumin nanoformulations: A review of pharmaceutical properties and preclinical studies and clinical data related to cancer treatment," *Biomaterials*, vol. 35, no. 10, pp. 3365–3383, 2014.

[7] M. M. Yallapu, M. Jaggi, and S. C. Chauhan, "Curcumin nanoformulations: a future nanomedicine for cancer.," *Drug Discov. Today*, vol. 17, no. 1–2, pp. 71–80, Jan. 2012.

[8] J. J. Johnson and H. Mukhtar, "Curcumin for chemoprevention of colon cancer," *Cancer Lett.*, vol. 255, pp. 170–181, 2007.

[9] C. Viseras, C. Aguzzi, P. Cerezo, and M. C. Bedmar, "Biopolymer–clay nanocomposites for controlled drug delivery," *Mater. Sci. Technol.*, vol. 24, no. 9, pp. 1020–1026, 2008.

[10] B. D. Kevadiya, G. V. Joshi, and H. C. Bajaj, "Layered bionanocomposites as carrier for procainamide," *Int. J. Pharm.*, vol. 388, no. 1–2, pp. 280–286, 2010.

[11] H. Kaygusuz and F. B. Erim, "Alginate/BSA/montmorillonite composites with enhanced protein entrapment and controlled release efficiency," *React. Funct. Polym.*, vol. 73, no. 11, pp. 1420–1425, 2013.

[12] F. Chivrac, E. Pollet, and L. Avérous, "Progress in nano-biocomposites based on polysaccharides and nanoclays," *Mater. Sci. Eng. R Reports*, vol. 67, no. 1, pp. 1–17, 2009.

[13] Z. Liu, Y. Jiao, Y. Wang, C. Zhou, and Z. Zhang, "Polysaccharides-based nanoparticles as drug delivery systems," *Adv. Drug Deliv. Rev.*, vol. 60, no. 15, pp. 1650–1662, 2008.

[14] K. Y. Lee and D. J. Mooney, “Alginate: Properties and biomedical applications,” *Prog. Polym. Sci.*, vol. 37, no. 1, pp. 106–126, 2012.

[15] A. D. Augst, H. J. Kong, and D. J. Mooney, “Alginate hydrogels as biomaterials,” *Macromol. Biosci.*, vol. 6, no. 8, pp. 623–633, 2006.

[16] Z. Ahmad and G. Khuller, “Alginate-based sustained released drug delivery systems for tuberculosis,” *Expert openion drug Deliv.*, vol. 5, no. 12, pp. 1323–1334, 2008.

[17] N. K. Sachan, S. Pushkar, A. Jha, and A. Bhattcharya, “Sodium alginate : the wonder polymer for controlled drug delivery,” *J. Pharm. Res.*, vol. 2, no. 7, pp. 1191–1199, 2009.

[18] H. Kaygusuz, M. Uysal, V. Ad mc lar, and F. B. Erim, “Natural alginate biopolymer montmorillonite clay composites for vitamin B2 delivery,” *J. Bioact. Compat. Polym.*, vol. 30, no. 1, pp. 48–56, 2015.

[19] H. H. Tønnesen and J. Karlsen, “Alginate in drug delivery systems.,” *Drug Dev. Ind. Pharm.*, vol. 28, no. 6, pp. 621–630, 2002.

[20] A. Shilpa, S. S. Agrawal, and A. R. Ray, “Controlled Delivery of Drugs from Alginate Matrix,” *J. Macromol. Sci. Part C Polym. Rev.*, vol. 43, no. 2, pp. 187–221, 2003.

[21] W. R. Gombotz and S. F. Wee, “Protein release from alginate matrices,” *Adv. Drug Deliv. Rev.*, vol. 64, pp. 194–205, 2012.

[22] C. Aguzzi, P. Cerezo, C. Viseras, and C. Caramella, “Use of clays as drug delivery systems: Possibilities and limitations,” *Appl. Clay Sci.*, vol. 36, no. 1–3, pp. 22–36, 2007.

[23] C. Viseras, P. Cerezo, R. Sanchez, I. Salcedo, and C. Aguzzi, “Current challenges in clay minerals for drug delivery,” *Appl. Clay Sci.*, vol. 48, no. 3, pp. 291–295, 2010.

[24] R. Suresh, S. N. Borkar, V. a Sawant, V. S. Shende, and S. K. Dimble, “Nanoclay Drug Delivery System,” *Int. J. Pharm. Sci. Nanotecnology*, vol. 3, no. 2, pp. 901–905, 2010.

[25] S. Pavlidou and C. D. Papaspyrides, “A review on polymer-layered silicate nanocomposites,” *Prog. Polym. Sci.*, vol. 33, no. 12, pp. 1119–1198, 2008.

[26] W. G. Fahrenholtz, “Clays,” in *Ceramic and Glass Materials: Structure, Properties and ProcessingStructure, Properties and Processing*, J. F. Shackelford and R. H. Doremus, Eds. Springer, 2008, pp. 111–133.

[27] D. R. Paul and L. M. Robeson, “Polymer nanotechnology: Nanocomposites,” *Polymer (Guildf).*, vol. 49, no. 15, pp. 3187–3204, 2008.

[28] a. López-Galindo, C. Viseras, and P. Cerezo, “Compositional, technical and safety specifications of clays to be used as pharmaceutical and cosmetic products,” *Appl. Clay Sci.*, vol. 36, pp. 51–63, 2007.

[29] J. Choy, S. Choi, J. Oh, and T. Park, “Clay minerals and layered double hydroxides for novel biological applications,” *Appl. Clay Sci.*, vol. 36, no. 1–3, pp. 122–132, 2007.

[30] F. Uddin, “Clays, nanoclays, and montmorillonite minerals,” *Metall. Mater. Trans. A Phys. Metall. Mater. Sci.*, vol. 39, no. 12, pp. 2804–2814, 2008.

[31] G. V. Joshi, B. D. Kevadiya, H. a. Patel, H. C. Bajaj, and R. V. Jasra, “Montmorillonite as a drug delivery system: Intercalation and in vitro release of timolol maleate,” *Int. J. Pharm.*, vol. 374, no. 1–2, pp. 53–57, 2009.

[32] “Barrier Properties of Ordered Multilayer Polymer Nanocomposites Part 1 (Nanotechnology).” [Online]. Available: http://what-when-how.com/nanoscience-and-nanotechnology/barrier-properties-of-ordered-multilayer-polymer-nanocomposites-part-1-nanotechnology/. [Accessed: 29-Jun-2015].

[33] S. Sinha Ray and M. Okamoto, “Polymer/layered silicate nanocomposites: A review from preparation to processing,” *Prog. Polym. Sci.*, vol. 28, no. 11, pp. 1539–1641, 2003.

[34] E. Jantratid, N. Janssen, C. Reppas, and J. B. Dressman, “Dissolution media simulating conditions in the proximal human gastrointestinal tract: An update,” *Pharm. Res.*, vol. 25, no. 7, pp. 1663–1676, 2008.

[35] C. Reppas and M. Vertzoni, “Biorelevant in-vitro performance testing of orally administered dosage forms,” *J. Pharm. Pharmacol.*, vol. 64, no. 7, pp. 919–930, 2012.

[36] E. Galia, E. Nicolaides, D. Hörter, R. Löbenberg, C. Reppas, and J. B. Dressman, “Evaluation of various dissolution media for predicting In vivo performance of class I and II drugs,” *Pharmaceutical Research*, vol. 15, no. 5. pp. 698–705, 1998.

[37] S. Klein, “The use of biorelevant dissolution media to forecast the in vivo performance of a drug.,” *AAPS J.*, vol. 12, no. 3, pp. 397–406, 2010.

[38] G. Garbacz and S. Klein, “Dissolution testing of oral modified-release dosage forms,” *J. Pharm. Pharmacol.*, vol. 64, no. 7, pp. 944–968, 2012.

[39] N. Kaewnopparat, S. Kaewnopparat, A. Jangwang, D. Maneenaun, T. Chuchome, and P. Panichayupakaranant, “Increased solubility, dissolution and physicochemical studies of curcumin-polyvinylpyrrolidone K-30 solid dispersions,” *Sci. Eng. Tech*, vol. 55, no. 7, pp. 229–234, 2009.

[40] a A. H. Sathali and J. Jayalakshmi, “Enhancement of Solubility and Dissolution Rate of Olmesartan Medoxomil By Solid Dispersion Technique,” vol. 3, no. 2, pp. 123–134, 2013.

[41] H. Chen, J. Wu, M. Sun, C. Guo, A. Yu, F. Cao, L. Zhao, Q. Tan, and G. Zhai, "N-trimethyl chitosan chloride-coated liposomes for the oral delivery of curcumin," *J. Liposome Res.*, vol. 22, no. 2, pp. 1–10, 2011.

[42] A. Karewicz, D. Bielska, A. Loboda, B. Gzyl-Malcher, J. Bednar, A. Jozkowicz, J. Dulak, and M. Nowakowska, "Curcumin-containing liposomes stabilized by thin layers of chitosan derivatives," *Colloids Surfaces B Biointerfaces*, vol. 109, pp. 307–316, 2013.

[43] C. Li, Y. Zhang, T. Su, L. Feng, Y. Long, and Z. Chen, "Silica-coated flexible liposomes as a nanohybrid delivery system for enhanced oral bioavailability of curcumin," *Int. J. Nanomedicine*, vol. 7, pp. 5995–6002, 2012.

[44] U. K. Parida, "Synthesis and Characterization of Chitosan-Polyvinyl Alcohol Blended with Cloisite 30B for Controlled Release of the Anticancer Drug Curcumin," *J. Biomater. Nanobiotechnol.*, vol. 02, no. 04, pp. 414–425, 2011.

[45] a. Anitha, V. G. Deepagan, V. V. Divya Rani, D. Menon, S. V. Nair, and R. Jayakumar, "Preparation, characterization, in vitro drug release and biological studies of curcumin loaded dextran sulphate-chitosan nanoparticles," *Carbohydr. Polym.*, vol. 84, no. 3, pp. 1158–1164, 2011.

[46] W. Sun, Y. Zou, Y. Guo, L. Wang, X. Xiao, R. Sun, and K. Zhao, "Construction and characterization of curcumin nanoparticles system," *J. Nanoparticle Res.*, vol. 16, no. 3, 2014.

[47] N. Suwannateep, W. Banlunara, S. P. Wanichwecharungruang, K. Chiablaem, K. Lirdprapamongkol, and J. Svasti, "Mucoadhesive curcumin nanospheres: Biological activity, adhesion to stomach mucosa and release of curcumin into the circulation," *J. Control. Release*, vol. 151, no. 2, pp. 176–182, 2011.

[48] A. Mukerjee and J. K. Vishwanatha, "Formulation, characterization and evaluation of curcumin-loaded PLGA nanospheres for cancer therapy," *Anticancer Res.*, vol. 29, no. 10, pp. 3867–3875, 2009.

[49] S. Dey and K. Sreenivasan, "Conjugation of curcumin onto alginate enhances aqueous solubility and stability of curcumin," *Carbohydr. Polym.*, vol. 99, pp. 499–507, 2014.

[50] A. F. Martins, P. V. a Bueno, E. a M. S. Almeida, F. H. a Rodrigues, A. F. Rubira, and E. C. Muniz, "Characterization of N-trimethyl chitosan/alginate complexes and curcumin release," *Int. J. Biol. Macromol.*, vol. 57, pp. 174–184, 2013.

[51] S. Song, Z. Wang, Y. Qian, L. Zhang, and E. Luo, "The release rate of curcumin from calcium alginate beads regulated by food emulsifiers," *J. Agric. Food Chem.*, vol. 60, no. 17, pp. 4388–4395, 2012.

[52] R. K. Das, N. Kasoju, and U. Bora, “Encapsulation of curcumin in alginate-chitosan-pluronic composite nanoparticles for delivery to cancer cells,” *Nanomedicine Nanotechnology, Biol. Med.*, vol. 6, no. 1, pp. 153–160, 2010.

[53] D. Guzman-Villanueva, I. M. El-Sherbiny, D. Herrera-Ruiz, and H. D. C. Smyth, “Design and in vitro evaluation of a new nano-microparticulate system for enhanced aqueous-phase solubility of curcumin,” *Biomed Res. Int.*, vol. 2013, 2013.

[54] T. S. Anirudhan, S. S. Gopal, and S. Sandeep, “Synthesis and characterization of montmorillonite/N-(carboxyacyl) chitosan coated magnetic particle nanocomposites for controlled delivery of paracetamol,” *Appl. Clay Sci.*, vol. 88–89, pp. 151–158, 2014.

[55] I. Salcedo, G. Sandri, C. Aguzzi, C. Bonferoni, P. Cerezo, R. Sánchez-Espejo, and C. Viseras, “Intestinal permeability of oxytetracycline from chitosan-montmorillonite nanocomposites,” *Colloids Surfaces B Biointerfaces*, vol. 117, pp. 441–448, 2014.

[56] S. Hua, H. Yang, W. Wang, and A. Wang, “Controlled release of ofloxacin from chitosan-montmorillonite hydrogel,” *Appl. Clay Sci.*, vol. 50, no. 1, pp. 112–117, 2010.

[57] S. M. Datta, “Clay-polymer nanocomposites as a novel drug carrier: Synthesis, characterization and controlled release study of Propranolol Hydrochloride,” *Appl. Clay Sci.*, vol. 80–81, pp. 85–92, 2013.

[58] S. Jain and M. Datta, “Montmorillonite-PLGA nanocomposites as an oral extended drug delivery vehicle for venlafaxine hydrochloride,” *Appl. Clay Sci.*, vol. 99, pp. 42–47, 2014.

[59] H. a. Patel, S. Shah, D. O. Shah, and P. a. Joshi, “Sustained release of venlafaxine from venlafaxine-montmorillonite-polyvinylpyrrolidone composites,” *Appl. Clay Sci.*, vol. 51, no. 1–2, pp. 126–130, 2011.

[60] H. Bajaj, B. Kevadiya, G. Joshi, H. Patel, and S. H. R. Abdi, “Montmorillonite-alginate composites as a drug delivery system: Intercalation and In vitro release of diclofenac sodium,” *Indian J. Pharm. Sci.*, vol. 72, no. 6, p. 732, 2010.

[61] B. D. Kevadiya, G. V. Joshi, H. M. Mody, and H. C. Bajaj, “Biopolymer-clay hydrogel composites as drug carrier: Host-guest intercalation and in vitro release study of lidocaine hydrochloride,” *Appl. Clay Sci.*, vol. 52, no. 4, pp. 364–367, 2011.

[62] R. I. Iliescu, E. Andronescu, C. D. Ghitulica, G. Voicu, A. Ficai, and M. Hoteteu, “Montmorillonite-alginate nanocomposite as a drug delivery system - Incorporation and in vitro release of irinotecan,” *Int. J. Pharm.*, vol. 463, no. 2, pp. 184–192, 2014.

[63] M. H. Penner, “Basic Principles of Spectroscopy,” in *Food Analysis*, S. S. Nielsen, Ed. Springer Science+Business Media, LLC, 2010, pp. 375–384.

[64] S. L. Upstone, “Ultraviolet / Visible Light Absorption Spectrophotometry in Clinical Chemistry,” in *Springer-Verlag Berlin Heidelberg*, R. A. Meyers, Ed. John Wiley & Sons Ltd, 2000, pp. 1699–1714.

[65] R. L. Wehling, “Infrared Spectroscopy,” in *Food Analysis*, 4th ed., S. S. Nielsen, Ed. Springer Science+Business Media, LLC, 2010, pp. 407–420.

[66] B. Fultz and J. Howe, “Diffraction and the X-Ray Powder,” in *Transmission Electron Microscopy and Diffractometry of Materials, Graduate Text in Physics*, Springer-Verlag Berlin Heidelberg, 2013, pp. 1–58.

[67] S. F. Wang, L. Shen, Y. J. Tong, L. Chen, I. Y. Phang, P. Q. Lim, and T. X. Liu, “Biopolymer chitosan/montmorillonite nanocomposites: Preparation and characterization,” *Polym. Degrad. Stab.*, vol. 90, no. 1, pp. 123–131, 2005.

[68] D. J. Phillips, S. R. Pygall, V. B. Cooper, and J. C. Mann, “Overcoming sink limitations in dissolution testing: a review of traditional methods and the potential utility of biphasic systems,” *J. Pharm. Pharmacol.*, vol. 64, pp. 1549–1559, 2012.

[69] F. Kong and R. P. Singh, “Disintegration of solid foods in human stomach,” *J. Food Sci.*, vol. 73, no. 5, pp. 67–80, 2008.

[70] W. F. Lee and L. L. Jou, “Effect of the intercalation agent content of montmorillonite on the swelling behavior and drug release behavior of nanocomposite hydrogels,” *J. Appl. Polym. Sci.*, vol. 94, no. 1, pp. 74–82, 2004.

[71] A. R. Ramadan, A. M. K. Esawi, and A. A. Gawad, “Effect of ball milling on the structure of Na+-montmorillonite and organo-montmorillonite (Cloisite 30B),” *Appl. Clay Sci.*, vol. 47, no. 3–4, pp. 196–202, 2010.

[72] K. Katti and D. Katti, “Effect Of Clay-Water Interactions On Swelling In Montmorillonite Clay,” *Civ. Eng.*, vol. 9, no. August, pp. 1–9, 1997.

[73] A. B. Morgan and J. D. Harris, “Exfoliated polystyrene-clay nanocomposites synthesized by solvent blending with sonication,” *Polymer (Guildf).*, vol. 45, no. 26, pp. 8695–8703, 2004.

[74] F. Franco, L. a. Pérez-Maqueda, and J. L. Pérez-Rodríguez, “The effect of ultrasound on the particle size and structural disorder of a well-ordered kaolinite,” *J. Colloid Interface Sci.*, vol. 274, no. 1, pp. 107–117, 2004.

[75] L. a. Pérez-Maqueda, A. Duran, and J. L. Pérez-Rodríguez, “Preparation of submicron talc particles by sonication,” *Appl. Clay Sci.*, vol. 28, pp. 245–255, 2005.

[76] H. A. Koeleman, R. van Zyl, Steyn, N. B. Boneschans, and H. S. Steyn, "Influence of montmorillonite on the dissolution and bioavailability of phenytoin," *Drug Dev. Ind. Pharm.*, vol. 16, no. 5, pp. 791–805, 1990.

[77] T. Takahashi and M. Yamaguchi, "Host-guest interactions between swelling clay minerals and poorly water-soluble drugs," *J. Colloid Interface Sci.*, vol. 146, no. 2, pp. 556–564, 1991.

[78] S. Kittinaovarat, P. Kansomwan, and N. Jiratumnukul, "Chitosan/modified montmorillonite beads and adsorption Reactive Red 120," *Appl. Clay Sci.*, vol. 48, no. 1–2, pp. 87–91, 2010.

[79] Y. L. Ma, Z. R. Xu, T. Guo, and P. You, "Adsorption of methylene blue on Cu(II)-exchanged montmorillonite," *J. Colloid Interface Sci.*, vol. 280, no. 2, pp. 283–288, 2004.

[80] M. Epstein and S. Yariv, "Visible-spectroscopy study of the adsorption of alizarinate by Al-montmorillonite in aqueous suspensions and in solid state," *J. Colloid Interface Sci.*, vol. 263, no. 2, pp. 377–385, 2003.

[81] B. D. Kevadiya, T. a. Patel, D. D. Jhala, R. P. Thumbar, H. Brahmbhatt, M. P. Pandya, S. Rajkumar, P. K. Jena, G. V. Joshi, P. K. Gadhia, C. B. Tripathi, and H. C. Bajaj, "Layered inorganic nanocomposites: A promising carrier for 5-fluorouracil (5-FU)," *Eur. J. Pharm. Biopharm.*, vol. 81, no. 1, pp. 91–101, 2012.

[82] F. Farshi Azhar and A. Olad, "A study on sustained release formulations for oral delivery of 5-fluorouracil based on alginate–chitosan/montmorillonite nanocomposite systems," *Appl. Clay Sci.*, vol. 101, pp. 288–296, 2014.

[83] G. Lagaly and S. Ziesmer, "Colloid chemistry of clay minerals: The coagulation of montmorillonite dispersions," *Adv. Colloid Interface Sci.*, vol. 100–102, pp. 105–128, 2003.

[84] J. Shen, X. Cao, and L. Jameslee, "Synthesis and foaming of water expandable polystyrene–clay nanocomposites," *Polymer (Guildf).*, vol. 47, no. 18, pp. 6303–6310, 2006.

[85] M. Xia, Y. Jiang, L. Zhao, F. Li, B. Xue, M. Sun, D. Liu, and X. Zhang, "Wet grinding of montmorillonite and its effect on the properties of mesoporous montmorillonite," *Colloids Surfaces A Physicochem. Eng. Asp.*, vol. 356, no. 1–3, pp. 1–9, 2010.

[86] G. V. Joshi, H. a. Patel, H. C. Bajaj, and R. V. Jasra, "Intercalation and controlled release of vitamin B6 from montmorillonite–vitamin B6 hybrid," *Colloid Polym. Sci.*, vol. 287, no. 9, pp. 1071–1076, 2009.

[87] S. D.Kumavat, Y. S.Chaudhari, P. Borole, P. Mishra, K. Shenghani, and P. Duvvuri, "Degradation studies of curcumin," *Int. J. Pharm. Rev. Res.*, vol. 3, no. 2, pp. 50–55, 2013.

[88] R. I. Iliescu, E. Andronescu, C. D. Ghiţulică, D. Berger, and A. Ficai, "Montmorillonite-alginate nanocomposite beads as drug carrier for oral administration of carboplatin-preparation and characterization," *UPB Sci. Bull. Ser. B Chem. Mater. Sci.*, vol. 73, no. 3, pp. 3–16, 2011.

[89] R. Mansa and C. Detellier, "Preparation and characterization of guar-montmorillonite nanocomposites," *Materials (Basel).*, vol. 6, no. 11, pp. 5199–5216, 2013.

[90] X. Wang, Y. Du, J. Luo, B. Lin, and J. F. Kennedy, "Chitosan/organic rectorite nanocomposite films: Structure, characteristic and drug delivery behaviour," *Carbohydr. Polym.*, vol. 69, no. 1, pp. 41–49, 2007.

[91] S.-T. Oh, O. Know, B.-C. Chun, J.-W. Cho, and J.-S. Park, "The effect of bentonite concentration on the drug delivery efficacy of a pH-sensetive alginate/bentonite hydrogel," *fibers Polym.*, vol. 10, no. 1, pp. 21–26, 2009.

[92] I. Stankovic, "Curcumin Chemical and Technical Assessment 61st JECFA," vol. 1, no. 8. pp. 1–8, 2004.

[93] S. M. H. Rahman, T. C. Telny, T. K. Ravi, and S. Kuppusamy, "Role of Surfactant and pH in Dissolution of Curcumin," *Indian J. Pharm. Sci. Pharm. Sci*, vol. 71, no. 2, pp. 139–142, 2009.

[94] T. Zöller and S. Klein, "Simplified biorelevant media for screening dissolution performance of poorly soluble drugs," *Dissol Technol*, vol. 14 , no. 4, pp. 8–13, 2007.

[95] H. Wei and R. Löbenberg, "Biorelevant dissolution media as a predictive tool for glyburide a class II drug," *Eur. J. Pharm. Sci.*, vol. 29, no. 1, pp. 45–52, 2006.

[96] J. Jinno, D. M. Oh, J. R. Crison, and G. L. Amidon, "Dissolution of ionizable water-insoluble drugs: The combined effect of pH and surfactant," *J. Pharm. Sci.*, vol. 89, no. 2, pp. 268–274, 2000.

Appendix 1

Preparation of Biorelevant Media

Preparation of fast state simulated gastric fluid using SIF powder original

Step 1: Preparation of NaCl/HCl solution for FaSSGF (1 Litre):

- Dissolve 2.00 g of NaCl in 0.9 L of purified water
- Adjust the pH to 1.6 with HCl and make up to volume (1 L) with purified water.

Step 2: Preparation of 1 L of FaSSGF

- Add 0.06 g of SIF Powder to approximately 500 mL of the NaCl/HCl solution at room temperature
- Make up to volume (1 L) with the NaCl/HCl solution

Preparation of fed state simulated intestinal fluid using SIF powder original

Step 1: Preparation of acetate buffer for FeSSIF (1 Litre):

- Dissolve 4.04 g of NaOH (pellets), 8.65 g of glacial acetic acid and 11.87 g of NaCl in 0.9 L of purified water
- Adjust the pH to 5.0 with either 1 N NaOH or 1 N HCl and make up to volume (1 L) with purified water

Step 2: Preparationof 1 L of FeSSIF:

- Add 11.2 g of SIF Powder to about 500 mL of buffer at room temperature and stir until SIF Powder has dissolved
- Make up to volume (1 L) with the buffer

Preparation of fast state simulated intestinal fluid using SIF powder FaSSIF-V2

Step 1: Preparation of maleate buffer for FaSSIF-V2 (1 Litre):

- Dissolve 1.39 g NaOH (pellets), 2.23 g of maleic acid and 4.01 g of NaCl in 0.9 L of purified water
- Adjust the pH to 6.5 with either 1 N NaOH or 1 N HCl and make up to volume (1 L) with purified water

Step 2: Preparation of 1 L of FaSSIF-V2

- Add 1.79 g of SIF Powder FaSSIF-V2 to about 500 mL of buffer at room temperature and stir until SIF Powder has dissolved
- Make up to volume (1 L) with the buffer and let FaSSIF stand for 1 hour. FaSSIF-V2 is ready for use.

Appendix 2

Calibration Curves

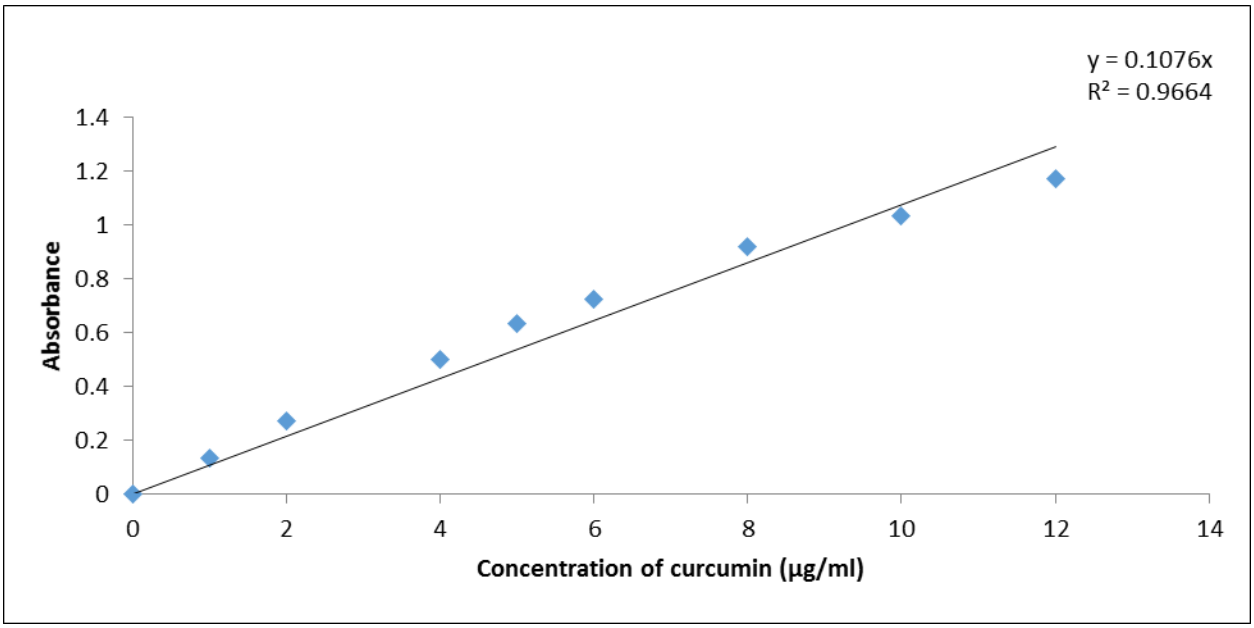

Calibration curve of curcumin in ethanol at λmax=425

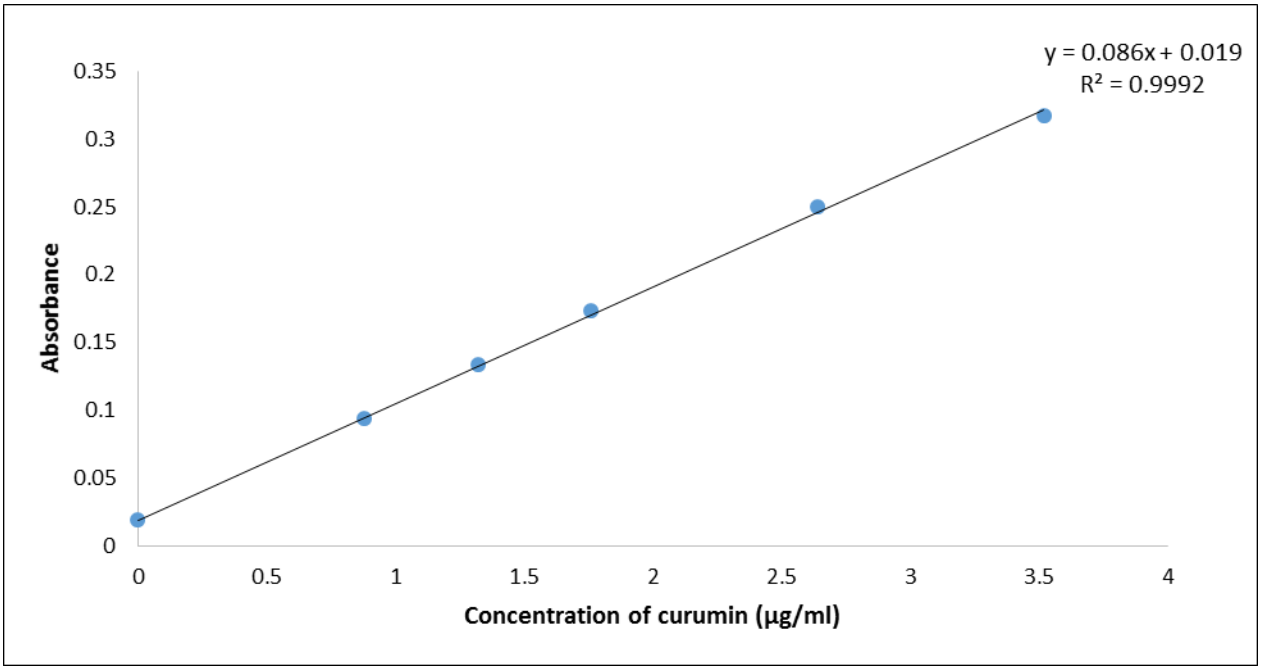

Calibration curve of curcumin in 3% $CaCl_2$ solution at λmax=464

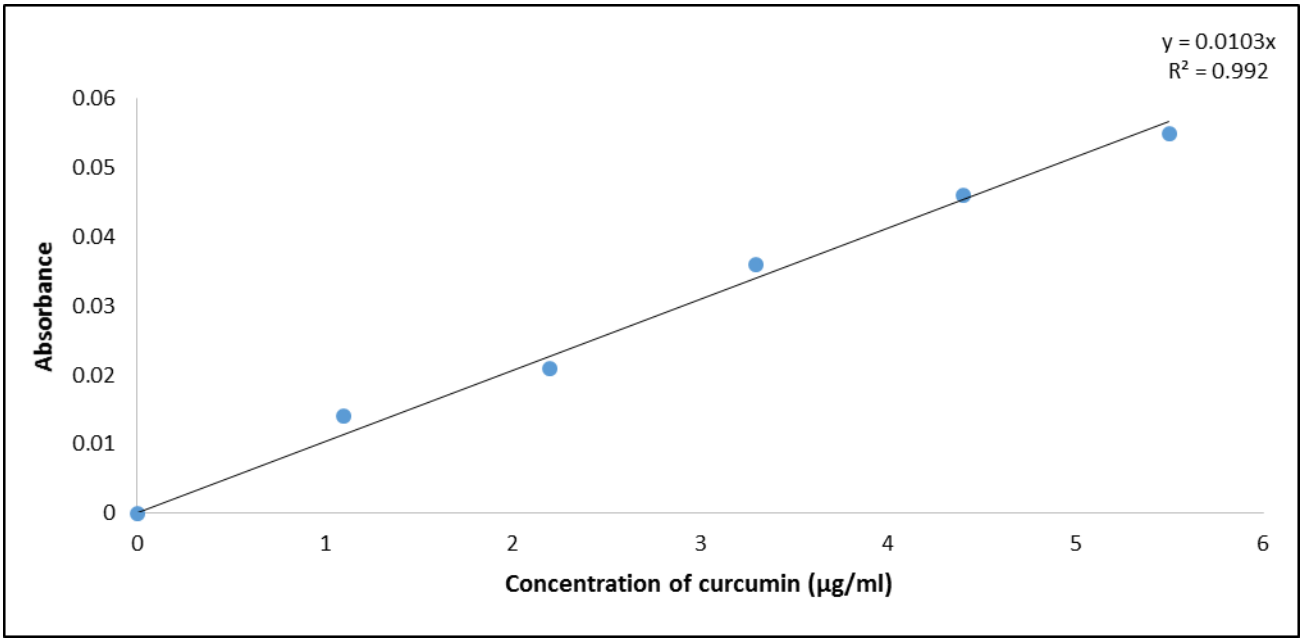

Calibration curve of curcumin in FaSSGF at λmax=425

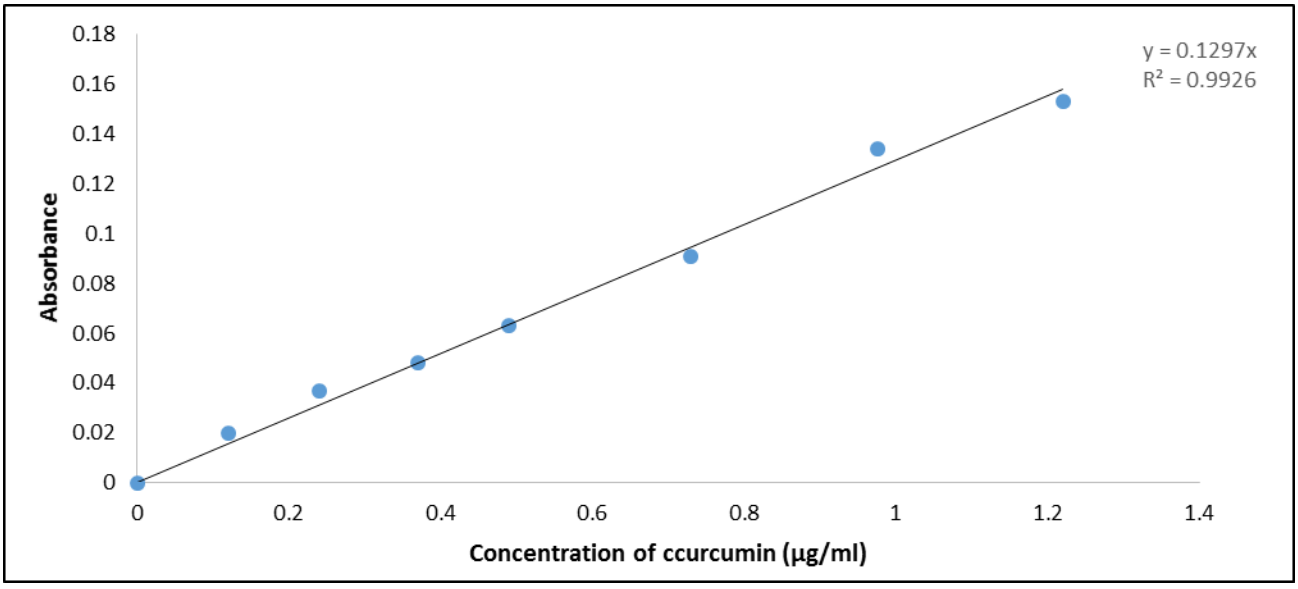

Calibration curve of curcumin in FeSSIF at λmax=424

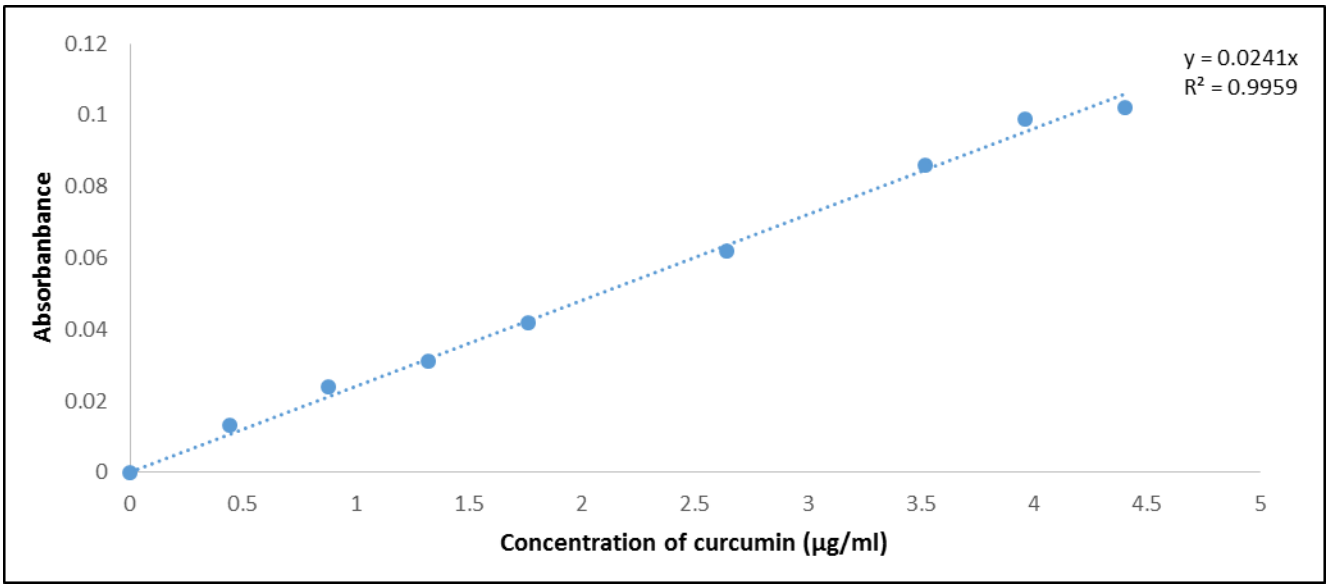

Calibration curve of curcumin in FaSSIF-V2 at λmax=418